PART I

EFFECT OF THE SURROUNDING GAS ATMOSPHERE ON THE LIQUID CONTENT OF FORMING HYDROCARBON DROPS

PART II

GAS ABSORPTION BY FALLING LIQUID DROPS: HYDROCARBON SYSTEMS

By

ÖNER HORTAÇSU

Bachelor of Science
Robert College
İstanbul, Turkey
1963

Master of Science
Oklahoma State University
Stillwater, Oklahoma
1965

Submitted to the Faculty of the Graduate College
of the Oklahoma State University
in partial fulfillment of the requirements
for the Degree of
DOCTOR OF PHILOSOPHY
July, 1970

PART I

EFFECT OF THE SURROUNDING GAS ATMOSPHERE ON THE

LIQUID CONTENT OF FORMING HYDROCARBON DROPS

PART II

GAS ABSORPTION BY FALLING LIQUID DROPS:

HYDROCARBON SYSTEMS

Thesis Approved:

R. N. Maddox
Thesis Adviser

John B. West

John H. Erbar

Clarence M. Cunningham

D. Dunham
Dean of the Graduate College

PREFACE

An improved understanding for the behavior of spray type contactors and reactors is possible through research on single and swarms of drops in gas phase. Studies at different stages of drop life are necessary for this understanding to be achieved.

In two parts, this thesis attempts to study the effect of the surrounding gas atmosphere on the liquid content of drops forming at a tip and gas absorption by falling liquid drops. For both parts of this study hydrocarbon systems were used.

I wish to gratefully acknowledge the help of various people to whom I owe the realization of this work.

My adviser, Dr. Robert N. Maddox, had a continued interest in my work and myself all through my years at Graduate School. I sincerely thank him for his help and guidance.

I also thank Dr. J. B. West, Dr. J. H. Erbar of the School of Chemical Engineering and Dr. Cunningham of the Chemistry Department for being members of my Advisory Committee and for their suggestions. Dr. W. Crynes' suggestions on the manuscript are also acknowledged.

I have enjoyed and profited from my association with all the members of the Chemical Engineering faculty; to them I will always be grateful. Here, I will like to mention Professor W. C. Edmister, Dr. R. L. Robinson and Dr. K. J. Bell, in addition to those mentioned above.

I thank Mr. E. E. McCroskey of the School of Chemical Engineering

for his indispensable help in procuring, setting up and operating the experimental apparatus. Thanks are also due to Mr. Preston Wilson and Mr. Arlin Harris of the Research Apparatus Development Laboratory for constructing the absorption column.

The School of Chemical Engineering provided and procured all of the financial help I received throughout the duration of this work, in addition to financing the expeimental apparatus and materials. I will always remain grateful to the School of Chemical Engineering for its very generous contribution.

Whatever I have been able to accomplish all through my life would not have been possible without the encouragement and support of my parents, brother and sister. Amy, in her position as wife, friend and colleague is an integral part of this work as she is of me.

TABLE OF CONTENTS

LIST OF TABLES

LIST OF FIGURES

PART I

EFFECT OF THE SURROUNDING GAS ATMOSPHERE ON THE LIQUID CONTENT OF FORMING HYDROCARBON DROPS

CHAPTER I

INTRODUCTION

Research on the effect of the surrounding liquid and feed rate to a forming drop or bubble for liquid-liquid systems and bubbles has not been extended to drops forming in gaseous atmospheres. This present work will probably initiate further studies to explore the effects of the variables pertinent to drops forming in soluble gas atmospheres.

Data presented here are basically on hydrocarbon systems. The range of the data is believed to be reasonably wide for a first study, however by no means extensive.

The experimental results have shown that at a constant drop formation time the atmosphere surrounding a drop could strongly affect the liquid in the drop.

CHAPTER II

LITERATURE SURVEY

There is no evidence in the literature that the effect of the surrounding gas atmosphere on the liquid content of forming drops has been studied. For very small drops formed by atomization, studies are available on the effect of pressure and temperature on the drop size in the combustion literature. The effect of chamber pressure, i.e. gas atmosphere density, on the stability of a liquid film on a sieve tray and consequently on the sizes of drops formed upon the break of the film was reported by Dombrowski and Hooper (9). Smaller drops were observed for denser atmospheres. This study (9) could be considered loosely related to the subject of this report.

In the absence of data on the effect of the gas atmosphere on forming drops this literature study will be concerned mainly with the available studies on gas-liquid (11, 12, 26, 46, 58, 60, 65) and liquid-liquid systems (35, 52, 53, 54). The effect of drop formation rate on the drop size will also be discussed.

If a liquid drop is formed infinitely slowly at a tip, pointing vertically down, the size of the drop is governed by Equation (1)

$$\sigma d_1 \pi = V_d (\rho_d - \rho_c) \left| \frac{g}{g_c} \right| \qquad (1)$$

Equation (1) is the basis of the pendant drop method for surface tension determinations. However, if the drops do not form slowly, the equilibrium condition assumed by Equation (1) does not apply.

The effect of formation time on the drop size was noticed by Harkins and Brown (28), who noted that faster forming drops, from a given tip, are larger than slower forming drops. The Harkins and Brown data on the effect of formation time on drop size are very limited in scope: only one liquid was used with one tip and drop weights were determined at eight different formation times. Harkins and Brown explained this behavior as the result of liquid streaming from the tip forcing its way into the drop detaching from the tip.

Tip calibration curves for gas absorption experiments by liquid drops are another source of data on drops forming from vertically downward tips in contact with gas (14, 39). In general, the literature data show that faster forming drops are larger than slower forming drops.

For all 17 tips calibrated by Dixon and Russel (14) drop volumes at five second formation time were smaller than the drop volumes at two second formation time. However, for tips of small internal diameters (0.403 mm - 1.15 mm), the Dixon and Russel curves show a maximum in drop volume between formation times of 0.5 and 2 seconds.

Hughes and Gilliland (39) reported calibration curves for three tips. Two of these tips showed a decreasing drop volume with increasing drop formation time, but the third, the smallest tip (d_1 = 0.52 mm), showed the opposite trend. Drop formation times reported by Hughes and Gilliland ranged from 0.25 sec. to 2.2 sec.

The maxima in drop sizes with increasing drop formation time, at fast formation rates, observed for some tips by Dixon and Russel, were also observed by Hayworth and Treybal (35) in their study on drops in liquid-liquid systems. The results of Hayworth and Treybal show that

from a nozzle velocity of 0.1 cm/sec. to about 10 cm/sec., drops increase in size with increasing nozzle velocity (smaller formation time) and the drop sizes decrease and become increasingly more erratic between nozzle velocities of 10 cm/sec. and 30 cm/sec.. Hayworth and Treybal (35) correlated their results in the form of Equation (2):

$$V_d + (4.11 \times 10^{-4}) V_d^{2/3} \left(\frac{\rho_d v_n^2}{\rho_d - \rho_c} \right) = (21 \times 10^{-4}) \left(\frac{\sigma d_1}{\rho_d - \rho_c} \right) + (1.069 \times 10^{-2}) \left[\frac{d_1^{0.747} v_n^{0.265} \mu_c}{\rho_d - \rho_c} \right]^{3/2} \qquad (2)$$

Equation (2) is based on a force balance of the surface tension, buoyant and kinetic forces acting on the drop. This force balance, if written in terms of volumes is:

$$V_d = V_\sigma + V_\infty - V_k \qquad (3)$$

Hayworth and Treybal's results showed that larger drops formed at larger tips. Larger drops were also observed in systems exhibiting higher interfacial tension and lower density difference between the phases. To a lesser extent, systems of increased continuous phase viscosities exhibited larger drops.

Null and Johnson (54) also studied the sizes of forming drops for liquid-liquid systems. Their geometrical models depended mostly on their measurements of drop height and the variation in the neck width at the point of detachment of the drop from the liquid stream. A set of experimentally determined correlation factors are necessary to determine drop sizes from the correlation proposed by Null and Johnson.

Results of Null and Johnson and the data of Hayworth and Treybal show larger drops for systems of high interfacial tension and low density differences. These results are consistent with a static balance, i.e. Equation (1), for an infinitely slowly forming drop. However, the Hayworth and Treybal correlation, reportedly predicted larger than actual drop sizes for two independent studies by Null (53) and Batson (1).

There is a controversy on the behavior of the drop size versus nozzle velocity plots available in the literature for liquid-liquid systems. The results of Null (52, 53) show only one maximum in drop size when plotted versus the nozzle velocity of liquid whereas Hayworth and Treybal (35) and Batson (1) reported two maxima in similar plots. Vilnits and Gelperin (61) reported work on drops forming both in air and immiscible liquid media. Their results for air were expressed as

$$\frac{d_e}{d_1} = 16.64 \times 10^{+3} \left[\left(\frac{v_n \mu_d}{\sigma} \right)^{0.767} \Big/ \mu_d^{1.7} \, Re_d^{0.92} \right] \qquad (4)$$

and for liquid-liquid systems

$$\frac{d_e}{d_1} = 4600 \left(\frac{v_n \mu_d}{\sigma} \right)^{0.42} \left(\frac{\mu_d}{\mu_d + \mu_c} \right) Re_d^{0.504} \qquad (5)$$

A recent article by Bayens and Laurence (2) reported the effect of the direction of mass transfer on the surface area of forming drops. The findings of this limited study showed that mass transfer from the liquid jet significantly decreased the interfacial area of the drops forming from this jet. However, increased mass transfer to the jet did

not affect the interfacial area of the resulting dispersion.

Recently, attempts have been reported to predict the formation of gas bubbles in liquids by a modified force balance (11, 12, 46, 57, 58, 69). This new trend is based on the equation

$$F_g - F_b = F_f + F_\sigma + F_\mu \tag{6}$$

Equation 6 was written for the two stages of the drop formation period by using different expressions for F_f and F_μ for each stage. The two stages are hypothetical and are differentiated by the start of necking at the drop base.

In summary, the literature data show that faster forming drops are larger than slower forming drops. However, at very fast formation rates (feed rate $\approx$ 10 cm/sec.) drop sizes are increasingly erratic and tend to get smaller with faster feed rates.

No study was encountered in the literature on the effect of the surrounding atmosphere on size or liquid content of forming drops.

CHAPTER III

EXPERIMENTAL APPARATUS AND MATERIALS

Experimental Apparatus

The experimental apparatus used to determine the liquid content of the drops in gas atmospheres of different solubility was made up of some parts of the apparatus used for the falling drop absorption studies (See Part II). Mainly the following equipment was used:

1. The drop catching assembly without the drop collection tube, Figure 14.
2. The drop forming assembly of the absorption column, Figure 13, including the top plate of the column but excluding valves V12 and V13 and also excluding the lines connecting them to the drop forming assembly.
3. Rotameter R3, Figure 12, and the gas transfer lines connecting the gas cylinder to rotameter R3, R3 to the saturators and the saturators to the gas inlet on the top plate.

The equipment was assembled as follows:

1. The top plate of the absorption column was bolted to the upper flange of the drop catching assembly and the interface sealed by an O ring.
2. The drop forming assembly was mounted on the top plate of the column and attached to it as in Figure 13.
3. The line for the incoming gas from rotameter R3 was attached

to the entry points available on the top plate, Figure 13.

4. A 1.7 cm I.D., 7.5 cm long glass tube was fitted to the center opening of a circular piece of one inch thick foam rubber, which was used to replace the drop collection tube at the bottom of the drop catching assembly. The upper end of the glass tube protruded two centimeters into the drop catching assembly. This glass tube was used as the exit for the liquid drops after they detached from the drop forming tip.

Glass weighing bottles were used to catch and weigh the drops. Stopcock grease was used to seal the ground glass joint between the cover and the body of the weighing bottle to eliminate loss of the absorbed gas and drop liquid prior to weighing and chromatographic analysis.

Experimental Materials

Hydrocarbon liquids used for drops were n-octane, n-nonane and n-decane. Most of the experimental data were taken using technical grade liquid hydrocarbons. For purposes of comparison with the technical grade liquid data, research grade n-nonane and n-decane were also used with some tips and some gas atmospheres.

The gases used were technical grade n-butane, technical grade propane, pure grade ethane, pure grade methane and commercial grade Freon 12.

All of the experimental materials, with the exception of Freon 12, were products of Phillips Petroleum Company, Bartlesville, Oklahoma. Freon 12 was a product of E. I. duPont de Nemours and Company of Wilmington, Delaware.

CHAPTER IV

EXPERIMENTAL PROCEDURE

The following experimental procedure was used for all runs, except for runs in air, of each of the hydrocarbon liquids used. For runs in air there was no reason to maintain an air flow to keep out undesirable gases from the drop formation chamber. The effect of the purge gas velocity present in the runs not with air was assumed to be negligible due to its magnitude, i.e. 17-22 cm/min.

1. Valves V16 and V17 Figure 13 being closed, about 200 ml of the liquid was poured into the main liquid reservoir.
2. Keeping V17 closed, V16 was opened and the liquid holding funnel was filled with the liquid.
3. The stainless steel tube holding the tip was removed from its entry point on the top plate. The tip to be used was cleaned by acetone, dried and attached to the lower end of the 1/8" stainless steel tube. The tube was then remounted to its place in the top assembly.
4. The flow of the gas to be used was started.
5. Keeping V16 open, V17 was opened allowing liquid out of the tip to remove entrained gas bubbles in the liquid lines.
6. Valve V16 was closed and after the liquid holding funnel was full of liquid, V17 was closed. The gas flow was left on for about fifteen minutes to completely purge the apparatus with

the gas to be used.

7. Valves V16 and V17 were reopened, maintaining a liquid flow rate through V16 faster than the flow rate through V17 to keep the liquid holding funnel full of liquid at all times.
8. A weighing bottle was inserted under the glass tube protruding from the drop forming chamber. The stopwatch was started and for 110-140 seconds the falling drops were caught in the weighing bottle. At the end of the measured time period, the weighing bottle was removed, the total time of sampling and the number of drops that fell into the bottle were recorded.
9. The weighing bottle with the sample was left open for a determined length of time, 3 minutes for n-octane drops and 5 minutes for n-nonane and n-decane drops, to let most of the absorbed gas escape. The weighing bottle was then closed.
10. The drop formation time was changed by changing the setting of valve V17 and steps 8 and 9 were repeated for a new sample in another weighing bottle.
11. After ten or eleven samples were obtained, the weighing bottles were weighed with the drop liquid.
12. For a run with a different tip, the tip was changed as in step 3 above, and steps 4-11 were repeated.

All parts of the drop forming assembly were thoroughly cleaned by acetone and dried before a different liquid was put into the system for a new set of runs. The apparatus was then rinsed with the liquid to be used before it was filled with it. The liquid in the saturators was also changed, after cleaning them with acetone, whenever a liquid change in the rest of the apparatus was necessary. Acetone was also

used to clean the weighing bottles after every use.

Analyses of the weighing bottle contents were made using the Varian Model 1200 Flame Ionization Chromatograph equipped with a Perkin Elmer Digital Integrator. A ten foot long 1/8" Stainless steel column packed with 10% S.E. 30 on Chromasorp P was used for separation. The oven temperatures and carrier gas (helium) flow rates to analyze the drops of different liquids were:

a. 110°C Oven temperature and 21 cc/min. He for n-octane

b. 125°C Oven temperature and 25 cc/min. He for n-nonane

c. 140°C Oven temperature and 26.5 cc/min. He for n-decane

All of the chromatographic analyses were performed using one microliter samples delivered by a 10 microliter Hamilton syringe, equipped with a Chaney adapter.

CHAPTER V

EXPERIMENTAL RESULTS AND DISCUSSION

Experimental Results

Experimental results are presented in Figures 1 through 7. Drop formation times within one to ten second range was explored in this study. Highly erratic drop weights were noticed at drop formation times of shorter than one second. At drop formation times longer than ten seconds, for most systems, the effect of drop formation time on the amount of liquid in the drop was rather small.

The data reported in this work as the amount of liquid in the drop, are not the actual drop weights. One would have had to correct for the desorbed solute gas during drop collection if the actual drop weights were to be reported. The procedures and the problems encountered to correct for this effect are discussed in the second part of this thesis. Under the conditions of the experiments reported in this part (Part I), the problems encountered in correcting the absorption column results for drop collection would have multiplied. It is reasonable to assume that the actual drop weights were higher than the measured liquid weights due to the weight of the absorbed gas.

Effect of the Surrounding Gas Atmosphere on the Liquid Content of a Forming Drop

The experimental data show that drops of a liquid hydrocarbon forming at a specified formation time from a specific tip contained smaller amounts of the liquid if surrounded by a heavier hydrocarbon gas, e.g. n-butane, than if surrounded by a lighter hydrocarbon gas, e.g. methane. Thus, for hydrocarbon-hydrocarbon systems, one could correlate the liquid weight in a drop with the vapor pressure, molecular weight, molecular diffusivity, density of the gas. The solubility of the gas in the liquid phase will also correlate the data. For ideal systems vapor pressures could be used to calculate gas solubilities in the liquid phase using Raoult's law.

Drops forming in Freon 12 had liquid contents between those drops forming in ethane and propane. Molecular diffusivities of Freon 12 (dichlorodifluoromethane) in the hydrocarbon liquids studied are lower than the molecular diffusivities of n-butane in the same liquids. The molecular weight and density of Freon 12 on the other hand are larger than the similar properties of n-butane. However, the vapor pressure of Freon 12 at the experimental temperature, 24°C, is between the vapor pressures of propane and n-butane at 24°C. This point suggests that vapor pressure might be a better correlating parameter representing the gas phase than gas density, gas molecular weight and the molecular diffusivity of the gas in the liquid. Furthermore, drops forming in air contained the most liquid. These observations suggest that the gas solubilities, or absorbed gas concentration in the forming drop could better describe the variation of drop weight with the surrounding atmosphere. Additional experimental data are necessary to establish this point.

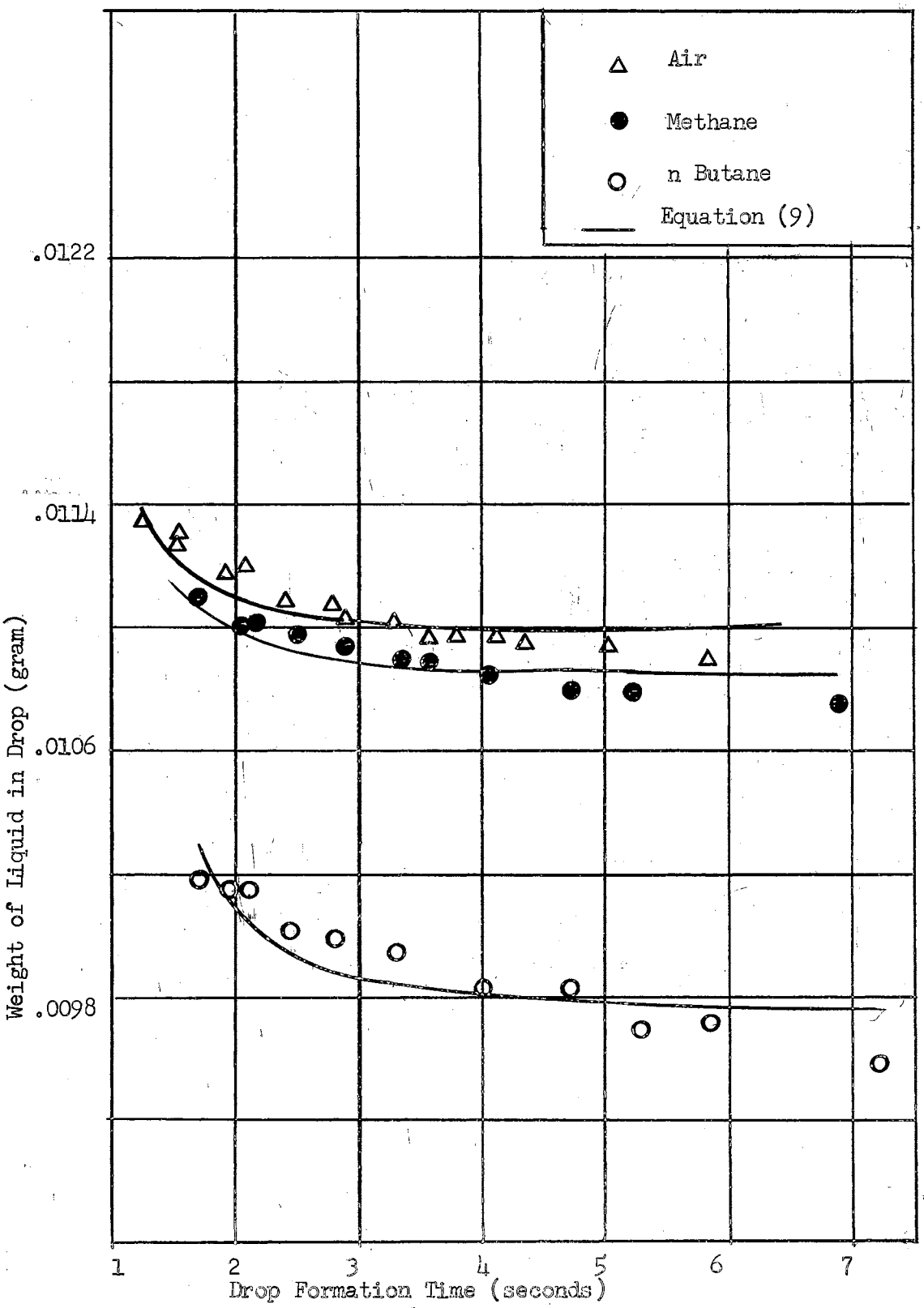

Figure 1. Data and Equation (9) Predictions for n Decane Drops Forming at Tip 2

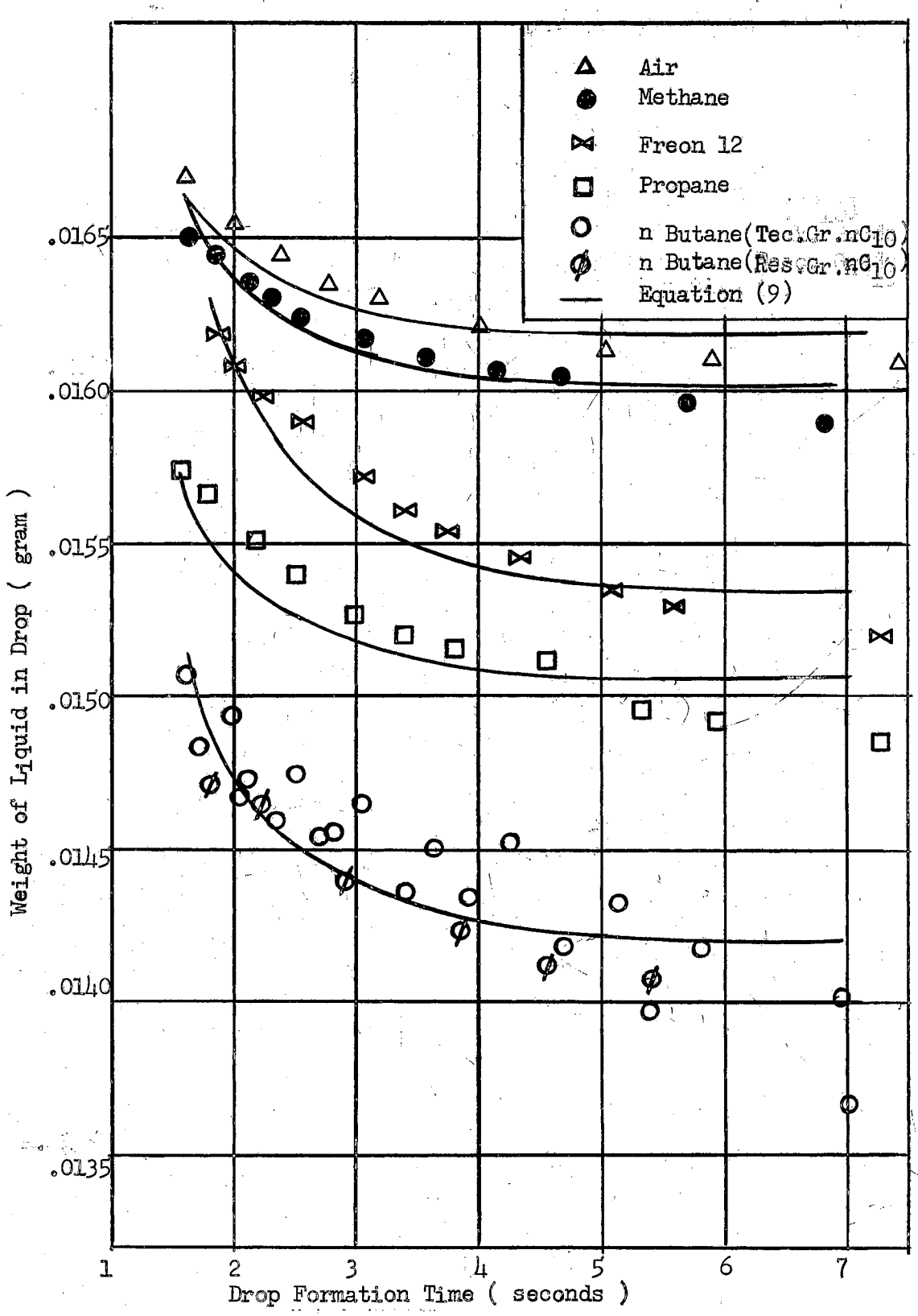

Figure 2. Data and Equation (9) Predictions for n-Decane Drops Forming at Tip 5

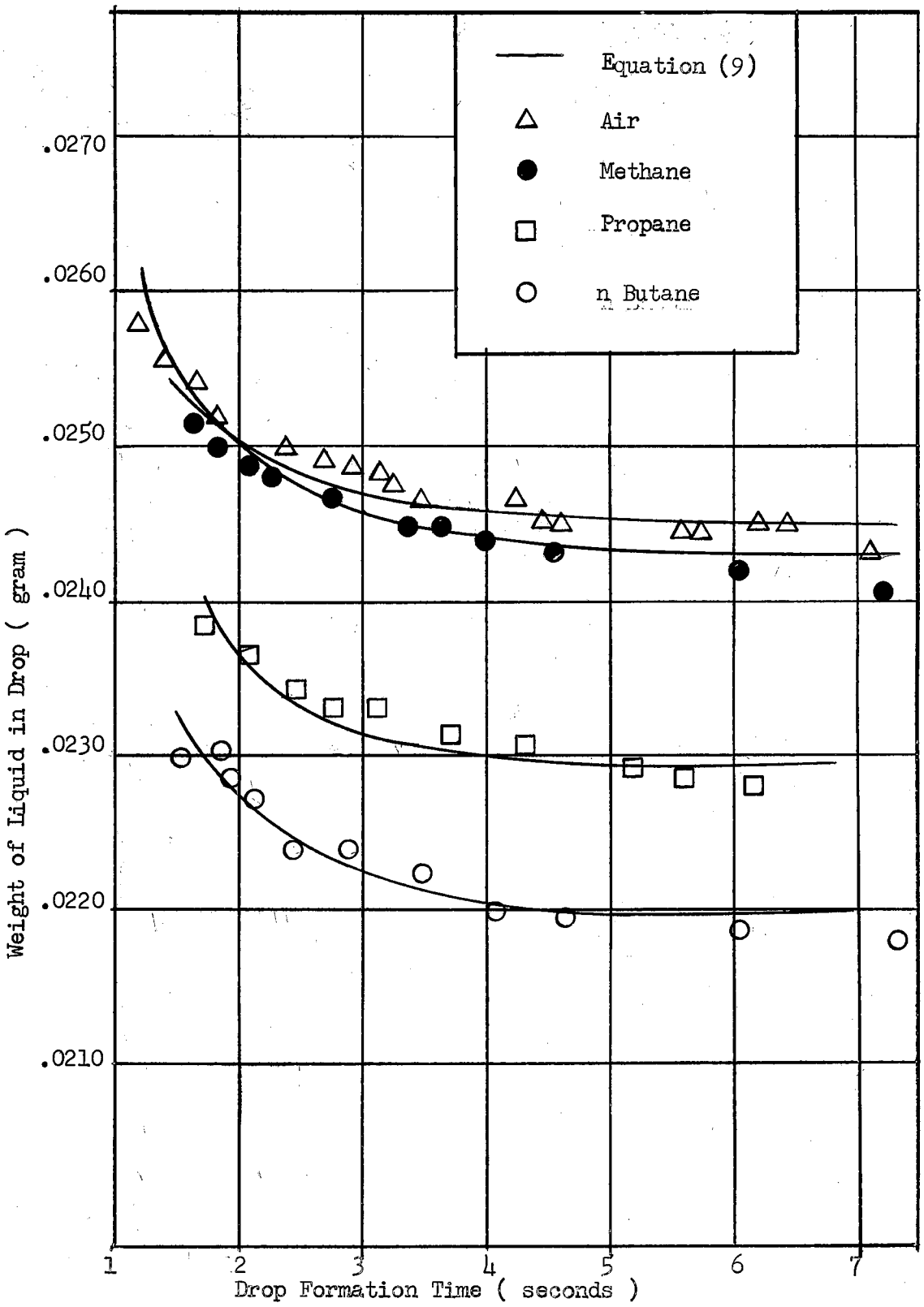

Figure 3. Data and Equation (9) Predictions for n Decane Drops Forming at Tip 7

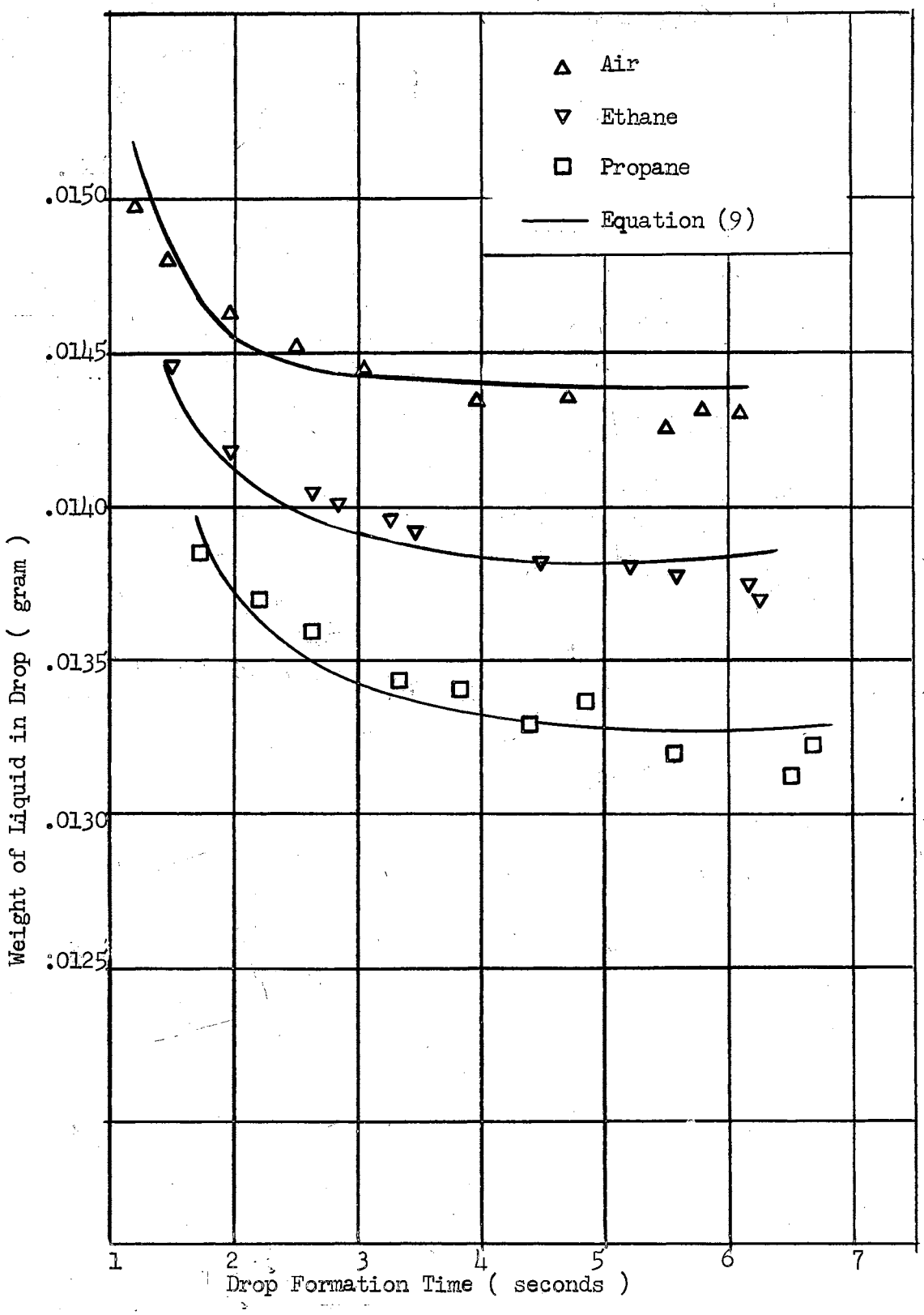

Figure 4. Data and Equation (9) Predictions for n Nonane Drops Forming at Tip 4

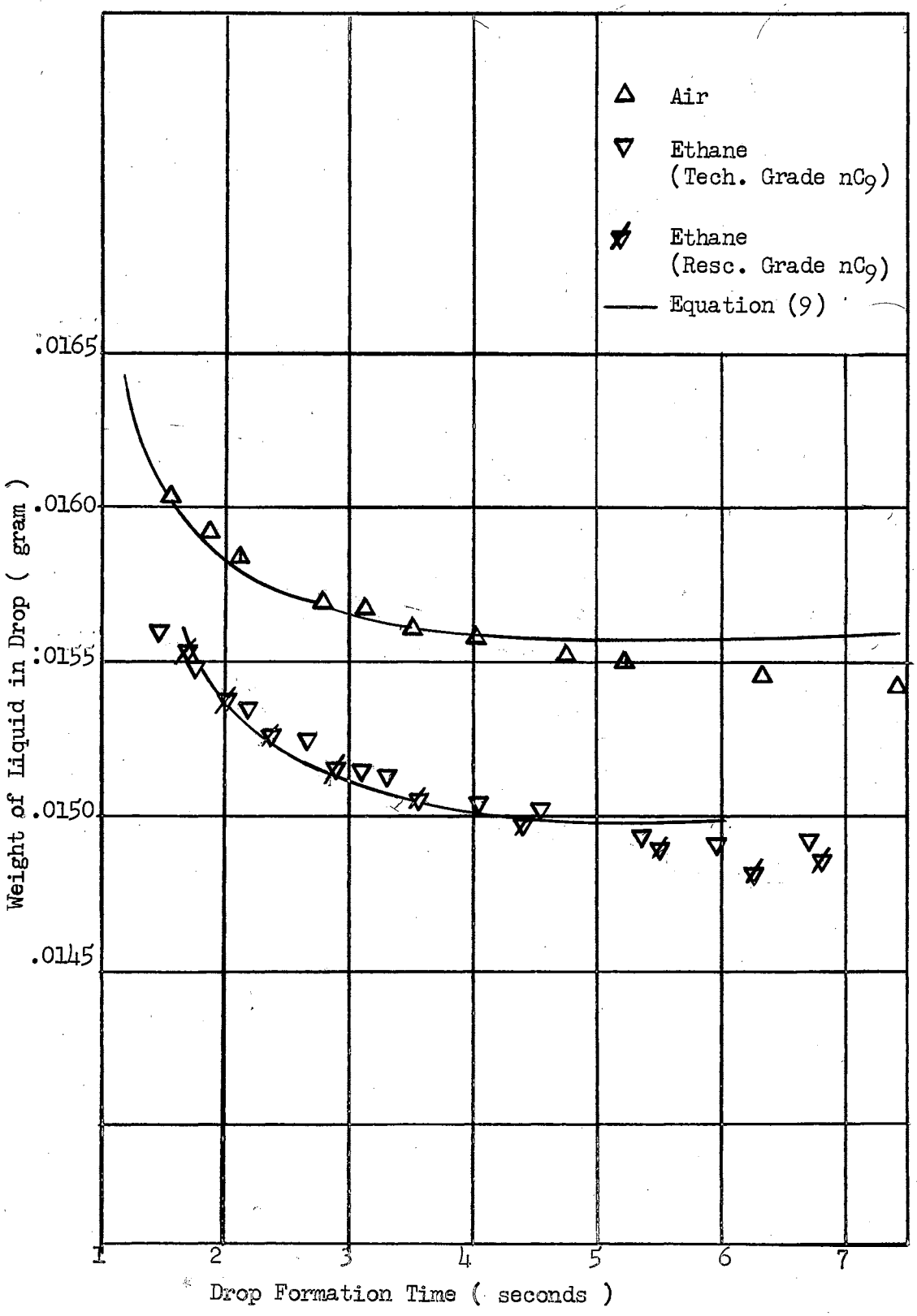

Figure 5. Data and Equation (9) Predictions for n Nonane Drops Forming at Tip 5

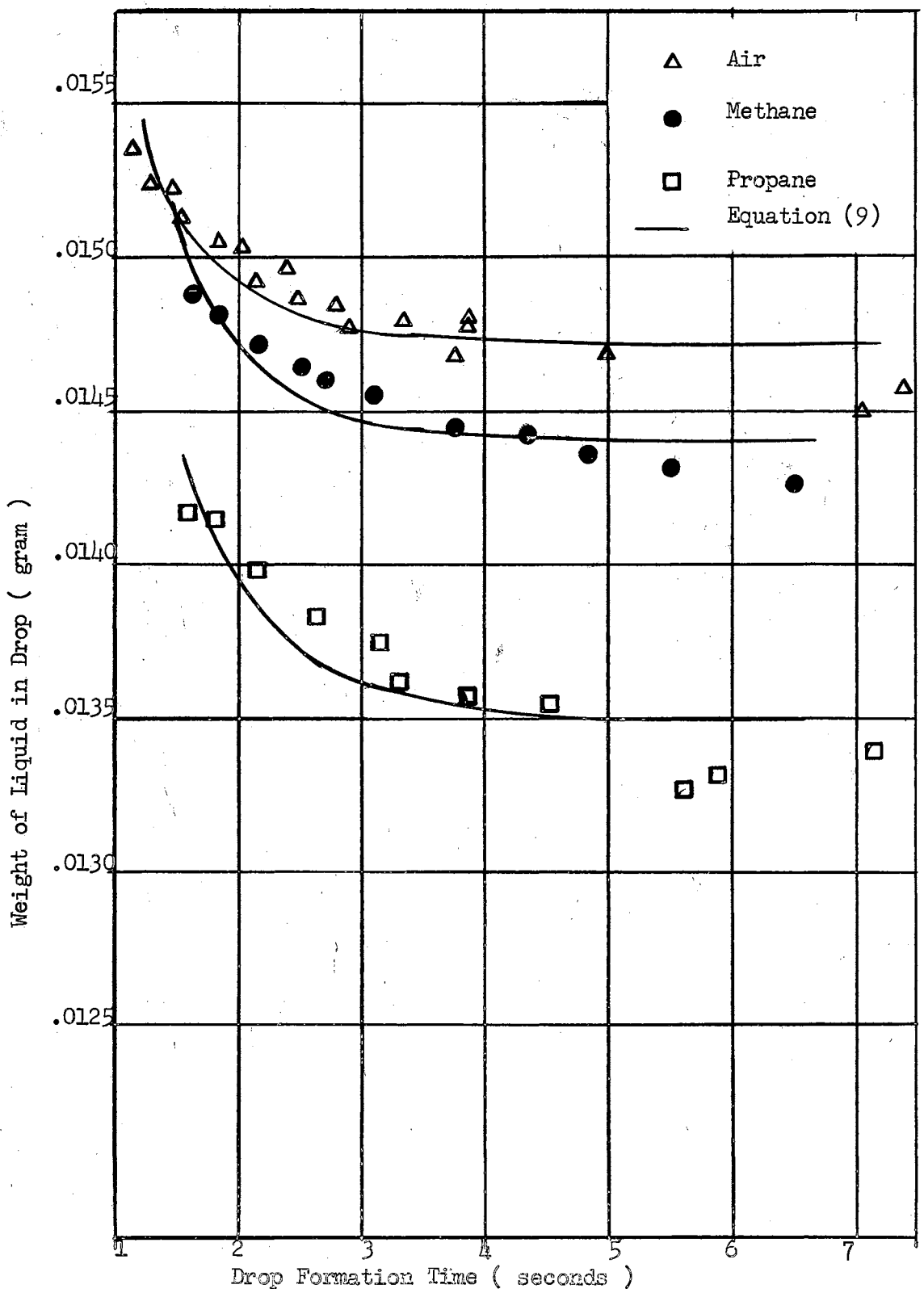

Figure 6. Data and Equation (9) Predictions for n Octane Drops Forming at Tip 5

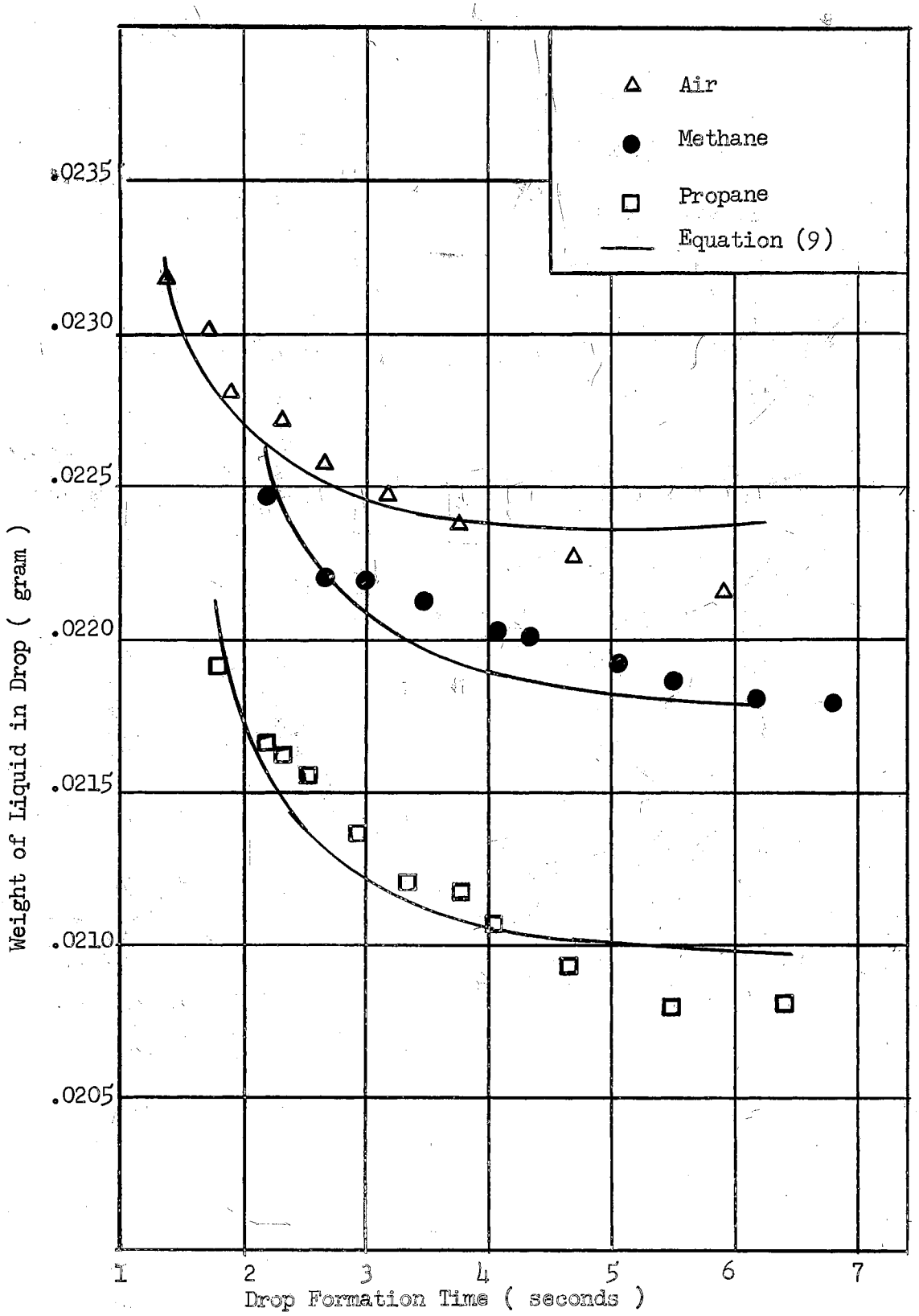

Figure 7. Data and Equation (9) Predictions for n Octane Drops Forming at Tip 7

Effect of Liquid Feed Rate on the Liquid Content of Forming Drops

Figure 8 shows the effect of liquid feed rate on the amount of liquid present in normal decane drops forming in four different gas atmospheres. For all systems the amount of liquid in the drops tends to increase with increasing liquid feed rate to the drop. This observation is explained by the Harkins and Brown (28) hypothesis that at faster formation rates, part of the liquid stream in the tip forming the drop, is forced into the drop during detachment. This observation is considered to give a general picture of the actual mechanism. Photographic studies on liquid-liquid systems show that (54) at faster liquid feed rates the length of the liquid jet extending out of the tip is increased. Due to inertial forces, at higher feed rates, the liquid jet is broken to leave some liquid in the drop. At even higher flow rates satellite drops form behind the main drop (35) with the snapping of the "neck" between the drop and the liquid jet. The presence of satellite drops is the main reason for the erratic literature data (35, 54) at high feed rates (low formation times).

Correlation of Data: Force Balance

A force balance on a forming drop can be written in the form

$$F_g - F_b - F_\sigma - F_f = 0 \qquad (7)$$

In general the forms of the F_g, F_b and F_σ terms, because of the nature of the forces involved can be represented in one way only. However, the form of F_f, which is the force due to the incoming liquid feed has varied between investigators (11, 12, 35, 46, 57, 60, 65). In Appendix A the basis of derivation of F_f and consequently the form of

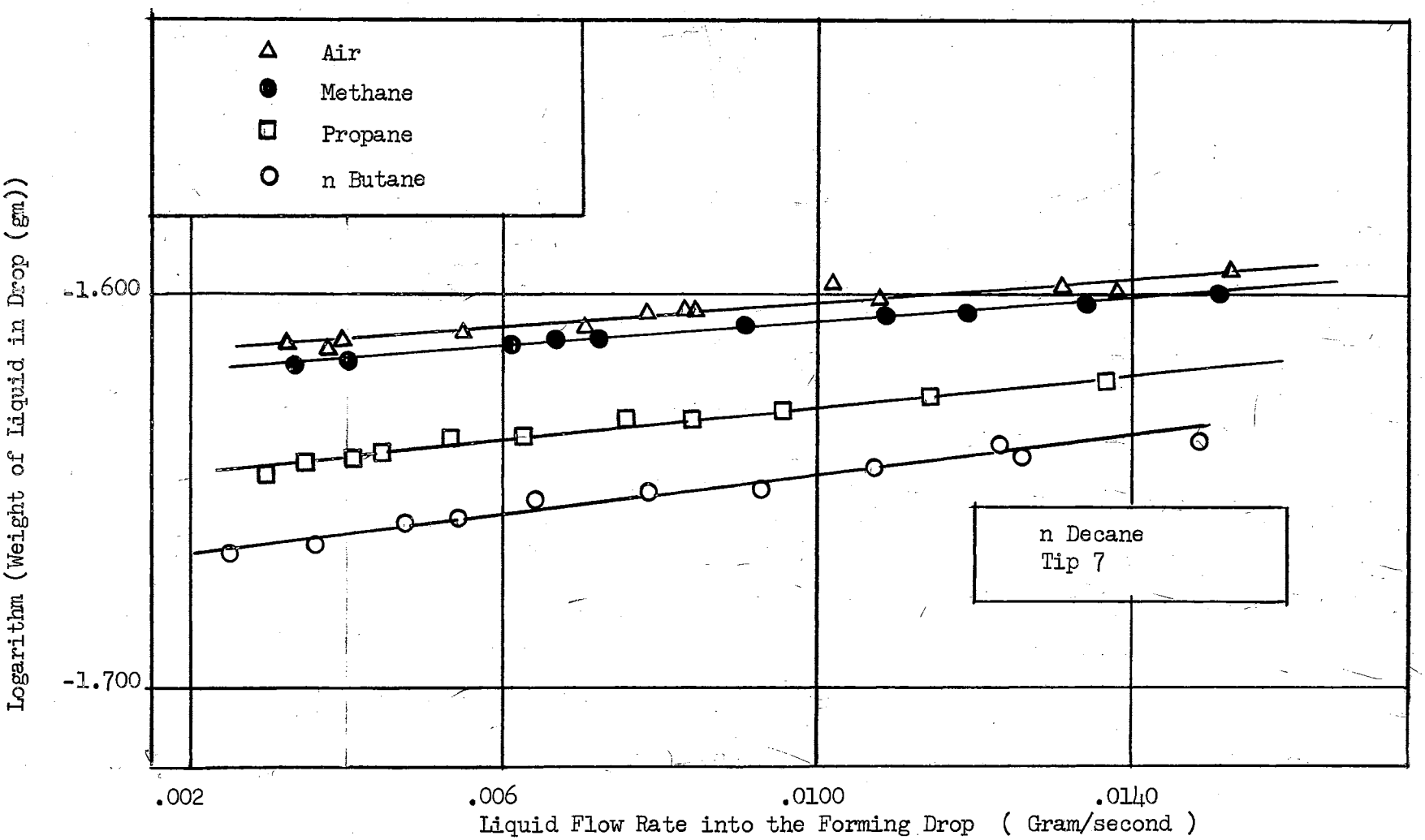

Figure 8. Effect of Liquid Flow Rate into the Forming Drop on the Final Drop Size

equation in terms of the system parameters is discussed in detail. Thus, in terms of the system parameters, Equation (7) is written as

$$M_d^2 - g\left(1 - \frac{\rho_c}{\rho_d}\right)\pi\frac{d_1^2}{4}\rho_d\theta_f^2 M_d + \psi\pi d_2\sigma\frac{d_1^2}{4}\rho_d\theta_f^2 = 0 \qquad (8)$$

Equation (8) above does not take into account the mass transfer into the drops during formation. Any model which will properly explain this condition has to take into account the proper variations in M_d, ρ_d and σ with the transfer of mass. At the present, there are no reliable correlations in the literature, nor data, to predict the variations in system parameters with mass transfer. From Figure 11 it could be calculated that the fractional saturations of the absorbed gases in the drops could not have exceeded 0.3 in the experiments performed. Variations in M_d and ρ_d for these gas concentrations could safely be neglected for all systems studied here.

Assuming 0.625 as the value of ψ in Equation (8)(from Harkins and Brown (28)), the predictions of Equation (8) were compared with the data. The comparisons showed that even though reasonably good values could be predicted for the hydrocarbon-air systems at formation times of about ten seconds, in general the predictions varied considerably from the data for shorter formation times. Equation (8) predictions seem to be almost unaffected by flow rate between ten and one second formation times, but the predicted drop weights rise sharply for drop formation times of less than one second. Literature models (11, 12, 46, 60, 65) modified for the case studied here also showed similar

trends.

The deviations of Equation (8) from data in the manner described above led the author to believe that an excess flow effect term, $F_\phi = \frac{\phi}{\theta_f}$ should be incorporated into Equation (8).

$$M_d^2 - g\left(1 - \frac{\rho_c}{\rho_d}\right)\pi \frac{d_1^2}{4} \rho_d \theta_f^2 M_d + \psi \pi d_1 \sigma \frac{d_1^2}{4} \rho_d \theta_f^2 + \frac{\phi}{\theta_f} = 0 \qquad (9)$$

This excess flow effect term seems to explain the unhindered growth ability of drops forming in a gas atmosphere as compared with the drops forming in liquid and bubbles forming in liquids, the growth of which are slowed by viscous forces.

Upon this modification, Equation (9) was fitted to the data (15, 50) and ϕ and ψ values evaluated for each tip and system studied. These curve fits were performed using two different values for the effective surface tension (F_σ term). One series of curve fits was made using the surface tension of the pure hydrocarbon liquid and another with the surface tension of the solute gas saturated hydrocarbon liquid. The hypothesis for the second type of fit was that a gas saturated drop surface exists all around the drop including the point of contact of the drop and the tip.

Mixture surface tensions were calculated using the method proposed by Deam (13), from pure component surface tensions calculated from equations of Ferguson (16) and Brock and Bird (4). The Brock and Bird equation is a corresponding states type general equation, whereas the Ferguson equation contains specific constants for different compounds. The constants for the Ferguson equation are not available in the

literature for all systems used for the present work. Mixture surface tensions calculated in this manner are given in Table I.

Table II shows the values of ϕ and ψ obtained from the curve fits. The values of ψ for the fits using a gas saturated liquid surface tensions vary from ψ of pure component surface tension in the ratio σ_m/σ (Figure 9). However, the values of ϕ from both types of curve fits are about equal for each tip and system. Thus, it appears that the effective surface tension is that of the pure liquid. This fact could be explained if one considers the forming drop as a slow liquid jet and the new area formed is near the nozzle. Thus, it is conceivable that even though most of the surface of the drop is saturated by the solute gas, the surface near the nozzle is not.

Variations in values (pure liquid surface tension) are probably due to different drop diameter to tip diameter ratios as shown by Harkins and Brown (28). Furthermore, it is conceivable that the heats of solution of the gases in the liquid phase and the small changes in the liquid properties with the absorbed gases also vary ψ. In fact the ψ values could be plotted as a function of σ_m, Figure 10, as well as a function of gas solubilities, using the tip diameter as the parameter.

In general, the ϕ values show an overall relationship to σ_m values as well, showing larger ϕ values for smaller σ_m. This trend is more definite for tips 2, 4 and 5 than for tip 7. A possible explanation for this trend could be that with decreased surface tension over most of the drop surface the expansion abilities of the drop with the incoming fluid is enhanced. Furthermore, larger ϕ values were obtained for larger tips. Thus, larger drops and smaller surface to

TABLE I

SATURATED MIXTURE SURFACE TENSIONS AT 23°C

(Deam's (13) Mixture Method)

System	$(\sigma_m)_{BB}$ (dynes/cm)	$(\sigma_m)_F$ (dynes/cm)
Methane-nDecane	23.28	23.17
Ethane -nDecane	22.26	--
Propane-nDecane	18.76	19.20
nButane-nDecane	7.00	--
Freon12-nDecane	16.77	--
Methane-nNonane	22.21	22.12
Ethane -nNonane	21.31	--
Propane-nNonane	18.08	18.27
nButane-nNonane	7.25	7.74
Freon12-nNonane	16.39	--
Methane-nOctane	21.30	--
Ethane -nOctane	20.45	--
Propane-nOctane	17.41	--
nButane-nOctane	7.31	--
Freon12-nOctane	15.84	--

$(\sigma_m)_{BB}$ - Pure σ's from Brock and Bird (4) @ T_r of mixture

$(\sigma_m)_F$ - Pure σ's from Ferguson (16) @ T_r of mixture

TABLE II

VALUES OF EQUATION (9) CONSTANTS FROM CURVE FITS

USING PURE LIQUID AND GAS SATURATED SURFACE TENSIONS

Tip	Gas	Liquid	Ψ_σ	$\Psi_{\sigma m}$	ϕ_σ	$\phi_{\sigma m}$
2	Air	nC_{10}	0.6791	0.6791	0.01201	0.01201
2	C1	nC_{10}	0.6721	0.6850	0.01517	0.009764
2	nC4	nC_{10}	0.6043	2.0478	0.03808	0.03807
4	Air	nC_9	0.6407	0.6407	0.04412	0.04412
4	C2	nC_9	0.6221	0.6575	0.06443	0.06450
4	C3	nC_9	0.5941	0.7442	0.10479	0.10474
5	Air	nC_{10}	0.6199	0.6199	0.06601	0.06601
5	C1	nC_{10}	0.6150	0.6245	0.09744	0.09744
5	C3	nC_{10}	0.5778	0.7281	0.11530	0.11527
5	F12	nC_{10}	0.5881	0.8290	0.26046	0.26042
5	nC4	nC_{10}	0.5445	1.8422	0.17013	0.16942
5	Air	nC_9	0.6229	0.6229	0.06187	0.06187
5	C2	nC_9	0.6000	0.6400	0.11081	0.11082
5	Air	nC_8	0.6237	0.6237	0.04618	0.04618
5	C3	nC_8	0.5723	0.7058	0.12942	0.12941
5	nC4	nC_8	0.6105	1.793	0.09345	0.09345
7	Air	nC_8	0.5971	0.5971	0.27151	0.27151
7	C1	nC_8	0.5835	0.5876	0.96471	0.96491
7	C3	nC_8	0.5620	0.6928	0.74866	0.74904
7	Air	nC_{10}	0.5934	0.5934	0.30031	0.30031
7	C1	nC_{10}	0.5865	0.5976	0.52086	0.52084
7	C3	nC_{10}	0.5553	0.6997	0.66517	0.66542
7	nC4	nC_{10}	0.5293	1.7960	0.58386	0.58382

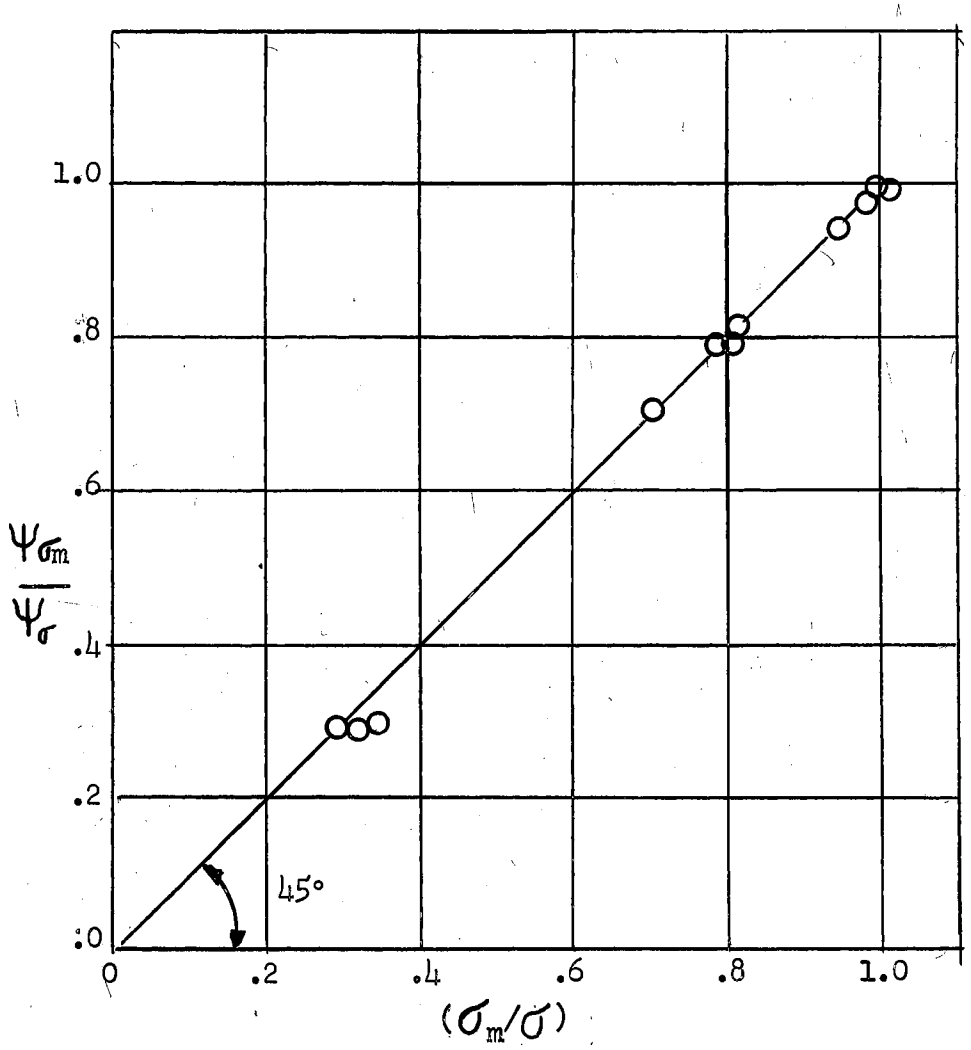

Figure 9. Relationship Between the Ratios σ_m/σ and $\Psi_{\sigma_m}/\Psi_\sigma$ from Equation (9) Curve Fits

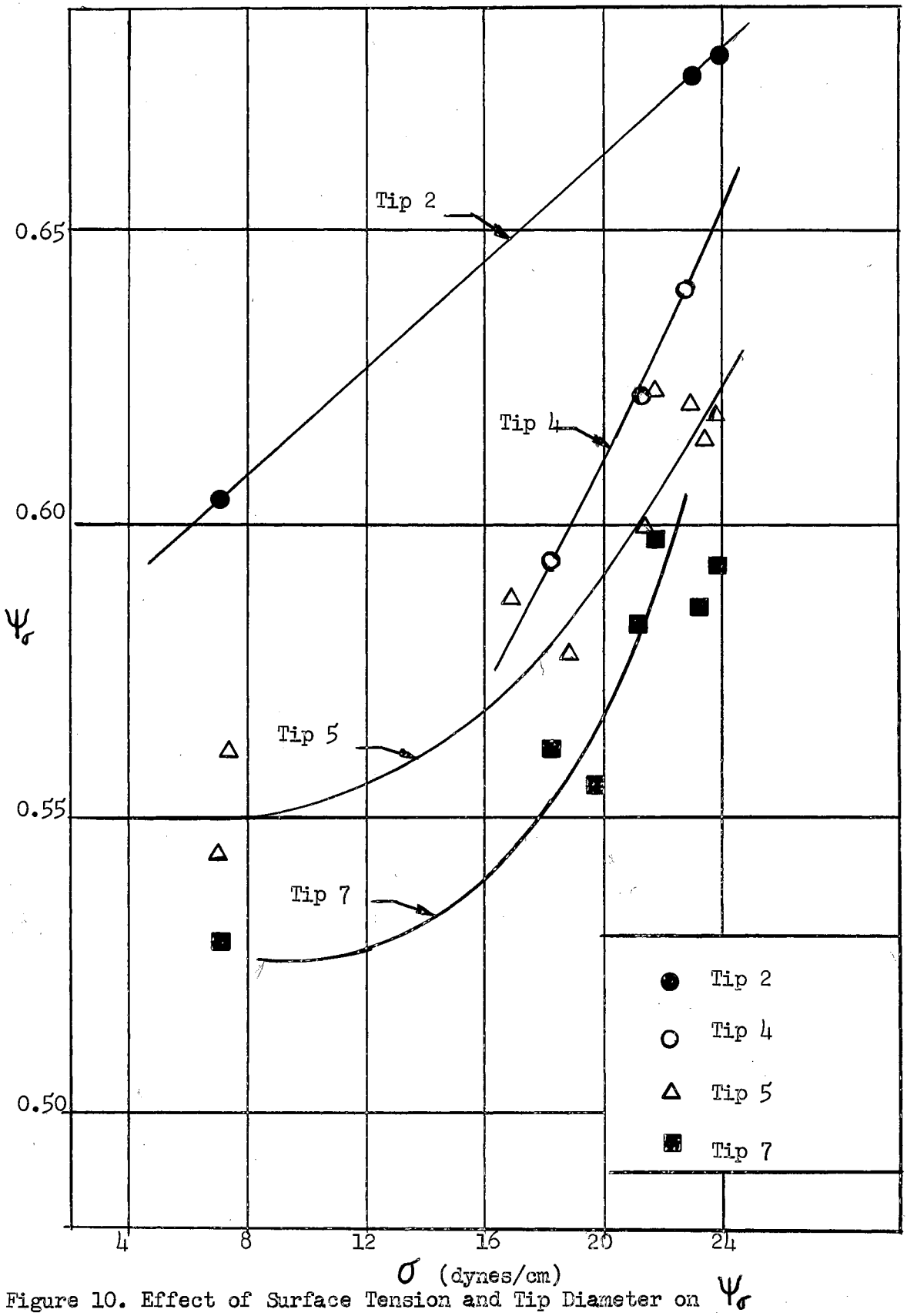

Figure 10. Effect of Surface Tension and Tip Diameter on ψ_σ

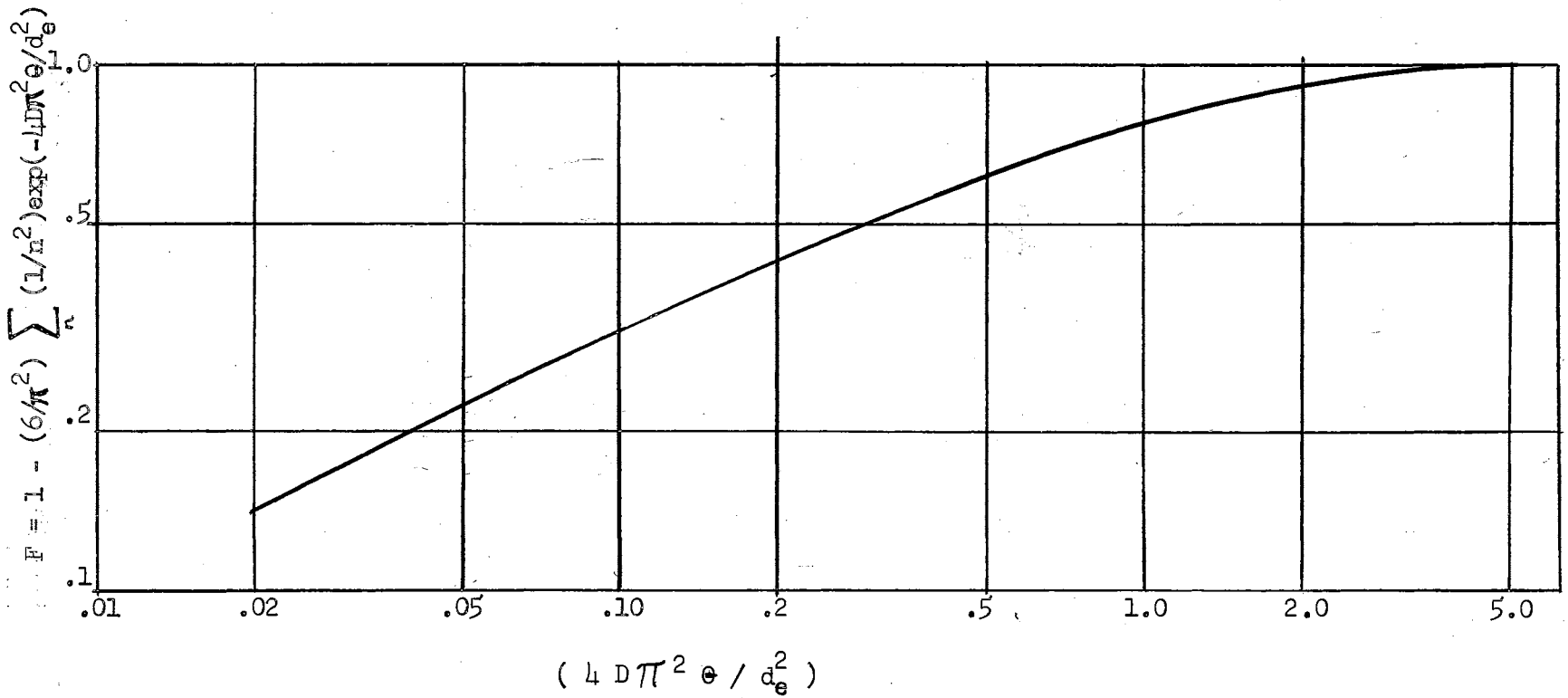

Figure 11. Fractional Saturations of Drops as a Function of the Diffusion Coefficient D, Time θ and Equivalent Drop Diameter d_e (Conduction in Spherical Drop)

volume ratios suggest that for a given surface tension, the excess flow effect is more pronounced for larger drops.

Correlation of Data: Dimensional Analysis

In an attempt to explain the data by means of a generalized equation a dimensional analysis approach was also tried. The background information on the hydrodynamics and mass transfer aspects of the drop formation machanism led the author to assume the following relationship:

$$\frac{(M_d)_{g,\theta_f}}{(M_d)_{air,}} = \text{constant} \left(\frac{d_1}{d_2}\right)^{P_2} (\theta_f)^{P_1} (d_1)^{P_3} (\mu_d)^{P_4} (\sigma)^{P_5} (\rho_d)^{P_6} (D_m)^{P_7} \quad (10)$$

Using dimensional analysis a number of dimensionless correlations were obtained from Equation (10). Forms of the dimensionless groups making up each of these dimensionless correlations were dependent upon the choice of the exponents, P_i, chosen to be determined from data. The dimensional analysis to obtain Equation (11) which was found to correlate the data is given in Appendix B. Through this analysis

$$\frac{(M_d)_{g,\theta_f}}{(M_d)_{air,}} = \text{constant} \left(\frac{d_1}{d_2}\right)^{P_1} \left(\frac{\theta_f \sigma^2 \rho_d}{\mu_d^3}\right)^{P_2} \left(\frac{d_1 \sigma \rho_d}{\mu_d^2}\right)^{P_3} \left(\frac{D_m \rho_d}{\mu_d}\right)^{P_7} \quad (11)$$

was obtained. The values of the constant and the exponents P_1, P_2, P_3 and P_7 were obtained by fitting the equation to experimental data by a nonlinear regression program (15) based on the method of

Marquardt (50). The liquid properties, σ, ρ_d and μ_d were obtained from Rossini, et. al. (63) and the liquid phase molecular diffusivities, D_m, were calculated from the Wilke-Chang (71) correlation. The values determined for the equation constant and the exponents were

$$\text{constant} = 6.787$$

$$P_1 = 0.281336$$

$$P_2 = -0.0338679$$

$$P_3 = -0.0403296$$

$$P_7 = 0.117188$$

The curve fit had an absolute average deviation of 1.3. percent with maximum deviations of 5.98 and -5.26 percent.

Weights of the liquid in the drops, $(M_d)_{g,\theta_f}$, varied about threefold over the range of the experimental conditions. However, the ratio, as presented in Equation (11) varies only from 0.85 to 1.07. This fact raises the questions about the usefulness of the fit obtained.

To obtain a more more meaningful result, the groups on the right hand side of Equation (11) were used to fit only the $(M_d)_{g,\theta_f}$ data. Calculations on this model resulted in Equation (12),

$$(M_d)_{g,\theta_f} = \text{constant} \left(\frac{d_1}{d_2}\right)^{P_1} \left(\frac{\theta_f \sigma^2 \rho_d}{\mu_d^3}\right)^{P_2} \left(\frac{d_1 v \rho_d}{\mu_d^2}\right)^{P_3} \left(\frac{D_m \rho_d}{\mu_d}\right)^{P_7} \qquad (12)$$

where constant = 0.8865

$$P_1 = 7.3697$$

$$P_2 = -0.0434488$$

$$P_3 = -0.0808437$$

$$P_7 = 0.0858291$$

Equation (12) fits the data with an absolute average error of 4.07 percent. Errors of all points range between 20 percent and -6.7 percent.

Combining the exponents of variables in Equation (12), one obtains

$$(M_d)_{g,\theta_f} = 0.8865 \frac{d_1^{7.2896} \; D_m^{0.085829} \; \mu_d^{0.29572}}{d_2^{7.36967} \; \sigma^{0.16698} \; \theta_f^{0.043449} \; \rho_d^{0.0434488}} \qquad (13)$$

Equation (12) was refitted to the data using the mixture surface tensions. The fit was not improved. The average absolute percent deviation was 4.88 and the range of errors was within 18.60 percent and -10. percent.

This result is in agreement with the mechanism postulated earlier by the force balance, in that the controlling surface tension at the drop-nozzle interface is that of the pure liquid.

CHAPTER VI

CONCLUSIONS AND RECOMMENDATIONS

The data presented in this work show that liquid drops forming from a tip at constant formation times have varying amounts of liquid in the drop depending on the gas atmosphere surrounding the drop during formation. For normal paraffinic gas-liquid systems the amount of liquid in the drop decreases with increasing solubility of the surrounding gas atmosphere, at a given drop formation time. Furthermore, data show smaller drops at longer formation times for a specific tip and gas-liquid system.

These data were correlated and analyzed in terms of a force balance on the forming drop as well as a dimensionless correlation. Two parameters contained in the force balance were evaluated from the data. One of these parameters was of the type used by Harkins and Brown (28) to account for the undetached portion of the drop liquid from the tip. The values of this parameter, evaluated from the data, are within the range of the Harkins and Brown values and correlate with the surface tension of the drop liquid saturated with the surrounding gas for each tip. The second parameter is incorporated with the excess flow term and for a given system, is a function of the tip size.

The dimensionless correlation derived to represent the data accounts for the mass transfer as well as the flow effects for all tips and systems studied.

The analysis of the data has shown that the controlling surface tension at the drop formation tip is the surface tension of the pure liquid.

Future work should include studies to determine the effect of the absorbed gas on the physical properties of the drop liquid during drop formation. An experimental procedure based on the modification of the procedures used by Constan and Calvert (7) or Groothuis and Kramers (23) could be used for this purpose.

PART II

GAS ABSORPTION BY FALLING LIQUID DROPS: HYDROCARBON SYSTEMS

CHAPTER I

INTRODUCTION

Study of gas absorption by liquid drops has not attracted nearly as much attention as the related subjects, mass transfer between gas bubbles and liquid drops in a continuous liquid phase. Single drop gas absorption studies available in the literature show that most of the data have been taken for water drops. Data on liquids other than water are scarce. Some of the available studies attempted to experimentally isolate mass transfer during different stages of drop life, i.e. formation, fall and collection, others did not.

At the present time, a rough picture of drop hydrodynamics exists. However, the volume and quality of the available data do not yet permit one to accurately relate hydrodynamics to the mass transfer phenomena. In this respect, information available from studies of related subjects could be used to serve as guidelines.

Industrial application of gas absorption by liquid drops is seen almost totally in spray equipment. Spray type contactors have some advantages over stagewise contactors. The advantages are: very low pressure drop and no packing or trays. However, spray equipment has generally been considered to be less efficient and uneconomical when compared to tray or packed columns and mechanically agitated gas-liquid (bubble) contactors. For practical applications, where multi-drop systems exist, direct application of single drop data should be made

with care.

The goals of the present study were:

1. To gain an understanding of gas absorption by liquid drops,
2. To obtain and evaluate gas absorption data for some hydrocarbon systems, and
3. To devise and study various end effect correction procedures for gas absorption by liquid drops.

For this purpose a ten foot tall absorption column was designed and constructed. Drops were collected in a drop catching unit remotely similar in design to that constructed by Garner and Kendrick (19).

The experimental results were analyzed and explained according to the theories and experimental data available in the literature. The experimental results of this study were also analyzed in terms of the different end effect correction procedures used.

This study is a first attempt to determine the gas absorption coefficients for hydrocarbon systems using a pure hydrocarbon gas, normal butane, in the gas phase. Thus, this study is also a first attempt in the use of pure highly soluble gases in gas absorption studies.

Experimentally, a problem to surmount was presented in the choice of an acceptable blanketing agent for the hydrocarbon systems used. Blanketing agents used by the earlier investigators in the drop collection stage were excluded from use here due to the low densities of the hydrocarbon liquids.

CHAPTER II

LITERATURE SURVEY

Available published studies on gas absorption by single drops are concentrated on water drops. Even though there are studies available on other liquids, these liquids seem to have been chosen randomly. In fact, some of the liquids used were industrial materials, which were mixtures of several chemically distinct compounds. This fact alone shows that a rigorous hydrodynamic understanding of the liquid drop in a gaseous atmosphere is not yet available. In the absence of a correct hydrodynamic picture, the available mass transfer results should be considered valuable in their own range, giving only a rough idea of the true picture.

A summary of the basic features of experimental studies on gas absorption by drops is given in Table III, at the end of the chapter.

Hydrodynamics of Liquid Drops in a Gas Atmosphere

Space does not permit one to include here a detailed survey of the literature available on the hydrodynamics of liquid drops in a gaseous atmosphere. However, the following points are given in an effort to summarize and evaluate the present state of the subject:

Fall velocities and drag coefficients are available for water drops at their terminal velocities. However, the results of these

studies do not show an overall consistency (17, 38). In any case, terminal velocity is seldom reached by the drops employed in absorption studies. Thus, the results of these hydrodynamic studies are not directly applicable.

For accelerating drops, velocity and/or drag coefficient data are very scarce. Data from accelerating solid spheres in liquids have been used to calculate fall times of drops in gases (17, 38). Some recent data (5) on drops of a variety of liquids in accelerated fall contradict the solid sphere data (34). This recent study shows that acceleration alone does not affect C_D as reported earlier. Liquid properties and impurities present in the liquid are reported to have a strong effect on drop hydrodynamics, and thus on C_D for accelerating drops.

Internal circulation has been studied (7, 17, 20, 21), however, the experimental methods used give large errors (7, 17, 20, 21). The equation

$$U_{ic} = \frac{U}{2\left(1+(\mu_c/\mu_d)\right)} \tag{14}$$

derived from the Hadamard-Rybczynski theory of internal circulation (27, 64) has been shown to give fair agreement with experimental data (20).

Oscillation of liquid drops has been investigated for drops suspended on a tip (7) and for drops in wind tunnels (17, 20, 21). Lamb's (47) equations for the frequency of oscillation, also (3), Equation (15), and the time dependency of the oscillation amplitude, Equation (16), are in fair agreement with published data (7, 17, 20).

$$f = \left(\frac{8 \cdot \sigma}{3 \pi M_d} \right)^{\frac{1}{2}} \tag{15}$$

$$B = B_o \exp (- 20 \theta \mu_d / (\rho_c d_e^2)) \tag{16}$$

The shapes of falling drops, with equivalent spherical diameters (d_e) between 1 and 5 mm, are of two semi-ellipsoids of revolution. These semi-ellipsoids have equal major and unequal minor axes, the flatter ellipsoid being at the front of the drop (17, 20, 62). For drops which have $1.0 < a/b < 2.1$ and $1 < E_o < 8.2$, Garner and Lane (20) proposed

$$\frac{a}{b} = 1 + 0.130 E_o \tag{17}$$

and Reinhardt (62) proposed

$$\frac{a}{b} = 1 + \frac{1.14}{9.0} E_o \tag{18}$$

Other correlations are also available (See (17) and (38) for a review). In general, the deviation between the surface area of the distorted drop and the surface area of an equivalent sphere is about 5% (21).

In conclusion, the hydrodynamic investigation of liquid drops in a gas atmosphere is not complete. One should try to gather information from studies on gas bubbles in liquids and from liquid-liquid drop systems (44) to predict the hydrodynamic behavior of liquid drops in gaseous atmospheres.

General Theory of Gas Absorption by Liquid Drops

Early researchers (14, 40, 69) assumed that gas absorption by liquid drops is a steady-state phenomenon. This assumption resulted in

$$K_L = \frac{G}{A\,\theta\,(C_g - C_L)} \tag{19}$$

for the liquid side mass transfer coefficient. Later it became evident that such an assumption was not valid for all cases and a non-steady-state approach should also be used. Such an assumption results in the well known expression

$$k_L = -\frac{V_d}{A\,\theta_a}\,\log_e\,(1 - F) \tag{20}$$

where, the fractional saturation F is defined as

$$F = \frac{C - C_o}{C^* - C_o} \tag{21}$$

For spherical drops, Equation (7) becomes,

$$k_L = -\frac{d_e}{6\,\theta_a}\,\log_e\,(1 - F) \tag{21}$$

To calculate the gas side mass transfer coefficient, one has to know the partial pressure of the dissolved gas rather than the concentration in the liquid phase.

Most liquid drop studies reported in the literature are not for perfect spheres. However, for the purpose of mass transfer coefficient calculations for falling drops, the drops are usually assumed to be spherical and the diameter of a sphere of equal volume is employed. Such an approximation ($\sim$5%) seems to be within the overall scatter of data. However, the frontal area of the drops is more active than the back area with respect to mass transfer. On this basis the error in

K_L could be magnified to about 15% (18).

For forming drops the drop surface area and volume should be corrected with respect to the formation rate. Dixon and Russel (14) experimentally determined the surface areas of forming water drops from seventeen tips. Their results showed that the ratio of the volume to the surface area of the drop is approximately constant.

The absorption time can be accurately determined for forming drops. However, for falling drops information is scarce on the velocities and drag coefficients of liquids in accelerating fall (See (17) and (38)). Fall times were calculated from Equation (38), page by some (14, 24, 25, 67), thus accounting for the effect of gravity only and neglecting the drag resistance and the buoyant force. More recently, researchers have attempted to compensate for the effects of distortion and acceleration on the velocity and drag coefficients of the drops (5, 17, 29, 62). As discussed earlier, accelerating drop hydrodynamics is not yet fully understood.

Studies of the effects of concentration level on the absorption coefficients (62), the additivity of individual phase resistances (39) and mechanism of interfacial resistance (19) are available for the general case of mass transfer and gas absorption.

Theory of Gas Absorption by Forming and Supported Drops

For absorption of carbon dioxide by forming water drops Dixon and Russel (14) postulated that

$$K_L = \frac{\text{constant } ((2/d_1) + \text{constant})}{\theta_f^{0.8}} \qquad (23)$$

In Equation (23), K_L is the overall mass transfer coefficient obtained

from Equation (19) using an arithmetic average for the gas concentration in the liquid for the formation time. They postulated that $(2/d_1)$, which is proportional to the square root of the liquid feed rate into the drop, is a measure of turbulence inside the drop.

Groothuis and Kramers (23) based their theory of sulfur dioxide absorption during the formation of hydrocarbon drops on the penetration theory. This results in

$$\frac{C - C_o}{C^* - C_o} \propto \frac{A}{V_d} \sqrt{\frac{D_m \theta_f}{\pi}} \tag{24}$$

for the liquid side coefficient.

Constan and Calvert (7) studied mass transfer to supported drops which had internal circulation and oscillation. Frossling's (18) equation for the gas side mass transfer

$$k_c = \frac{2.0\, D_V}{d_e} \left[1 + 0.276\, Re^{1/2}\, Sc^{1/3}\right] \tag{25}$$

coefficient gave results in fair agreement with the experimental overall gas side mass transfer coefficients. The data for the gas side coefficients were obtained by measuring the sublimation rates of naphthalene spheres in air currents. For the liquid side mass transfer coefficients, Constan and Calvert noted that, for a given drop and fractional saturation, the ratio of D_e to D_M is dependent on the film thickness, which in turn is a function of the internal circulation velocity in the drop. Their theory for supported drops was based on non-steady state mass transfer.

Constan and Calvert's (7) attempts to explain gas absorption by drops with controlled forced circulation through the drop were not very successful. Fresh liquid was introduced and old liquid was constantly

withdrawn from the drop. Equation (19) was used for drops with controlled forced circulation to calculate mass transfer coefficients, postulating constant drop concentration.

Hughes and Gilliland (39) extended Dixon and Russel's (14) work. They added the effect of drop oscillation on mass transfer to forming drops in addition to the effect of the internal circulation caused by fresh liquid feed. Hughes and Gilliland proposed

$$(k_L)_f \approx a'' \left(\frac{d_2}{d_1}\right)^{2(1-n)} \frac{d_e^{1-2n}}{\theta_f^{1-n}} + b'' \frac{d_e^{2m-\frac{1}{2}}}{\theta_f^{m}} \qquad (26)$$

where the first term shows the effects of internal circulation and the second term shows the effects of oscillation. From Equation (26) they derived

$$\frac{C - C_o}{C^* - C_o} = f\left[a_1' \left(\frac{d_1}{d_2}\right)^{2(1-n)} Ti_f^{n} + b_1' Ti_f^{i-m} \sqrt{\frac{g_c \sigma \rho_d d_e}{\mu_d^2}} \right] \qquad (27)$$

where n and $m \approx 0.2 - 0.4$ and a_1', b_1', a'' and b'' are constants In summary, absorption by forming drops can not be considered purely a steady-state phenomenon. A correct approach must consider the dependence of drop gas concentration on absorption and also on the rate of fresh liquid introduced into the drop. For supported drops which have been formed prior to the start of the absorption period, an unsteady-state approach should also be used.

Theory of Gas Absorption by Falling Liquid Drops

Some of the earlier workers, specifically Whitman et al. (70), Dixon and Russel (14) and Johnstone and Williams (40) used an equation

of the form of Equation (19) to evaluate mass transfer coefficients. A steady state assumption inherent in Equation (19) is not valid for absorption by falling drops. However, for Johnstone and Williams' (40) work, the use of a constant driving force could be warranted. In their work (40), the absorbed gas reacted with a reagent present in the drop liquid and lost its identity. If care is taken and an excess of reagent is present and the reaction rate is high, this absorption could be considered as steady state. Johnstone and Williams used this method for the determination of gas side coefficients.

For the liquid side mass transfer coefficients of falling liquid drops, the only correct approach is to use the unsteady state assumption as given in Equation (20).

An attempt to explain the effects of system variables on the reported mass transfer coefficients is an important task. For the gas side mass transfer coefficient, Hatta, et al. (31, 32) proposed

$$k_g = \beta U^n \tag{28}$$

where, U is the drop fall velocity, β and n are constants which were found to be 0.000097 and 0.25, respectively. This equation is based on the assumption that the gas film thickness is inversely proportional to U^n. Shabalin (66), for drops at terminal velocity, found n to be between 0.75 and 0.80. Johnstone and Williams (40) used

$$\bar{k}_g = \frac{\sqrt{D_m / d_e}}{1.5\ R\ T} \left(2\ g\ L \right)^{\frac{1}{4}} \tag{29}$$

for a spherical drop falling a distance L from rest. They also accounted for the effect of the countercurrent gas velocity by

$$\bar{k}_g = \frac{\sqrt{D_m / d_e}}{1.5\ R\ T} \cdot \frac{\left[\left(U_g + 2\ g\ L \right)^{3/2} - U_g^{3/2} \right]}{\left(2\ g\ L \right)^{\frac{1}{2}}} \tag{30}$$

where U_g is the gas velocity. Recently Plit (56) proposed a dimensionless correlation

$$Nu = 0.125 \times 10^{-8} \left(\frac{D_m}{D_v\ Pr}\right)^{-1.96} \left(\frac{\mu_c}{\mu_d}\right)^{0.5} \left(\frac{d_e^2\ \rho_d}{\sigma}\right)^{0.205} \left(\frac{U\ d_e\ \rho_d}{\mu\ g}\right)^{1.75} \left(\frac{U\ \mu_c}{\sigma}\right)^{0.15} \tag{31}$$

for absorption of ammonia by water drops of large diameter.

Liquid side mass transfer mechanisms of different systems in drops of varying sizes could be compared on equal basis in terms of the ratios of effective to molecular diffusivities, i.e. D_e/D_m. This ratio also gives an idea of the internal drop hydrodynamics. The major drawback of this method is that molecular diffusivities of gases in liquids are not well known for all systems. Himmelblau (37) recently presented molecular diffusivity data for several systems in a review article.

Effective diffusivities of gases in liquid drops could be calculated from

$$\frac{C - C_o}{C^* - C_o} = 1 - \left(6/\pi^2\right) \sum_{n=1}^{\infty} (1/n^2) \exp\left(-4\, n^2 \pi^2\, D_m\, \theta_a / d_e^2\right) \tag{32}$$

Equation (32) is for diffusion into a sphere with constant surface concentration; a condition which is satisfied by absorption of slightly soluble gases and also by absorption of pure gases. Equation (32) is analogous to the classical solution for heat conduction into a sphere of constant surface temperature. Solutions for the mass transfer case are available in the literature (8, 55).

Equation (32) is for a stagnant sphere. Departures from the stagnant sphere case are handled by substituting an effective diffusivity, D_e for D_M, where

$$D_e = D_m + D_c \tag{33}$$

At the present, an exact quantitative relationship relating the drop hydrodynamics to the liquid side mass transfer coefficient does not exist. However, some trends are evident from literature data. In general, the liquid side mass transfer coefficients are higher for hydrodynamically less stable drops. This is exhibited by higher D_e/D_M values. Internal circulation decreases the stagnant film thickness of the drops and thus increases the mass transfer rate. However, internal circulation currents tend to have a smaller effect on the mass transfer to large drops. In large drops, due to the higher degree of deformation, large volumes of liquid in the drop are bypassed by the internal circulation currents (21).

Small drops and drops of high surface tension and low viscosity liquids tend to have more hydrodynamical stability (17, 20, 21). Furthermore, as the drops age, i.e. longer absorption times, they tend to gain more stability. Oscillations and internal circulations present in the forming drop are magnified by the detachment of the drop from the tip and the snapping of the drop tail to the drop body. Periodic eddy shedding also affects oscillations (17, 20, 38). However, since these motions dissipate energy, they tend to die down with drop age. Equation (16) was proposed (47) for the decay of the

$$B = B_o \exp\left(- 20\mu_d / (\rho_c d_e^2)\right) \qquad (16)$$

amplitude of oscillations due to viscous action.

Experimental Apparatus and Methods for Gas Absorption by Liquid Drops

Two major types of experimental apparatus have been used to determine gas absorption by liquid drops; namely:

a. Absorption tubes and chambers with slow or zero gas velocity in which drops form and/or fall,

b. Wind tunnel studies used to support formed drops or to suspend detached drops during the absorption period.

Whitman et al. (69) used an apparatus which consisted of an absorption tube 60 cm. long and 6.5 cm. in diameter. The drop liquid was stored in a constant head tank. The drops formed in the absorption tube from a tip in contact with the solute gas at constant time intervals. The detached drops fell 52 cm. into the drop collection tube and were blanketed from the solute gas by a layer of kerosene in the collection tube. The solute gas was saturated with the drop liquid to prevent evaporation from drops. The absorbed gas concentration in the liquid was chemically determined. Hatta, et al. (31, 33) and Dixon and Russel (14) used apparatus basically similar to the apparatus of Whitman, et al. However, they varied the drop fall height. Guyer, et al. (24, 25) also used the same type of apparatus with fixed (24) and variable height (25) experiments for the desorption of CO_2 from CO_2 saturated water drops into gas streams.

In an effort to experimentally isolate the absorption during drop formation from absorption during fall, Johnstone and Williams (40) altered the top section of an apparatus which was similar to that used by Whitman. In this new version the drops were formed in an insoluble gas atmosphere (air) and made contact with the solute gas after they began to fall. This type of apparatus was also used by Shabalin (66), Hughes and Gilliland (39) and Rabovskii and Shinyaeva (59). Johnstone and Williams and Robovskii and Shinyaeva also varied the gas velocity in the absorption tube.

Shabalin used an absorption apparatus which had a ten meter inert gas section above an absorption tube of variable height. In the ten meter inert gas section, drops attained velocities equal or very close to their terminal velocities

Garner and his coworkers (20, 21) used a wind tunnel, constructed by Garner and Kendrick (19) for their mass transfer studies. In this equipment the drops were formed in an inert gas chamber and after detachment from the tip were held for the desired time length in the wind tunnel by a gas stream. To be able to hold the drop stationary, the gas stream had a velocity equal in magnitude and opposite in direction to the terminal velocity of the drop used for the experiment. At the end of the desired length of the absorption period, the gas flow was terminated by the introduction of the drop catching unit into the wind tunnel. The drop catching design of Garner and Kendrick (19) was also unique in that an inert gas (air) blanket was used to isolate the splashing drop from the solute gas. The amount of absorbed gas was volumetrically measured after desorption from the collected drops.

Constan and Calvert (7) also used a wind tunnel for their study of drops supported on capillaries. These drops were formed outside the absorption chamber on hypodermic capillaries and then introduced into the chamber in a shield. The shield was then removed around the tip, exposing the drop to the gas stream. At the end of the absorption period, the liquid drop which had absorbed some sulfur dioxide was dipped into a hydrogen peroxide solution. The conductivity of the solution was measured to determine the amount of sulfur dioxide absorbed by the drop. Constan and Calvert also prepared drops with constant internal circulation by suspending the drop from the tip of two

concentric tubes. Fresh liquid was forced into the drop from the central tube and liquid was withdrawn from the annulus. The amount of absorbed gas was determined volumetrically from readings on a gas syringe holding the solute gas supply. A similar set up was also used by Groothuis and Kramers (23) for the study of gas absorption by forming drops.

Comparison of Experimental Results with Theoretical Predictions: Forming and Supported Drops

Whitman, et al. (69) calculated mass transfer coefficients for forming drops by extrapolating their data for drops forming and falling in a solute gas atmosphere. The values they report for the mass transfer coefficients are lower than expected and indicate the absence of turbulence in the drop. However, their mass transfer coefficients for falling drops indicate the presence of turbulence in the drops.

Dixon and Russel's (14) data for forming drops were correlated as a function of the time of formation of the drop and the reciprocal of the internal tip diameter as shown in Equation (23). This correlation gave a fair fit to their data.

A modification of the Dixon and Russel model is the Hughes and Gilliland model for forming drops, Equations (26) and (27). Equation (27) indicates that the first term on the right hand side, which shows the effect of internal circulation, governs for large values of d_2/d_1. For small d_2/d_1 ($d_2/d_1 < 5$), the second term governs and k_L is strongly affected by $Ti_f = (\mu_d \theta_f / (\rho_d d_e^2))$.

This model agrees well with the Dixon and Russel data (14).

Groothuis and Kramers (23) attempted to correlate their fractional

saturation data for forming drops with respect to dimensionless time, i.e $(4D_M\Theta/d_e^2)^{\frac{1}{2}}$. The equivalent spherical radius, r_e, used by Groothuis and Kramers was obtained from Dixon and Russel data to be 0.061. The r_e values from Dixon and Russel data vary between 0.50 and 0.64, most of the r_e values being in the 0.58-0.64 range. The approximate value used for r_e could partially explain the deviation between the data and the correlation proposed.

Gas side mass tranfer coefficients obtained by Costan and Calvert (7) for suspended naphthalene spheres show fair agreement with the predictions of Equation (25) proposed by Frossling (18). The results show that the effect of oscillations on the external mass transfer coefficients is not pronounced for oscillation velocities less than the gas stream velocity. They also observed that this result is in agreement with the results of related heat transfer studies.

For the liquid side mass transfer coefficients of supported liquid drops Constan and Calvert used the conventional log-log $(4D_e\Theta/d_e^2)$ vs. fractional saturation, F, plot. For the propylene glycol-sulfur dioxide system, the oscillating drop data showed higher F values than the stagnant drop data, both data being higher than the curve predicted by Equation (32) for the case of molecular diffusion. For the ethylene glycol-sulfur dioxide and glycerine-sulfur dioxide systems, data showed no significant differences between the stagnant and oscillating drops. For these systems the data fell very near the curve predicted by Equation (32); in fact for $(4D_e\Theta/d_e^2) > 10^{-2}$ the majority of the data points were lower in fractional saturation than the values predicted for molecular diffusion. Since the drops were formed outside the absorption chamber, the model used is adequate. Errors in d_e and

D_M would affect the experimental and predicted $D_e\theta/r_e^2$ values equally. The reason for this very unusual behavior of data could be the fact that Constan and Calvert did not correct their dissolved gas concentrations for gas desorption from the drop liquid during removal from the absorption chamber. The data could be "corrected" for this effect aposteriori by assuming that the lowest experimental F value is equal that predicted by molecular diffusion alone. The proportionality factor thus determined could then be used for correcting other data. The scatter of Constan and Calvert data is about ± 30%.

Comparison of Experimental Results with Theoretical Predictions: Falling Drops

Whitman, et al.'s (69) absorption data show that at longer drop formation times (θ_f = 5-6 sec.) up to 52% of the absorption took place during drop formation. Thus, the overall mass transfer coefficients reported by Whitman, et al., if considered for fall only, are wrong.

Hatta, et al. (34) committed the same error as Whitman. For the liquid side mass transfer coefficients they reported D_e/D_M values of 60 to 70. They were not able to relate these high D_e values, at least in part, to the results of an earlier theoretical work (33) where they had studied the effects of internal circulation and oscillations on the mass transfer coefficients.

For the gas side mass transfer coefficient, the model proposed by Hatta, et al. (31) which reportedly fits Hatta's (32) and Shabalin's (66) data was also found to fit Johnstone and Williams' (40) data when U was taken to be the gas velocity. For the exponent Hatta reported an average value of 0.25 (0.22 - 0.28) and Shabalin 0.75 - 0.80. Johnstone

and Williams' data was found to give about 0.25. These results substantiate the hypothesis that the gas film thickness is an inverse function of the interfacial velocity as also predicted by Frossling's equation, i.e. Equation (25), (18).

Shabalin's drops were at terminal velocity and drops used by the other researchers, (32, 40) were not. The discrepancy among the values of the exponent in Equation (28) could be due to the fact that Shabalin's value could be considered to be a point value at terminal velocity and the other values are averanges for the total fall period with acceleration. The variation in the exponent values as reported by Hatta could be an indication to a relationship between the value of the exponent and the interfacial velocity. Values of β seem to be dependent on the system and also on the drop size.

Hughes and Gilliland (39) corrected their absorption results for the additional gas absorption by the liquid drops from the kerosene blanket in the drop catcher, before the drop liquid was removed for analysis. Their article (39) indicates that they believed they were the first to find that the drop liquid could pick up additional carbon dioxide from kerosene before sample removal. With this in mind they attempted to correct the data reported by Shabalin for the effect of the liquid cover. In fact, Shabalin (66) had noticed the disadvantage of a kerosene blanket and replaced the kerosene with transformer oil. His experiments showed that carbon dioxide solubility in transformer oil was negligible. However, Garner and Lane (20) showed that carbon dioxide does dissolve in drops of transformer oil in a wind tunnel, thus Shalalin's results did probably need correction.

Hughes and Gilliland were not able to explain their data in terms

of drop hydrodynamics via eddy diffusion approach. Their proposed explanation was in terms of Sherwood number. They noted that:

1. Sh $\propto$ oscillation amplitude, and
2. Stagnant film thickness in drop: 0.1 - 0.5% of drop diameter.

Thus, with drop age, according to Equation (16), the oscillation amplitude decreases, in turn increasing the amount of stagnant liquid in the drop. Their data were correlated as

$$Sh = 106\ Sc^{1/3} \exp(-20\ Ti) \qquad (34)$$

Garner and Lane (20) corrected their carbon dioxide absorption data for desorption to the inert gas blanket they employed in the drop catcher. An explanation as to how these correction factors were determined was not found in Garner's published work (20, 21). The correction factors indicate that 26 - 30% of the actual carbon dioxide absorbed by the drops in the wind tunnel was lost to the inert gas blanket.

Drops studied by Garner and Lane achieved a wide range of fractional saturations, i.e. between 0.126 and 0.935, for different systems. Their results were reported in terms of point ratios of D_e/D_m versus absorption times. The absorption time ranged up to 20 seconds, being extended by the use of the wind tunnel. The results show that for all systems the diffusivity ratio is initially low, passes through a maximum and then decreases, reaching an asymptotic value of between 1 and 2.5 at longer absorption times. The asymptotic values 1 and 2.5 are in agreement with the theoretical considerations of pure molecular diffusion and a completely circulating drop as

Predicted by Kronig and Brink (45). The authors explain the initially low values of the diffusivity ratio via the hypothesis: "The inert gas that surrounds the drop during formation has to be replaced by the CO_2 for the absorption to start. After this displacement, up to two seconds are required for the establishment of a concentration gradient between the drop surface and the inside." The maximum D_e/D_m values reported by Garner and Lane are between 9 and 83. A $(D_e/D_m)_{max} = 9$ was reported for transformer oil drops and $(D_e/D_m)_{max} = 83$ was reported for water drops. Drops of other liquids studied exhibited $(D_e/D_m)_{max}$ values between 9 and 83.

Tests on contaminated and uncontaminated kerosene drops showed that contaminated kerosene drops stopped circulating, $1 < D_e/D_m < 2$, after 2-10 seconds of absorption time, whereas uncontaminated drops showed higher mean diffusivity ratios after 10 seconds. This observation is in parallel with Buzzard's (5) observations on the drag coefficients of falling drops. These observations support the theory which states that surface active agents tend to decrease the hydrodynamic stability of liquid drops. Furthermore, Lamb's theory (47) of the decay of drop oscillations with time, Equation (16), is also substantiated by the evidence that shows a decay in diffusivity ratio with time.

Based on their measurements of drop internal circulation velocities, Garner and Lane (17) calculated internal Reynolds numbers. The data were correlated as

$$\log\left[(D_e - D_m) \times 10^{-5}\right] = \text{constant} + \log\left[(Re)_{internal}\right] \qquad (35)$$

This correlation is also in fair agreement with Constan and Calvert's data (7) on drops with constant internal circulation.

In similar experiments Garner and Lihou (21) noted that a plot of

fractional saturation versus drop size showed a maximum at d_e = .51 for the CO_2-water system. This supports the hypothesis that internal circulation in large deformed drops is less effective in increasing the mass transfer than in smaller drops.

Studies on absorption of water vapor from various gases by drops of water soluble liquids, i.e. glycols, etc., showed trends similar to other gas absorption results (20, 21). Garner and Lane (20) show lower maximum D_e/D_m values, 1.7 - 4.0, and also slower rate of dampening of hydrodynamic activity of the glycol drops than the CO_2 absorbing water drops. These lower D_e/D_m values are partially due to relatively high gas phase resistance, about 30%, in water vapor absorption. Rabovskii and Shinyaeva (59) varied the interfacial velocity between the drop and the gas by varying the gas velocity in the column, 0.4 - 3.0 m/sec. Their results for k_g and the average interfacial velocity, U_{av} were plotted according to Equation (28), and slopes varying between 0.98 and 1.80 were obtained. These values are nearer to Shabalin's (66) values than the values from other sources (32, 40). This seems reasonable since at a gas velocity of about 3.0 m/sec., the interfacial velocity is near the terminal velocity of the drops, as was the case with the drops used by Shabalin. When considered in terms of D_e/D_m, the Rabovskii and Shinyaeva data are in the range of Garner and Lane (20) data, i.e. 1.2 D_e/D_m 10. The majority of the data is near D_e/D_m = 2.5, the value predicted by Kronig and Brink (45) for fully circulating drops.

TABLE III

EXPERIMENTAL STUDIES ON MASS TRANSFER BETWEEN A LIQUID DROP AND ITS SURROUNDING ATMOSPHERE

(MAINLY GAS ABSORPTION)

REFERENCE	LIQUID	GAS	STAGE	MASS TRANSFER MECHANISM STU.	HYDRODYNAMIC MECHANISM STU.	VARIABLES STUDIED
Whitman, et.al.(69)	H_2O	CO_2	fl;(fm)	ABS; (k_L)	-	Θ_{fm};gsc
	H_2O	NH_3+Air	fl+fm	ABS; (k_g)	-	
	H_2O	Air	fl+fm	EVA; (k_g)	-	gvl
Hatta, et. al.(32)	H_2O	$NH_3 + O_2$	fl+fm	ABS; (k_g)	-	dfh;dsz ?
Hatta and Baba(34)	H_2O	CO_2	fl+fm	ABS;(k_L;F)	-	dfh;dsz
Guyer, et. al. (25)	H_2O+CO_2	Air	fl+fm	DES; (F)	-	tem;dsz; dfh;Θ_{fm}
	H_2O+CO_2	Air+ CO_2				
Guyer, et. al. (26)	H_2O+CO_2	Air+ CO_2	fl+fm	DES; (F)	-	gsc;dsz; Θ_{fm};dfh
Johnstone and Williams (40)	H_2O+H_2SO_4	NH_3+Air	fl+fm	ABS; (k_g)	-	gvl
	H_2O+NaOH	SO_2+Air				
	H_2O+NaOH+H_2O_2	H_2S+Air				
	H_2O+NaOH	HCl+Air				
	H_2O+NaOH	CO_2+Air				

TABLE III (Continued)

Johnstone and Williams (40)	H_2O	-	fl	-	shp;vel	dsz
Shabalin (66)	H_2O H_2O	NH_3+Air(?) CO_2	fl	ABS; (K_g) ABS; (K_L)	Θ_{fl}	dfh;dsz;?
Dixon&Russel (14)	H_2O	CO_2	fm;(fl+fm)	ABS; (K_L)	-	dsz;Θ_{fm}
Groothuis and Kramers (23)	H_2O nC_9 nC_{10} nC_{12} nC_{16}	SO_2	fm	ABS; (K_L)	-	dsz(?); Θ_{fm};tem
Garner and Lane (20)	H_2O Dekalin 4 Kerosenes Mentor 28 Transformer Oil	CO_2+Air	fl(**)	ABS;(D_e/D_m)	icv;osf;shp	tem;dsz;abt
	Glycerol Propylene Glycol Methanol Amine Ethanol Amine Ethylene Glycol	Air+H_2O	fl(*),(**)	ABS;(D_e/D_m)	icv;osf;shp	tem;dsz;abt
Plit (56)	H_2O	NH_3+Air(?)	fl(?); ?	ABS; (K_g)	?	?

TABLE III (Continued)

Garner and Lihou (21)	Diol Diol+5%IBA Diol+10%IBA Diol+20%IBA Diol+40%IBA Diol+60%IBA Diol+80%IBA Isobutanol(IBA) 98%Glycerol 78%Glycerol Tetrabro'meth'n nC_7 iC_8 H_2O	CO_2; CO_2+Air	fl (**)	ABS; $(F;D\theta/d_e^2)$	shp;vel; icl	abt;dsz; gsc
Rabovskii and Shinyaeva(59)	Diethylene-Glycol	N_2+H_2O O_2+H_2O $C_2H_2+H_2O$ CO_2+H_2O $C_2H_2Cl_2+H_2O$	fl(**)	ABS;(K_g)	-	gvl
Constan and Calvert (7)	Glycerine PropyleneGlycol EthyleneGlycol	SO_2	fm	ABS;$(D_m\theta/d_e^2)$	osa;osf;icv	gvl;dsz;θ_{fm}
	Naphthalene	Air	fm(**)	SUB;(K_g)	Osa;osf	gvl;dsz
Makino and Takashima (49)	H_2O H_2O+10%KI	I_2+Air	fl;cl	ABS;(K_g)	acc;	θ_{fm};dsz; gvl;dfh

(*) - Water vapor absorbed by the liquid drop
(**)- Experiments performed in a wind tunnel by suspending the drop in the middle of the gas flow

TABLE III (Contined)

List of Abbreviations

Column 4: STAGE

cl - drop collection stage
fl - drop fall stage
fm - drop formation stage
( ) - area of study was of minor interest in this work

Column 5: MASS TRANSFER MECHANISM(S) STUDIED

ABS - gas absorption by liquid drops
DES - gas desorption from liquid drops
EVA - evaporation of drop liquid
SUB - sublimation from solid sphere

Column 6: HYDRODYNAMIC MECHANISM(S) STUDIED

acc - acceleration effect on mass transfer
icl - internal circulation (presence/absence)
icv - internal circulation velocity
osa - drop oscillation amplitude
osc - drop oscillations (presence/absence)
osf - drop oscillation frequencies
shp - drop shapes
vel - drop fall velocities

Column 7: VARIABLES STUDIED

abt - absorption time (wind tunnel experiments)
dfh - height of fall of drops
dsz - drop size
gsc - solute concentration in gas phase
gyl - gas velocity
tem - system temperature
θ_{fm} - drop formation time

CHAPTER III

EXPERIMENTAL APPARATUS AND MATERIALS

A sketch of the apparatus used for the study of gas absorption by falling liquid drops is given in Figure 12.

Absorption Column

Main Body of the Absorption Column

The main body of the absorption column was made of 3½ inch I.D. Lucite tubing. The column was made of five, two-foot sections. Each piece had ½ inch thick flanges, eight inches in diameter, at both ends. These pieces were bolted together at the flanges and sealed with O-ring seals to form the column. Two, three, four and five of these pieces were used for runs at different fall heights.

All of the column sections had truncated circle cross sections. A truncated circle shape was chosen over the more conventional circular shape in an effort to offset the disadvantages of a circular column in case of a probable future photographic study. A circular column gives a deformed drop image. For photographic studies a rectangular column could have been used, but such a column is harder and more expensive to construct.

Six gas sampling ports, designated as GP in Figure 12, were located at different parts of the column to obtain gas samples for the gas phase concentration determinations. Four of these gas sampling

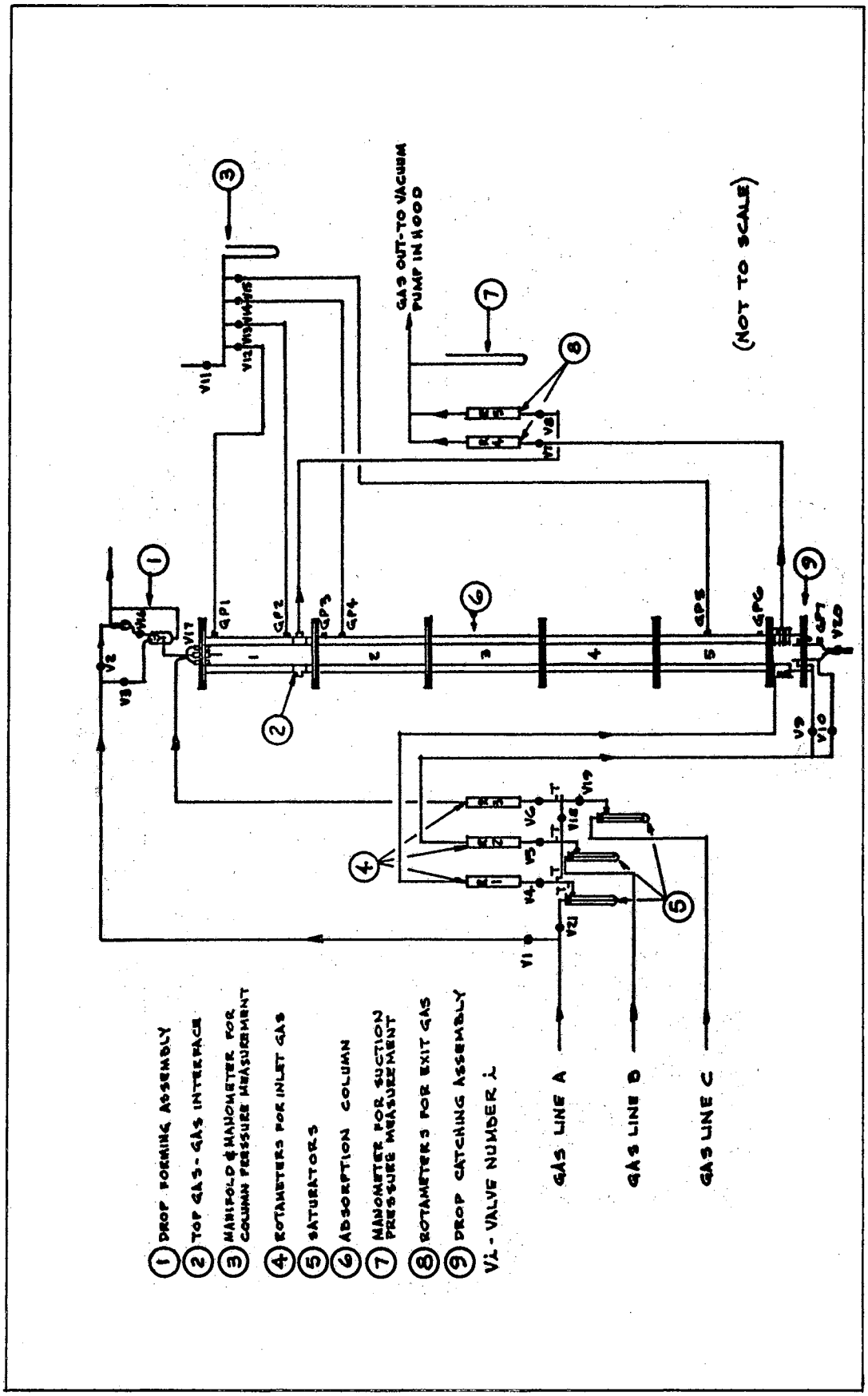

Figure 12. Experimental Apparatus

ports were connected to a manometer to measure the pressure in the column.

The upper suction ring, located in the lower part of section 1 of the column, was also constructed of Lucite and consisted of two rows of holes drilled on 1½ inch long 2 inch I.D. Lucite tubing. The suction ring was closed at both ends by 1½ inch I.D. Lucite baffles. Gas coming out of the upper suction ring was carried away in 3/8 inch O.D. copper tubing, passed through rotameter R5 and discharged into the hood from the vacuum pump. The center of the upper suction ring was 2-3/8 inches above the lower face of column section 1.

Drop Forming Assembly

Figure 13 shows the drop forming assembly located at the top of the column. A glass vessel of 200 ml. volume was used as the main liquid reservoir (MLR). MLR was connected to the constant liquid head reservoir (CLHR) by ¼ inch Tygon, copper and glass tubing. The glass tubing was an extension of the CLHR body, copper tubing was used to connect valve V16 and from the valve to the MLR, Tygon tubing was used. Valve V16 was a 20 turn, 1/8 inch Ideal needle valve with a bronze body and a 18-8 stainless steel needle. The orifice opening of the valve was 1/16 inch in diameter. Valve V16 was used to regulate the liquid flow from the MLR to the CLHR.

The shell of the constant liquid head reservoir was made of 60 mm. O.D. glass tubing and it was 14.5 cm. long from base to the top. The liquid holding funnel (LHF), which was in the CLHR, was also made of glass. It was 3.5 cm. long from base to tip and had a 3.5 cm. diameter at the base. Liquid coming from the MLR through valve V16 entered the

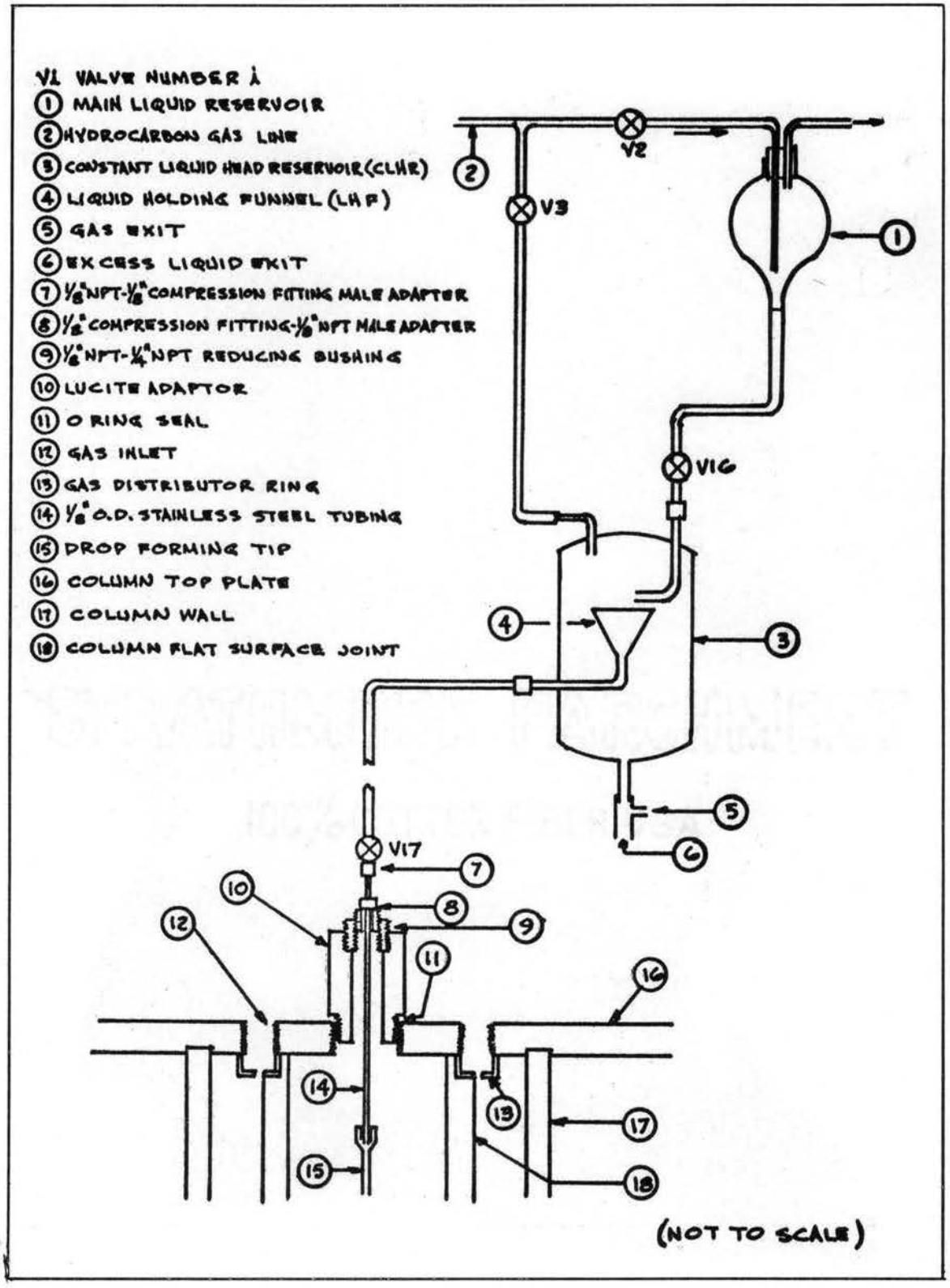

Figure 13. Drop Forming Assembly

CLHR from the L-shaped glass tubing at the upper right hand corner and dripped into LHF.

During experimental runs, the liquid holding funnel was kept full by maintaining a faster slow rate into it than the rate of formation of the drops at the tip. The excess liquid which spilled from the LHF was collected in a 200 ml. volumetric flask placed under the bottom CLHR exit.

Liquid from the liquid holding funnel passed through the ¼ inch copper tubing connecting the CLHR to V17, which regulated the liquid flow rate to the drop forming tip. Valve V17 was exactly of the same type as V16. However, a vernier scale was attached to the valve stem of V17, to enable an easier resetting of the valve at the desired drop forming rate. A 12.2 cm. long 1/8 inch O.D. 1/16 inch I.D. stainless steel tube was attached, with a compression fitting, to the exit end of V17. This stainless steel tube was attached to the top center of the absorption column via a 1/8 inch NPT male adapter and a Lucite adapter. The lower end of the stainless steel tube was 1-5/8 inches below the bottom face of the top plate. The vertical distance between the lower end of the stainless steel tube and the top of the LHF was 22-1/8 inches. The stainless steel tube had a tapered lower end made to fit the standard luer hubs of the drop forming tips. The lower end of the tips were 3 inches below the bottom face of the top plate.

The Lucite adapter, connecting the drop forming assembly with the top plate of the absorption column, was attached to the column top plate with a threaded joint and sealed with two rubber O-rings.

A Lucite gas distributing ring was attached to the lower face of the column top plate around the 1/8 inch stainless steel tube entrance.

This gas distributing ring was used to introduce nitrogen to the top section of the column as a blanket gas for the absorption runs. For the cup correction factor runs, some of the hydrocarbon gas entering the column was introduced through the distributing ring.

Drop Catching Assembly

Figure 14 shows a sketch of the drop catching assembly attached to the bottom end of the absorption column main body. The drop catching assembly was made of two parts. The upper section was used for the entrance of the hydrocarbon gas and the lower blanket gas, i.e. Freon 12, and also for the exit of these two gases by suction. This upper section was made of 3½ inch I.D. Lucite tubing (circular cross section) and was flanged to the lower end of column section 5. The interior partitions of this section, as seen in Figure 14, were also made of Lucite. The second part of the drop catching assembly was really the part that caught the drops and was mainly an open end (top) 9 cm. long 50 mm. O.D. glass tubing. At the lower end of the drop catching tube were two ground glass ball-socket joints and a rubber septum socket used as a gas sampling port, i.e. GP7. The ground glass ball joint on the side of the drop catching tube was used for the introduction of Freon 12 when a fast Freon 12 purge of the drop catcher was needed. The ball joint at the bottom of the drop catching tube was used to draw the liquid sample out. In order not to disturb the gas profile in the column, while the liquid sample was being drawn out, V20, a Teflon stopcock, with a 3 mm. bore, was attached to the sample exit of the drop catching tube by means of a ground glass socket matching the ground glass ball joint on the drop catching tube. To the other end

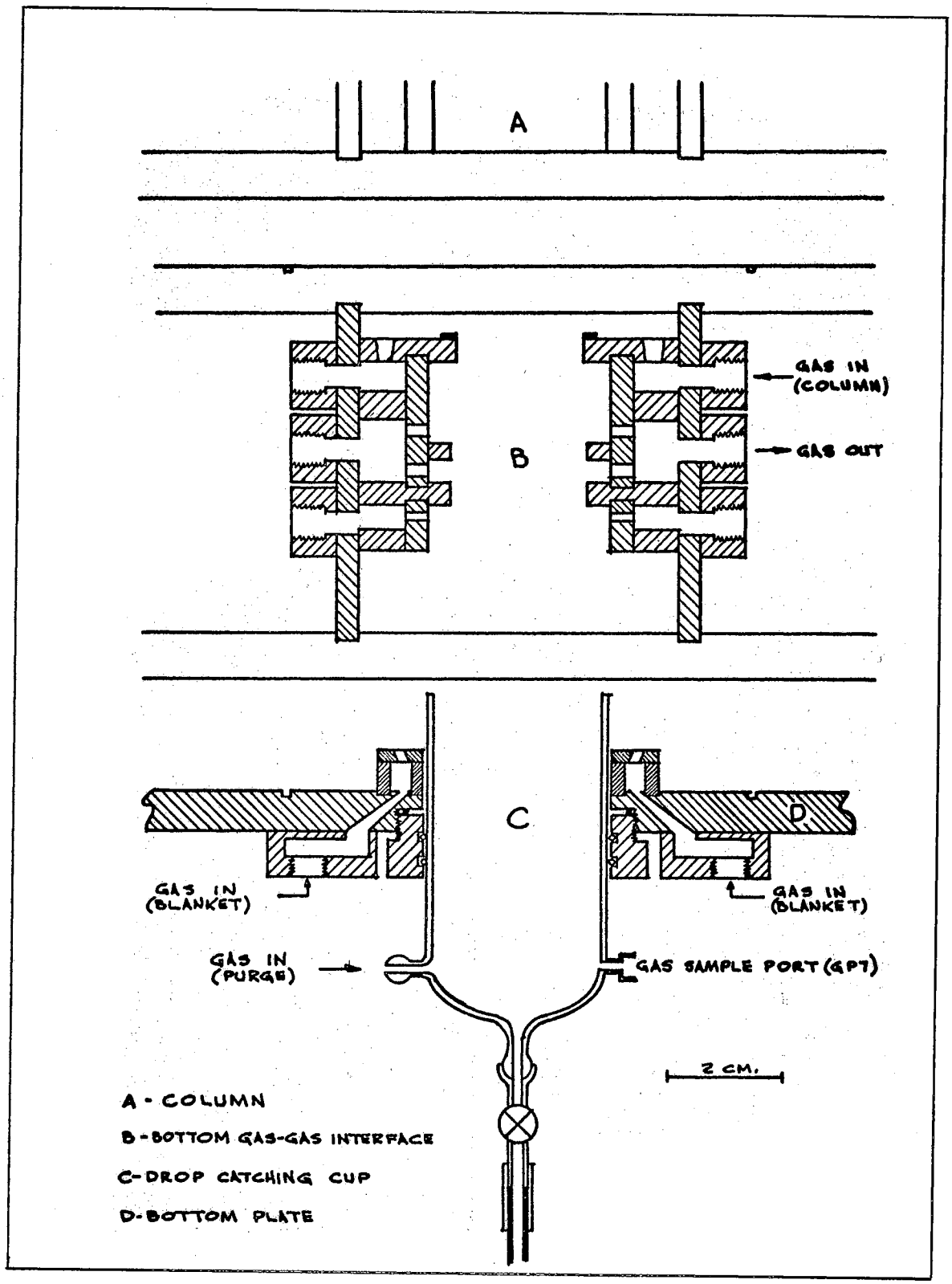

Figure 14. Drop Catching Assembly

of the stopcock a 7.6 cm. long piece of ¼ inch stainless steel tube was attached. Tygon ends of the sample vials were connected to the lower end of this stainless steel tube during sample removal.

The drop catching tube was attached to a Lucite adapter which fitted tightly around the glass tube. This connection was sealed with two O-rings. The Lucite adapter was attached to the bottom plate of the absorption column, which was attached to the bottom of the upper section of the drop catching assembly via a threaded joint. An O-ring sealed the threaded joint between the Lucite adapter and the bottom plate of the absorption column. The open end of the drop catching tube extended 1.6 cm. into the upper part of the drop catching assembly and was surrounded by a gas distributor ring. This gas distributor ring was made of Lucite and was attached to the absorption column bottom plate. The lower blanket gas, i.e. Freon 12, was introduced into the drop catching assembly from this distributor ring.

Auxiliary Equipment

The following equipment was also used with the absorption equipment:

1. Drop Forming Tips: Seven different tips were available, although not all of these seven tips were used for each liquid. Specifications of all of these seven tips are given below:

Drop Forming Tip Dimensions

Tip No.	Gage	O.D.(mm)	I.D.(mm)
T1	18	1.24	0.84
T2	14	2.10	1.60
T3	12	2.76	2.16
T4	11	3.05	2.38
T5	10	3.40	2.68
T6	**	4.07	3.20
T7	**	5.38	4.53

All of the tips were made of stainless steel, were 4 cm. long and had 90° ends. Tips T1 through T5 were commercially available hypodermic needles. Tip T1 was made from a Yale 18 gage standard tapered end hypodermic needle by carefully filing the long needle to the desired length and then polishing it with a very fine emory cloth to a smooth finish. Tips T2 through T5 were Hamilton hypodermic needles with 90° ends. Tips T6 and T7 were manufactured in the O.S.U. Research Apparatus Development Laboratory from stainless steel tubing and mounted on standard luer hubs.

2. Rotameters: All of the rotameters used for gas flow measurements were Matheson 600 series rotameters of the following kinds:

Rotameter No.	Matheson No.
R1	603
R2	602
R3	603
R4	603
R5	604

Valves V4 and V6 were fine needle valves that came attached to rotameters R1 and R3, respectively. Valve V5 was an Ideal needle valve exactly similar to V16 described above. Valves V7 and V8 were 1/4 inch stainless steel needle valves. These valves were not fine metering valves.

3. Saturators: The saturators were used to saturate the column gases with the liquid under study. They were 60 cc. liquid holding capacity side-arm Pyrex test tubes. These test tubes were closed by Neoprene stoppers at the top, through which an 8 mm. O.D. glass tube extended almost to the bottom of the test tube. Each saturator was about half filled with liquid. Three saturators in series were used for all gases entering the column. For the hydrocarbon gas, however, a liquid trap was connected in series, after the saturators and before the rotameter valve, to knock out the entrained liquid. Each set of three saturators were connected to each other by heavy wall ¼ inch Tygon tubing.

   Glass T's, equipped with rubber septa were connected to the gas lines just before the rotameter valves to obtain gas samples.

4. Manometer Manifold for Column Pressure Measurement: A water-filled U-tube manometer was used to measure the column pressure at four of the gas sampling ports, i.e. GP1, GP2, GP4 and GP5. Valves V12 - V15, used for the isolation of each pressure tap, were 1/8 inch spring loaded valves. Valve V11 was a ¼ inch stainless steel valve used to equalize the pressure in the manifold when needed.

5. Vacuum Pump: A Welch Model 1402 Dua Seal Vacuum Pump was used to draw the gases out of the absorption column. The vacuum pump was placed in the hood to enable a safe exhaust of the column gases. A mercury-filled U-tube manometer was connected between the exit gas rotameters R4 and R5 and the vacuum pump to measure the suction generated by the pump.

6. Other Auxiliary Equipment:

   a. Valve V1 was a 1/8 inch valve used to turn the hydrocarbon gas flow on to the drop forming assembly for the correction runs to saturate the liquid with the gas.

   b. Valves V2 and V3 were 1/8 inch valves, used to regulate the flow of the hydrocarbon gas to the main liquid reservoir and to the constant liquid head reservoir during correction factor runs.

   c. Valves V9 and V10 were ¼ inch valves used to divert the Freon 12 flow directly to the drop catching tube entrance from its usual distributor ring entrance.

7. Gas Transfer Lines: Gas transfer lines were mostly of ¼ inch copper tubing with flared fittings. Whenever flexibility was needed in the lines, ¼ inch I.D. Tygon tubing was used. The hydrocarbon gas line to the drop catching assembly was mostly of Tygon tubing.

Sampling Equipment

Drop Sample Containers

Drop samples were transferred from the drop catching tube into small (2.5 ml.) glass vials by a 5.5 cm. long piece of Tygon tubing

fitted to their open ends. The vial-Tygon tubing connections were sealed with an epoxy glue.

Syringes

Hamilton Series 1000 gas tight syringes were used to obtain gas samples from the absorption column for chromatographic analysis. Two of these syringes were of 2.5 ml. volume and one was of 1 ml. volume. Twenty-two gage 2.5 inch long standard tapered tip Trylon hypodermic needles were used with the gas tight syringes.

A 10 μl Hamilton syringe with a Chaney adapter attachment and a fixed needle was used for taking liquid samples from the vials for chromatographic analysis.

Analytical Equipment

Gas chromatographs were used for both the liquid and gas analyses necessary for this work. For analysis of the column gases to determine the column gas profile, a F&M Model 500, thermal conductivity type gas chromatograph was used. A 7 ft., $\frac{1}{4}$ inch column, packed with 50-80 mesh Poropak Q was used with this chromatograph.

For the analysis of the liquid drops a Varian Model 1200 Flame Ionization gas chromatograph equipped with a Varian backflush valve was used. The column in the Varian 1200 was a seven ft. long, 1/8 inch diameter column packed with 100-120 mesh Poropak Q.

Both chromatographs were equipped with Honeywell strip chart recorders, Perkin Elmer Model D2 Digital Integrators and Kienzle digital printers.

Experimental Materials

All hydrocarbons, liquid and gas, used for the experiments were products of Phillips Petroleum Company, Bartlesville, Oklahoma. The liquid hydrocarbons used were normal-octane, normal-nonane and normal-decane; all were technical grade. Technical grade normal-butane was used as the hydrocarbon gas. Water washed nitrogen was used as the blanket gas in the drop formation area and commercial grade Freon 12 was used as the blanket gas in the drop catching assembly.

Helium was used as the carrier gas for both chromatographs. For the flame ionization chromatograph (Varian 1200) hydrogen and compressed air were used to obtain the hydrogen flame at the detector.

CHAPTER IV

EXPERIMENTAL PROCEDURE

Five different types of experimental runs were made for gas absorption measurements by liquid drops. The differences between these runs mainly were the types of gases that occupied different sections of the column. Table IV shows the gases that occupied different sections of the column for each type of run, as well as the purpose of the run.

Details on the operating states of the different components of the experimental apparatus for different types of experimental apparatus are given in Table V. Table V is based on the sketch of experimental apparatus in Figure 12. Information in Table V on the operating states of V10, V20 and V12 through V15 may need more explanation. Valve V10 was used for a fast purge of the drop collection chamber whenever necessary and was opened for this purpose between runs. While the drops were falling, valve V10 was always kept closed. Valve V20 was also opened to facilitate a fast purge of the drop collection chamber. Furthermore, V20 was also used to control transfer of the drop liquid collected in the drop collection chamber to the sample vial. Thus, V20 was closed for part of the run time, i.e. sampling period, and open for the rest, i.e. transfer period.

Spring loaded valves V12-V15 were used to check the column pressure. Thus they were intermittently opened and closed. Since there was little pressure deviation along the column, usually the

TABLE IV

EXPERIMENTAL RUN TYPES (CLASSIFIED ON THE BASIS OF THE GASES OCCUPYING COLUMN SECTIONS)

Col'n Sec'tn / Run Type	Formation	Fall	Collection	Purpose of Run
A	N_2	HC	F12	To determine the amount of solute gas absorbed by falling drops--not corrected for desorption during collection.
B*	HC	HC	F12	To determine the amount of solute gas desorbed during collection in F12; used to correct coefficient from A for collection effect.
C	N_2	HC	HC	To determine the amount of solute gas absorbed during fall and during collection in HC gas. Correct for collection effect from D, or extrapolate to zero fall height to obtain absorption for fall only.
D	N_2	N_2	HC	To determine the amount of solute gas absorbed by liquid during collection in HC gas.
E	HC	HC	HC	To determine the absorption during drop formation and stabilization.

N_2 - Nitrogen

F12 - Freon 12

HC - Hydrocarbon Gas (n-butane)

(*) - For B type runs, the drop liquid was initially saturated with the solute gas, i.e. valves V1, V2 and V3 open.

TABLE V

OPERATING STATES OF THE EXPERIMENTAL APPARATUS COMPONENTS AS SHOWN IN FIGURE 1

Run Type / Component	A	B	C	D	E
Gas Cylinder Connected to:					
Gas Line A	HC	HC	HC	N_2	HC
Gas Line B	F12	F12	-	HC	-
Gas Line C	N_2	-	N_2	-	-
Gas Carried by Rotameter:					
R1	HC	HC	HC	-	HC
R2	F12	F12	-	HC	-
R3	N_2	HC	N_2	N_2	HC
R4	HC & F12	HC & F12	-	N_2 & HC	HC
R5	HC & N_2	HC	HC & N_2	-	HC
Valve V1	C	O	C	C	C
V2	C	O	C	C	C
V3	C	O	C	C	C
V4	O	O	O	O	O
V5	O	O	C	O	C
V6	O	O	O	O	O
V7	O	O	C	O	O
V8	O	O	O	C	O
V9	O	O	O	O	C
V10	C/O	C/O	C/O	C/O	C
V12-V15	INT	INT	INT	INT	INT
V16	O	O	O	O	O
V17	O	O	O	O	O
V18	C	O	C	O	O
V19	O	C	O	C	C
V20	C/O	C/O	C/O	C/O	C/O
V21	O	O	O	C	O

Code: HC - Hydrocarbon Gas
N_2 - Nitrogen Gas
F12 - Freon 12 Gas
O - Open
C - Closed
C/O - Closed and Open during a Run
INT - Intermittently Closed and Opened during a Run

reading from V14 was recorded.

The procedure for an experimental run was as follows:

1. Set the operating states of the experimental apparatus components as given in Table V.
2. With V20 open, turn on the vacuum pump and initiate gas flow, starting the flow of the hydrocarbon gas last (See Appendix D for gas flow rates).
3. Slowly close V20, while observing the column pressure reading from manometer with V14 open. Regulate the rotameter settings to obtain a column internal pressure 1-5 cm. of water above atmospheric.
4. Take gas samples, about 1 cc, from the various gas sampling ports along the column and analyze in the FM 500 chromatograph to determine the gas concentration profile in the column.
5. If the chromatographic analysis shows undesirable mixing of gases in the column, e.g. hydrocarbon gas in the collection chamber in type A runs, regulate the gas flow rates in and out the column. If necessary, purge the drop collection chamber by diverting most of the gas flow through V9, to eliminate mixing of gases in the column.
6. After the desirable gas-gas interfaces have been established in the column, start forming drops, i.e. open V16 and V17, at a constant rate, with V20 closed.
7. After a constant drop rate has been established, recheck the column gas profile. If the gas profile in the column is found satisfactory, attach a sample vial to the stainless

steel stem of V20. Open V20 and transfer the collected drop liquid into the sample vial. Close V20, start timer and discard the liquid.

8. Attach a clean sample vial, from ice box storage, gas tight to V20 stem via a screw type hose clamp.
9. With V20 closed, collect liquid above it for the desired length of sampling period. At the end of the sampling period, open V20 permitting the collected liquid to flow into the sample vial. Close V20 at the end of the desired transfer period. Start collecting the next sample. Disconnect sample vial from the stem of V20, discard this first sample.
10. Attach a new vial on to V20 stem as described in step 8. Position a screw type pinch clamp loosely on the Tygon tube section of the sample vial, between the vial glass part and V20-Tygon tube attachment. Proceed as in step 9 above to collect and transfer sample into vial. However, after transferring the sample into vial, close the pinch clamp on Tygon tubing tightly. Disconnect vial from V20 stem and close the open end of the Tygon tube with a gas tight rubber septum. Mark the vial for identification and place it in ice.
11. Attach a new sample vial to the stem of V20 and repeat steps 8, 9 and 10 for duplicate and/or triplicate samples at the same sampling and transfer period.
12. After duplicate or triplicate samples have been collected from a given tip, stop drop liquid flow by closing V16

and V17.

13. To change tips, loosen the 1/8 inch compression fitting, i.e. 7 in Figure 13 and 1/8 inch NPT male adapter, 8. Remove the 1/8 inch stainless steel tube holding the drop forming tip. Replace with a new tip, already cleaned with acetone. Reassemble the tip holding assembly.
14. Open V16 and V17 and let liquid run out from tip fast until all air bubbles are removed.
15. Perform steps 6-14 above to obtain a new set of drop samples with the new tip.

Preliminary experiments showed that 75 seconds and 15 seconds should be used as the lengths of sampling and transfer periods, respectively. This conclusion was based on the following considerations:

1. The sampling and transfer periods should be the same for all tips and all liquids.
2. Enough sample should be collected even from the smallest tip, for an easy sampling for chromatographic analysis.
3. Sampling and transfer periods should be long enough to enable the operator to work at a fast, but not at an overly hurried pace, while changing vials, etc. Reasonable slack time should be available in case of minor mishaps while changing vials.

When it was necessary to change the liquid phase, the liquid in the drop forming assembly and the saturators was drained. After draining, all glassware and all liquid lines in the drop forming assembly, including V16 and V17, were cleaned with acetone and dried. New liquid

was then put in the saturators and the drop forming assembly. Step 14, above, was then performed to eliminate any trapped air bubbles from the liquid lines below the liquid holding funnel in the constant head reservoir.

Liquid Sample Handling and Sample Removal for Analysis

Sample vials containing samples of liquid drops were closed gas tight as in step 9 above, marked for identification and kept in ice. To obtain a liquid sample from the vial for chromatographic analysis, the sample vial was removed from ice, the pinch clamp was loosened, permitting the liquid access to the upper end of the Tygon tube attached to the sample vial. The contents of the vial were then agitated by shaking and inverting the vial a few times to ensure sample homogeneity. Then, the syringe needle was introduced into the vial through the rubber septum at the end of the Tygon tubing to obtain a sample for analysis. One microliter liquid samples were used for chromatographic analyses. After a sample was removed from the sample vial, the vial was put back into ice for the period of analysis. Usually duplicate and sometimes triplicate analyses were made of a sample. The sample was kept in ice until the end of the last analysis and then discarded. The sample vials were drained and cleaned by acetone before being reused in a new run.

CHAPTER V

EXPERIMENTAL RESULTS AND DISCUSSION

This chapter commences with the presentation of the experimental data in the form of observed solute gas concentrations in the analyzed liquid samples. This is followed by a discussion of the methods used in handling the experimental data to evaluate quantities indicative of the mass transfer rates and mechanisms involved. The calculated values of these quantities are also presented, as well as a comparison of the different methods used for correction for the end effects.

From available theory and literature data, mass transfer coefficients are predicted for the systems studied. These values are then compared with those obtained experimentally. The chapter is concluded with a discussion of the experimental errors involved.

Experimental Results

The results of various types of runs performed on the absorption column are given in Table VI. The run types, as noted in the first column of Table VI, are characterized by the gases occupying different sections of the column. Differences between run types were summarized in Table IV. In Table VI, column five shows the number of samples taken from the drops formed by a given tip and, in parentheses, the total number of chromatographic analyses performed on all the samples of that tip. The sample concentration was taken to be the arithmetic

TABLE VI

EXPERIMENTAL RESULTS - ABSORPTION COLUMN

Run Type	Column Length (Ft)	System	Tip No.	Samples & (Analyses)	Drop Gas Conc. (Wt. Fr.)	Exp. Error Avg. Abs. (%)
A	6	nC_4-	1	3;(7)	0.0085	7.5
			2	3;(6)	0.0104	3.8
		nC_{10}	5	3;(7)	0.0118	3.2
			7	3;(5)	0.0136	4.0
A	6	nC_4-	1	3;(6)	0.0137	12.
			2	3;(6)	0.0249	13.
		nC_9	3	3;(6)	0.0174	3.3
			5	3;(7)	0.0196	2.6
			7	2;(4)	0.0191	3.9
A	6	nC_4-	1	3;(6)	0.0201	11.
			2	3;(6)	0.0257	6.1
		nC_8	5	3;(8)	0.0264	1.0
			7	3;(6)	0.0355	3.9
B	6	nC_4-	1	2;(5)	0.0243	22.
			2	3;(6)	0.0362	4.1
		nC_{10}	5	3;(7)	0.0495	4.0
			7	3;(7)	0.0680	6.3
B	6	nC_4-	1	3;(6)	0.0230	13.
			2	3;(6)	0.0209	7.8
		nC_9	3	3;(6)	0.0654	2.4
			5	3;(6)	0.0645	3.8
			7	3;(5)	0.0759	2.1
B	6	nC_4-	1	3;(5)	0.0311	10.
			2	3;(6)	0.0481	9.4
		nC_8	5	3;(6)	0.0719	3.8
			7	3;(6)	0.0687	2.7
C	10	nC_4-	1	2;(3)*	0.0773	4.0
			1	2;(2)**	0.1030	0.78
		nC_{10}	2	3;(4)	0.1138	4.3
			3	3;(4)	0.1170	2.7
			5	3;(4)	0.1257	2.1
			7	3;(4)	0.1260	3.7

TABLE VI (Continued)

C	10	nC_4-	1	2;(3)*	0.1109	0.48
			1	2;(2)**	0.1285	0.70
		nC_{10}	2	3;(3)	0.1232	3.1
			3	2;(3)	0.1261	2.7
			5	3;(3)	0.1251	0.80
			7	3;(4)	0.1261	2.0
C	10	nC_4-	1	2;(3)	0.0918	2.9
(***)			2	2;(3)	0.1213	2.1
		nC_{10}	3	2;(2)	0.1242	6.3
			5	2;(3)	0.1247	0.80
			7	2;(3)	0.1295	0.85
C	6	nC_4-	1	2;(3)*	0.1063	3.4
			1	2;(3)**	0.1283	2.6
		nC_{10}	2	3;(5)	0.1030	0.55
			3	3;(4)	0.1221	2.2
			5	3;(4)	0.1113	3.3
			7	3;(4)	0.1132	2.3
C	4	nC_4-	1	3;(4)	0.1054	2.7
			2	3;(4)	0.1197	3.4
		nC_{10}	3	3;(3)	0.1227	0.19
			5	3;(4)	0.1226	2.6
			7	3;(3)	0.1226	2.3
C	6	nC_4-	1	3;(6)	0.1575	2.9
			2	3;(6)	0.1200	4.5
		nC_9	3	3;(6)	0.1404	6.1
			5	3;(6)	0.1427	6.5
			7	3;(6)	0.1196	3.6
C	6	nC_4-	1	2;(4)*	0.1371	2.0
			1	2;(4)**	0.1504	1.7
		nC_8	2	3;(6)	0.1446	5.7
			3	3;(4)	0.1433	3.5
			5	3;(4)	0.1462	3.3
			7	3;(4)	0.1430	3.6
D	6	nC_4-	1	3;(6)	0.1465	3.3
			2	3;(6)	0.1148	1.9
		nC_9	3	2;(4)	0.1313	5.6
			5	3;(6)	0.1189	2.0
			7	3;(6)	0.0959	1.2

TABLE VI (Continued)

E	4	nC_4-	1	2;(3)	0.1075	0.30
			2	2;(2)	0.1245	2.6
		nC_{10}	3	2;(3)	0.1195	1.9
			5	2;(2)	0.1238	1.9
			7	2;(2)	0.1328	1.0

(*) - Only one sample was taken
(**) - Two samples were taken
(***) - A three way valve was used as V20 for this run (Figure III), to minimize the contact between the sample liquid and the drop catcher atmosphere.

average of the analysis values when more than one analysis was made on a sample. The reported concentrations for each tip are the averages of sample concentrations. Average absolute experimental errors are reported in column seven of Table VI to indicate the scatter among the observed sample concentrations.

All the reported weight fractions of the absorbed hydrocarbon gas ($n\text{-}C_4$) are on Freon 12 free basis. Freon 12 was used as the blanket gas at the drop collection chamber and has no effect on the absorbed normal butane concentration in the drop at the termination of the drop fall. Equations (26) and (29) discussed below, have been developed to correct the observed n-butane concentration in the liquid sample for desorption to the blanket gas.

Handling of Experimental Data for Mass Transfer Coefficients and Related Calculations

The length of the absorption period is a common parameter to all of the calculations made using the experimental data to calculate mass transfer coefficients and effective diffusivities. Lengths of the absorption periods used in this study were not experimentally measured, but calculated. A discussion of the method used to calculate this parameter is presented below, prior to the discussion on the calculation of mass transfer coefficients and other related calculations.

Calculation of the Absorption Periods

For all types of runs, with the exception of Type E runs, the absorption periods involved in this work were taken as the lengths of the periods the falling drops of different sizes were in contact with the

solute gas, i.e. n-butane. Thus, this period is equal to the time it required for a liquid drop to fall between upper nitrogen-n-butane interface and the lower n-butane - Freon 12 interface.

Drop fall times were calculated from

$$\frac{d^2L}{d\theta^2} = \frac{g(\rho_d - \rho_c)}{\rho_d} - (6/8)\, C_D \frac{\rho_c}{d_e \rho_d} \left(\frac{dL}{d\theta}\right)^2 \qquad (36)$$

Equation (36) was obtained from Hughes and Gilliland (38). A fourth order Runge-Kutta method was used for the integration of Equation (36) along the length of the column. However, as briefly discussed in Chapter II, there is considerable controversy in the literature on the proper value of C_D for falling drops. Some recent works by Buzzard and Nedderman (5), Harper, et al. (30) and Kenning (41) have contributed considerably to the available knowledge in the subject. Harper, et al. (30) and Kennig (41) note that for liquid drops falling in gas, the drag coefficient should be rather insensitive to surface effects. The experimental data given by Buzzard and Nedderman (5) show that for uncontaminated liquids C_D could be considered constant for $Re \gtrsim 1000$ and for contaminated liquids C_D could be considered constant for $Re \gtrsim 1600$. Based on this information and also on a drag coefficient versus surface tension plot given by Buzzard and Nedderman, a value of 0.55 was used for the liquid drops encountered in this project.

Table VII shows the fall times and Reynolds numbers at different points along the absorption column for C_D = 0.45, 0.50, 0.55, 0.60, 0.65, 0.70 for a n-C_{10} drop in n-C_4 formed from Tip 5 at 2.7 seconds, (d_e = 0.348 cm.). Column 8 of Table VII is for C_D calculated from

$$C_D = \frac{48}{Re} + 0.60 \qquad (37)$$

TABLE VII

EFFECT OF DRAG COEFFICIENT C_D ON DROP FALL TIME

C_D	0.45	0.50	0.55	0.60	0.65	0.70	Eq.(37)	Eq.(38)
L (cm.)	θ_{fall} (sec)	θ_{fall} (sec)	θ_{fall} (sec)	θ_{fall} (sec)	θ_{fall} (sec)	θ_{fall} (sec)	θ_{fall} (sec)	θ_{fall} (sec)
25	0.231	0.231	0.231	0.232	0.233	0.233	0.234	0.226
50	0.331	0.332	0.333	0.334	0.335	0.336	0.337	0.319
100	0.480	0.484	0.486	0.488	0.493	0.496	0.498	0.452
150	0.605	0.610	0.615	0.620	0.624	0.632	0.631	0.553
200	0.714	0.724	0.733	0.742	0.750	0.757	0.756	0.639
250	0.821	0.833	0.844	0.857	0.868	0.880	0.873	0.714
300	0.922	0.937	0.953	0.963	0.983	0.999	0.992	0.782

as suggested by Hughes and Gilliland (38) for accelerating drops. Column 9 of Table VII shows the fall times calculated by the assumption of zero drag from

$$\theta_f = \sqrt{\frac{2L}{g}} \tag{38}$$

Mass Transfer Coefficients and Ratios of Effective to Molecular Diffusivities for Falling Drops from Type A and Type B Run Results - (Corrected for End Effects)

Mass transfer coefficients and effective-to-molecular-diffusivity ratios for falling drops calculated from the results of Type A and Type B runs are given in Table VIII. The fractional saturation concentration of the dissolved n-butane in the drop liquid at the end of the fall period was calculated from the fractional saturation concentrations obtained from Type A and Type B runs for the given liquid, drop size and fall height from Equation (39)

$$\frac{C_d}{C^*} = \frac{C_s^A}{C_s^B} \tag{39}$$

Equation (39) is derived in Appendix F. The saturation concentrations of n-butane in the liquids used were determined chromatographically and checked by Raoult's Law predictions (See Appendix E).

The mass transfer coefficients were calculated from

$$K_L = \frac{d_e}{6\theta_a} \log_e (1 - F) \tag{40}$$

An overall absorption coefficient based on the liquid side is used on the left hand side of Equation (40) instead of the more commonly used liquid film coefficient. For the case of this study Equation (40) should be valid since the gas phase consisted of pure solute gas

TABLE VIII

K_L AND D_e/D_m FROM TYPE A AND TYPE B RUN RESULTS - SIX FOOT COLUMN

Tip No	d_e (cm)	θ (sec)	Type A	Type B	Corrected F	K_L cm/sec	D_e/D_m
nC_4-nC_{10} System (C^* = 0.246 wt. fraction nC_4 in nC_{10})							
1	0.264	0.365	0.0346	0.0989	0.350	0.052	32.6
2	0.308	0.355	0.0423	0.147	0.288	0.0493	29.5
5	0.351	0.347	0.0480	0.201	0.239	0.0461	25.9
7	0.403	0.340	0.0553	0.277	0.200	0.0439	23.2
nC_4-nC_9 System (C^* = 0.276 wt. fraction nC_4 in nC_9)							
1	0.262	0.366	0.0496	0.0834	0.595	0.111	93.5
2	0.305	0.355	0.0901	0.0757	-	-	-
3	0.329	0.353	0.0630	0.237	0.268	0.0480	23.5
5	0.348	0.347	0.0710	0.234	0.303	0.0603	35.2
7	0.400	0.342	0.0692	0.275	0.252	0.0583	31.3
nC_4-nC_8 System (C^* = 0.297 wt. fraction nC_4 in nC_8)							
1	0.259	0.369	0.0676	0.105	0.645	0.121	92.0
2	0.302	0.357	0.0865	0.162	0.534	0.108	78.9
5	0.344	0.349	0.0890	0.242	0.368	0.0755	43.3
7	0.395	0.344	0.120	0.232	0.517	0.139	129.2

saturated with the drop liquid and, therefore, the gas film resistance could be neglected.

A brief discussion of the advantages and disadvantages of expressing mass transfer results in terms of D_e/D_m was given in Chapter II. Effective diffusivities calculated from Equation (19) (Chapter II), using the corrected fractional saturations of the drops and the calculated absorption times, are presented as the ratios $\phi = D_e/D_m$. The molecular diffusivities used for these calculations were calculated from the Wilke-Chang correlation (71)

$$D_m = 7.4 \times 10^{-10} \frac{T (\phi MW_d)^{\frac{1}{2}}}{\mu_d \, mv_d^{0.6}} \qquad (41)$$

The physical properties of the system in Equation (41) were obtained from Reid and Sherwood (61). The molecular diffusivities calculated from Equation (41) for the systems studied, at 24°C., were:

$$D_m \ (nC_4\text{-}nC_{10}) = 1.94 \times 10^{-5} \text{ cm.}^2/\text{sec.}$$

$$D_m \ (nC_4 - nC_9) = 2.38 \times 10^{-5} \text{ cm.}^2/\text{sec.}$$

$$D_m \ (nC_4 - nC_8) = 2.91 \times 10^{-5} \text{ cm.}^2/\text{sec.}$$

Mass Transfer Coefficients for Falling Drops from Type C and Type D Run Results - (Corrected for End Effects)

Table IX contains the corrected drop fractional saturations, the absorption times and the calculated overall mass transfer coefficients K_L (based on the liquid side) for the nC_4-nC_9 system from the results of Type C and Type D runs. Equation (42), derived in Appendix E was used

$$C_d = (C_s^C - C_s^D)/(1 - (C_s^D/C^*)) \qquad (42)$$

to convert the observed sample compositions to the drop compositions at the end of the fall period. The mass transfer coefficients were calculated from Equation (40). Effective-to-molecular-diffusivity ratios are not reported in Table IX. In particular the drops of Tips 1, 2 and 3 exhibited very low corrected fractional saturations. At these very low concentrations, for the system and fall heights studied, D_e/D_m ratios of less than one were obtained.

Mass Transfer Coefficients for Falling Drops from the Results of Type C Runs - (Corrected for End Effects)

Table X shows that Type C runs were made at varying column lengths, i.e. varying absorption times. For runs made in this manner a classical method of end effect correction is the extrapolation of the observed solute concentrations to zero absorption time. Figure 15 shows the extrapolation as well as the data. The extrapolation was made to the time it takes each drop to fall from rest to the upper suction rings where the inert gas blanket and the solute gas formed an interface. The solute gas concentration determined from this extrapolation was then subtracted from the observed sample concentrations to determine the solute concentration in the drop at the end of the fall period. Table X shows the absorption periods for each drop for different column heights as well as the overall mass transfer coefficients K_L (based on the liquid side) calculated from Equation (40) as previously. K_L's for Tips 2, 4 and 5 at the 6 ft. column height were not calculated since, due to the scatter, the data points fell below the concentration determined by the extrapolation procedure. Ratios of D_e to D_m were also not reported, since due to the very low fractional saturations obtained with this correction procedure, D_e/D_m values of less than one

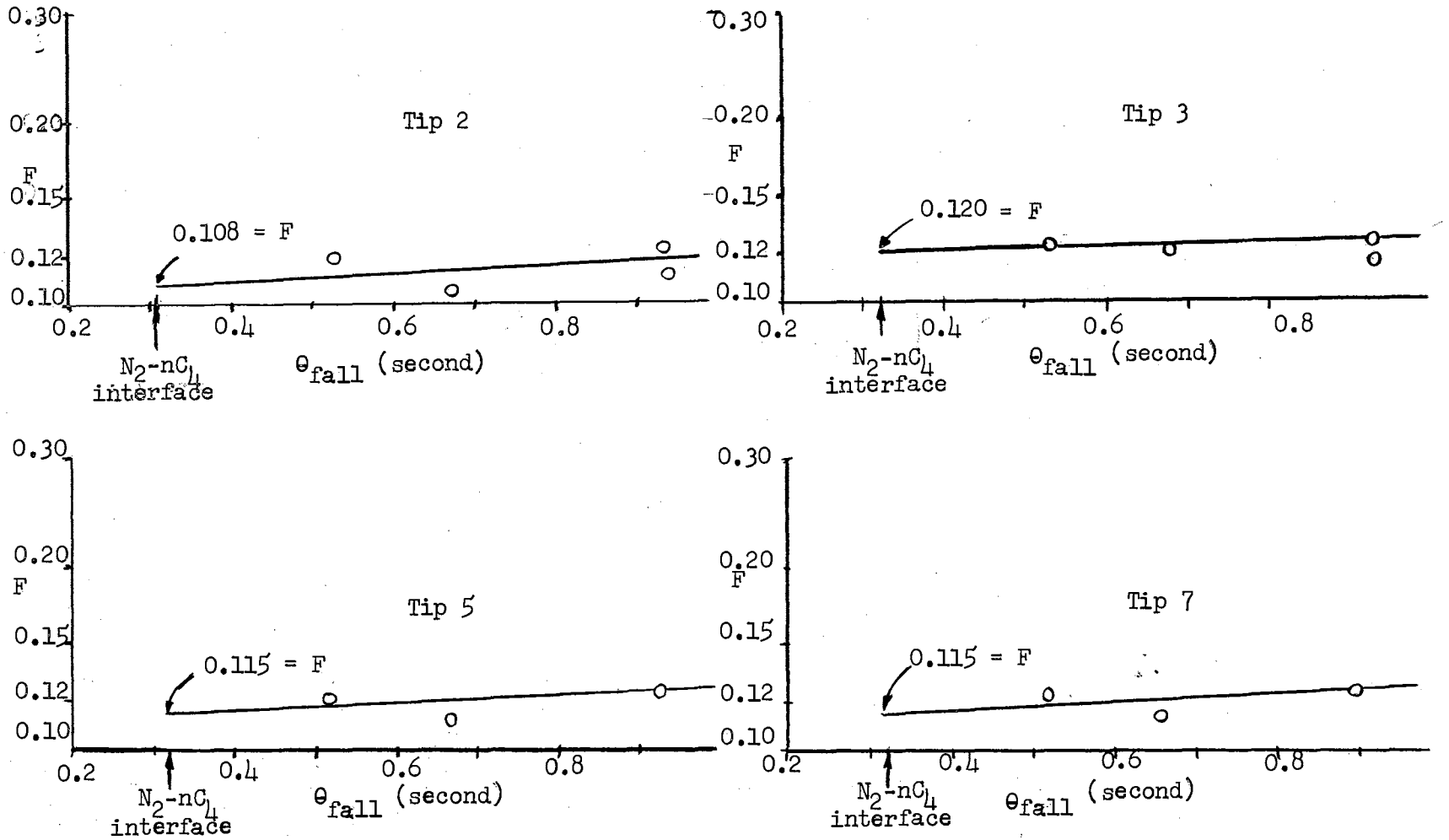

Figure 15. Type C Run Results - Extrapolation to Zero Absorption Time

TABLE IX

MASS TRANSFER COEFFICIENTS FOR SIX FOOT COLUMN FROM TYPE C AND TYPE D RUN RESULTS: nC_4-nC_9 SYSTEM

Tip No	d_e (cm)	θ_a (sec)	F Type C	F Type D	F Eq.(42)	K_L (cm/sec)
1	0.262	0.366	0.572	0.533	0.0855	0.0107
2	0.305	0.355	0.435	0.416	0.0312	0.00454
3	0.329	0.353	0.507	0.475	0.0620	0.00096
5	0.348	0.347	0.518	0.431	0.153	0.00277
7	0.400	0.342	0.435	0.343	0.133	0.00279

TABLE X

MASS TRANSFER COEFFICIENTS FROM TYPE C RUN RESULTS; CORRECTED FOR COLLECTION EFFECT BY EXTRAPOLATION TO ZERO CONTACT TIME: nC_4-nC_{10} SYSTEM

Tip No	d_e (cm)	4 ft. Column θ_a (sec)	4 ft. Column K_L (cm/sec)	6 ft. Column θ_a (sec)	6 ft. Column K_L (cm/sec)	10 ft. Column θ_a (sec)	10 ft. Column K_L (cm/sec)
1	0.264	0.211	0.0044	0.365	0.0148	0.638	0.0049
2	0.308	0.207	0.0119	0.355	-	0.615	0.00358
3	0.332	0.205	0.00297	0.351	0.00216	0.605	0.00055
5	0.351	0.203	0.00935	0.347	-	0.598	0.00042
7	0.403	0.202	0.0101	0.340	-	0.582	0.00518

were obtained.

Comparison of the Results of Different Cup Correction Procedures Used

Experimentally obtained overall liquid phase mass transfer coefficients, K_L, for falling drops under different experimental conditions have already been presented, in Tables VIII, IX and X. A comparison of these values show differences in terms of K_L values, obtained via different collection cup correction procedures. These procedures were discussed in the preceding section and also in Appendix F. The choice of one of these correction procedures as the correct one should be based on a consistency test between the data and available theory. Such a check is attempted in the latter part of this chapter and a choice is made. However, it should be recognized from the values given in Tables VIII, IX and X, that in general, the K_L values decrease with increasing drop diameter. As will be discussed later, this trend is not in accord with most of the presently available knowledge in the subject.

Figures 16, 17 and 18 show the data presented in Tables VIII, IX and X as well as some theoretical predictions of the related K_L values. A discussion of this comparison will be made later.

A comparison of the experimentally determined K_L's on the basis of the cup correction procedures shows that the cup correction procedure involving Equation (42) and that involving extrapolation of Type C results to $\theta_a = 0$ result in K_L's of similar magnitude. Use of Equation (42) involves Type C and Type D run results for similar size drops of the same system. However, the K_L values obtained from the correction

of Type A and Type B run results, via Equation (39) are considerably higher than the others.

The closeness of the K_L's in Table IX and Table X could be based on the results of Type C runs, which are common to the two cup correction procedures used to acquire these results. This point will be discussed later when comparing the experimental results with those theoretically predicted.

Figure 19 shows a plot of D_e/D_m values versus d_e as given in Table VIII. In general, for a given drop diameter D_e/D_m values increase with decreasing molecular weight. Also the surface tension of the liquids studied decrease with decreasing molecular weight. This indicates that D_e/D_m is higher for liquids of lower surface tension, indicating a higher drop instability for drops lower surface tension.

The trend of D_e/D_m with respect to drop size will be discussed later in detail. However, D_e/D_m ratios consistently larger than 2.5 from Type A Type B run results indicate internally circulating drops on the basis of the Kronig-Brink model ( ); a situation expected in falling drops in the size range studied.

Predicted Mass Transfer Coefficients for Falling Liquid Drops

One has to first predict gas and liquid film mass transfer coefficients, i.e. k_c ($k_g = k_c/RT$) and k_L respectively, from available theory, to be able to predict K_L or K_g. The overall liquid and gas phase mass transfer coefficients K_L and K_g are related to the film coefficients, on the basis of the two film theory (70), as follows:

$$\frac{1}{K_L} = \frac{1}{k_L} + \frac{1}{K_e k_c} \qquad (43)$$

$$K_g = \frac{1}{k_c} + \frac{K_e}{k_L} \tag{44}$$

At this point the inclusion of k_c, the gas film mass transfer coefficient may look unnecessary since the gas phase did not include any intentionally added inert diluents with the solute gas. However, in Type A, C and D runs the liquid drops were formed in a nitrogen atmosphere and fell in this atmosphere a distance of about 47 cm. It has been suggested by Garner and Lane (20) that such drops, upon entering the solute gas region retain a thin layer of the inert gas around them. Garner and Lane suggested a period of about two seconds for complete displacement of such a blanket. Thus, it would also be proper to include a gas film resistance term to the present set of proposed calculations to account for the probable presence of a nitrogen blanket around the drop as it falls through the n-butane atmosphere.

The gas film mass transfer coefficients for the systems studied were calculated from Frossling's equation (18)

$$k_c = 2 \frac{D_v}{d_e} \left[1 + 0.276 \, R_e^{1/2} \, S_c^{1/3} \right] \tag{25}$$

Equation (12) has been used with confidence in the literature for k_c predictions and has been found to give good agreement with data (7). Gas film mass transfer coefficients calculated from Equation (25) for the nC_4-nC_{10}, nC_4-nC_9 and nC_4-nC_8 systems at the 6 ft. column height are tabulated in Table XI. Average drop velocities, in the absorption region, have been used for Reynolds Number calculations in Equation (25). The molecular diffusivity of n-butane in the hypothesized nitrogen shroud around the liquid drop has been calculated from the ideal gas approximation of the Chapman-Enskog equation (61) to be

TABLE XI

PREDICTED MASS TRANSFER COEFFICIENTS FOR SIX FOOT HEIGHT OF FALL

Tip No	d_e (cm)	$(k_c)_c$ (cm/sec)	$(k_L)_{c1}$ (cm/sec)	$(k_L)_{c2}$ (cm/sec)	$(k_L)_{c3}$ (cm/sec)	$(K_L)_{c1}$ (cm/sec)	$(K_L)_{c2}$ (cm/sec)	$(K_L)_{c3}$ (cm/sec)	K_e
nC_4-nC_{10} System									
1	0.264	6.09	0.0082	0.0066	0.185	0.0082	0.0066	0.0868	2.10
2	0.308	5.67	0.0083	0.0062	0.174	0.0083	0.0062	0.0816	2.10
5	0.351	5.33	0.0084	0.0058	0.164	0.0084	0.0058	0.0769	2.10
7	0.403	5.00	0.0085	0.0055	0.155	0.0085	0.0055	0.0727	2.10
nC_4-nC_9 System									
1	0.262	6.08	0.0091	0.0082	0.205	0.0091	0.0082	0.0948	2.13
2	0.305	5.70	0.0092	0.0078	0.193	0.0092	0.0078	0.0892	2.13
3	0.329	5.50	0.0093	0.0075	0.186	0.0092	0.0075	0.0859	2.13
5	0.348	5.35	0.0094	0.0073	0.182	0.0093	0.0073	0.0841	2.13
7	0.400	5.03	0.0095	0.0069	0.172	0.0094	0.0069	0.0795	2.13
nC_4-nC_8 System									
1	0.259	6.10	0.0100	0.0106	0.227	0.0100	0.0106	0.103	2.16
2	0.302	5.70	0.0102	0.0098	0.214	0.0101	0.0098	0.0974	2.16
5	0.344	5.37	0.0103	0.0093	0.203	0.0103	0.0092	0.0923	2.16
7	0.395	5.03	0.0104	0.0088	0.191	0.0104	0.0087	0.0869	2.16

0.0625 cm.^{2}/sec. The molecular parameters pertinent to this calculation have been obtained from Reid and Sherwood ((61).

Prediction of liquid film mass transfer coefficients, k_L, for the systems studied were based on the penetration (36) surface renewal (10) theories. As tabulated in Table XI, three sets of k_L values were calculated from the assumed model

$$k_L = \sqrt{\frac{4 D_m}{\pi \theta_c}}$$

The discrepancy between the three sets of k_L values arises from the assumptions made in calculating θ_c, the contact time. The following are the assumptions made in θ_c calculations:

1. θ_c is the total time the drop was in contact with the solute gas during fall, i.e. $\theta_c = \theta_a$. The θ_{c_1} designations in Table XII and the corresponding $(k_L)_{\theta_1}$ designations in Table XI refer to this assumption. On the basis of the surface renewal theory, this assumption means that the drop surface was renewed only once during fall. This procedure was followed recently by Makino and Takashima (49).
2. θ_c is the time it takes for an internal circulation current to sweep the perimeter of a circle with a diameter equal to the drop diameter, i.e. $\theta_c = d_e/U_{ic}$. The internal circulation velocities of the drops were calculated from Equation (14)

$$U_{ic} = \frac{U}{2\left(1 + \mu_d/\mu_c\right)} \qquad (14)$$

derived from the Hadamard-Rybczynski model (27, 64). Average drop velocities, U, during drop fall in contact with solute gas were used in Equation (14). θ_c's

calculated in this manner are designated as θ_{c2} in Table XII and the corresponding $(k_L)_{c2}$ in Table XI.

3. The third assumption made for θ_c calculation is a classical assumption to similar calculations for gas bubbles and liquid-liquid systems. This method assumes that the surface renewal time θ_c is the time it takes the drop to travel a distance of one diameter, i.e. $\theta_c = \theta_a/(L/d_e)$. The fall velocities of the liquid drops are much higher than the velocities attained by bubbles in liquid or by liquid-liquid systems. Thus, the surface renewal times calculated in this way for liquid drops falling in gas are very short. θ_{c3} and $(k_L)_{c3}$ designations are used in Table XII and Table XI, respectively, for the values obtained from this assumption.

Liquid phase molecular diffusivities, D_m, used in Equation (45) were calculated from the Wilke-Chang correlation (71), Equation (41).

Vapor-liquid equilibrium constants, K_e, used in Equations (30) and (31) for n-butane in n-decane, in n-nonane and in n-octane were of the form

$$K_e = \frac{y_e}{x_e} \tag{46}$$

and were calculated from equilibrium vapor and liquid compositions.

The overall liquid phase mass transfer coefficients calculated using $(k_L)_{c1}$, $(k_L)_{c2}$ and $(k_L)_{c3}$ and common $(k_c)_c$ values are given in Table XI and designated as $(K_L)_{c1}$, $(K_L)_{c2}$ and $(K_L)_{c3}$, respectively.

Comparison of the Experimental Results with Theoretical Predictions and Available Literature Information

A comparison of the predicted and experimentally obtained K_L values for the nC_4-nC_{10}, nC_4-nC_9 and nC_4-nC_8 systems at the six foot column length are given in Figures 16, 17 and 18. Figures 16 and 17 also include a line which indicates the predicted K_L values for a solid drop. Solid drop K_L values were calculated from Equation (40).

The calculated absorption time during fall, θ_a, for drops of diameter d_e was used in Equation (40). The fractional saturations, F, were calculated for each drop for the given θ_a from Equation (32), presented earlier. This line based on molecular diffusivity only establishes the lower limit of the K_L's for the nC_4-nC_9 and nC_4-nC_{10} systems for the range of drop sizes shown. This theoretical lower limit suffers from the errors introduced into its calculation by the D_m prediction by Equation (41), θ_a prediction and the assumption of drop sphericity. This uncertainty could be as much as 20%.

However, most of the K_L's from extrapolated Type C results are more than 20 percent lower than the predicted theoretical limiting value. A possible partial explanation for this discrepancy could be found in the extrapolation technique. This end effect correction procedure, though widely used, inherently assumes similar drop hydrodynamics at all points along the column during fall. The fact that the hydrodynamics of the drop changes during fall has been well established (17, 20, 21, 38).

The $(K_L)_{c1}$ and $(K_L)_{c2}$ lines are close together since $(\theta_c)_1$ and $(\theta_c)_2$ for these drops and systems were found to be close together (see

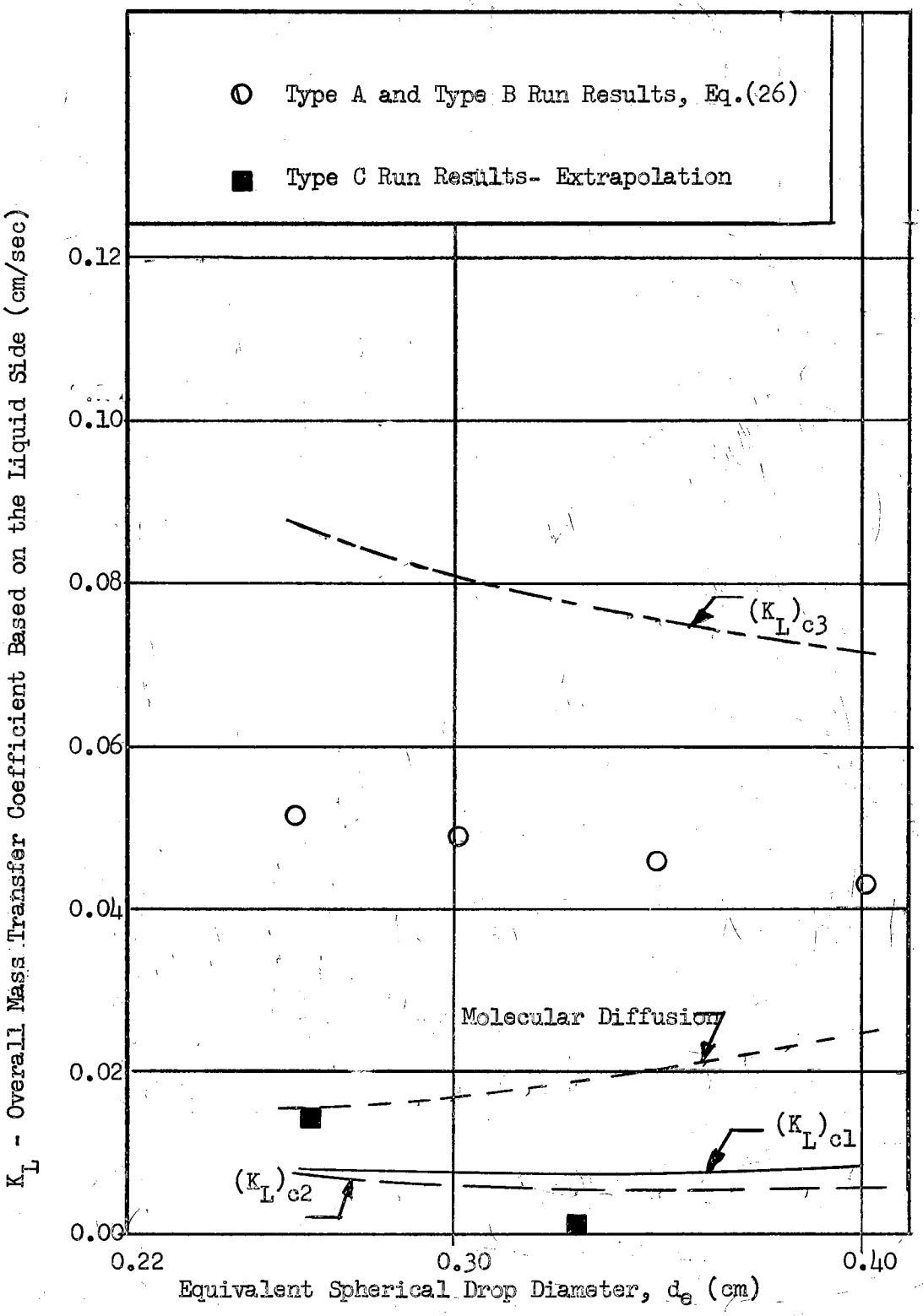

Figure 16. Experimental and Predicted K_L's for nC_4-nC_{10} System (Six Foot Column Data)

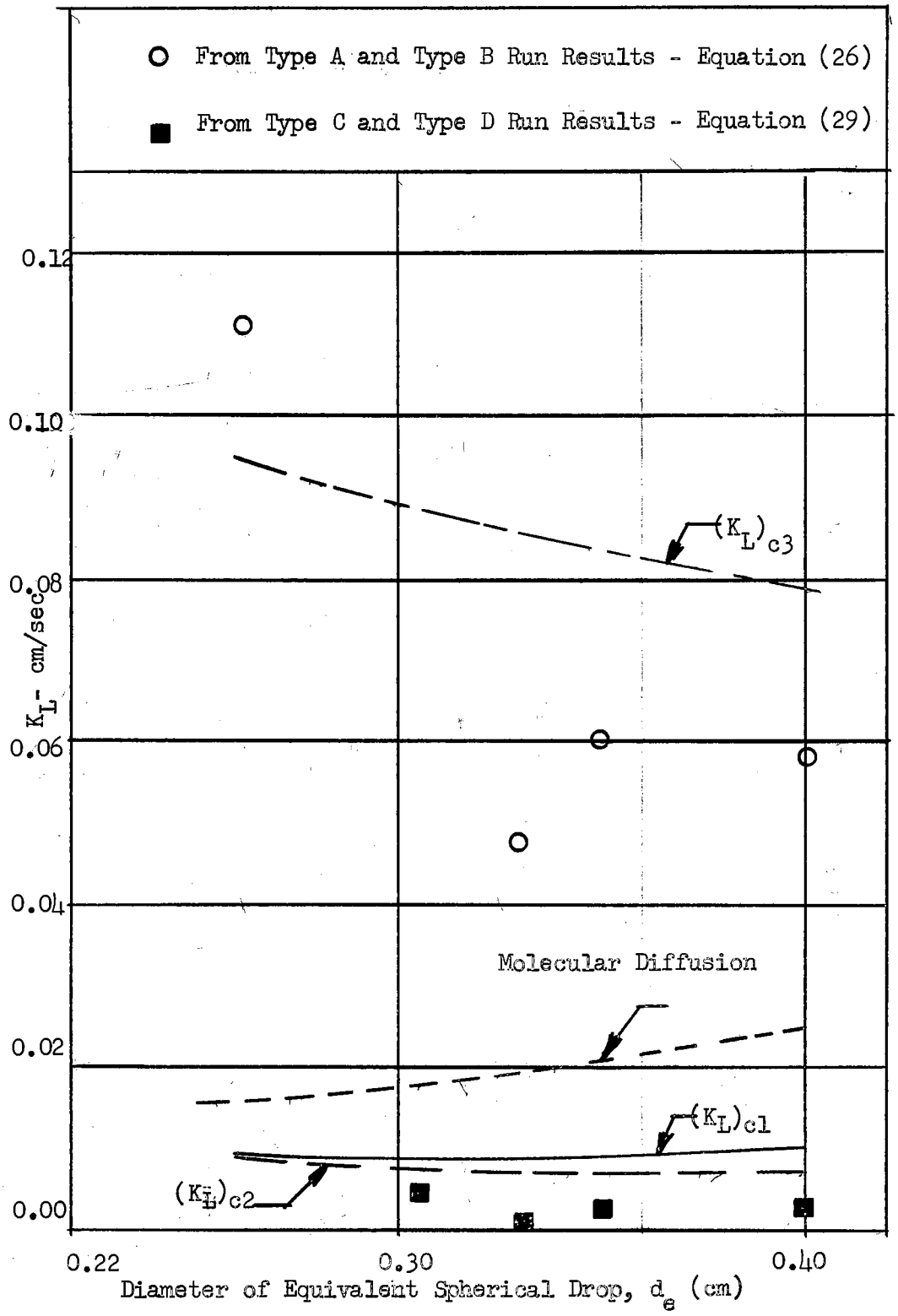

Figure 17. Experimental and Predicted K_L's for nC_4-nC_9 System (Six Foot Column Data)

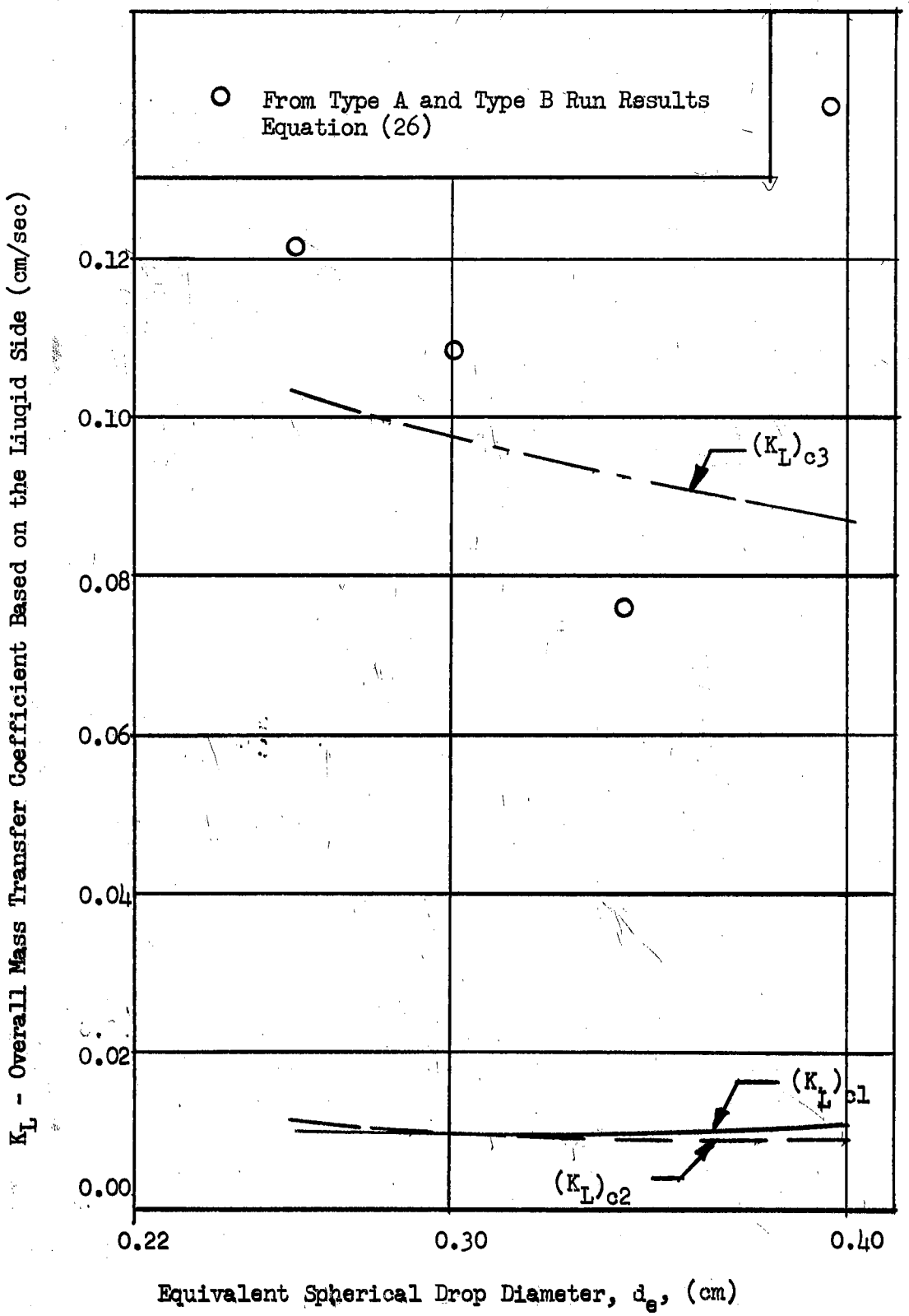

Figure 18. Experimental and Predicted K_L's for nC_4-nC_8 System (Six Foot Column Data)

TABLE XII

SURFACE RENEWAL TIMES, INTERNAL CIRCULATION VELOCITIES AND OSCILLATION FREQUENCIES FOR DROPS IN THE SIX FOOT COLUMN

System	Tip No	d_e (cm)	$\theta_{c1}=\theta_a$ (sec)	θ_{c2} (sec)	θ_{c3} (sec)	U_{ic} (cm/sec)	f (1/sec)
nC_4-nC_{10}	1	0.264	0.365	0.575	7.24	1.44	58.0
	2	0.308	0.355	0.653	8.22	1.48	46.1
	5	0.351	0.347	0.730	9.16	1.51	37.9
	7	0.403	0.340	0.822	10.30	1.54	30.8
nC_4-nC_9	1	0.262	0.366	0.450	7.20	1.83	58.1
	2	0.305	0.355	0.504	8.14	1.90	46.1
	3	0.329	0.353	0.541	8.74	1.91	41.2
	5	0.348	0.347	0.566	9.08	1.93	37.9
	7	0.400	0.342	0.638	10.27	1.97	30.8
nC_4-nC_8	1	0.259	0.369	0.330	7.18	2.37	58.0
	2	0.302	0.357	0.387	8.11	2.45	46.0
	5	0.344	0.349	0.432	9.02	2.50	37.9
	7	0.395	0.344	0.485	10.21	2.56	30.7

Table XII). The author believes that the θ_{c_1} calculation is inherently weak since it assumes a surface renewal time to a drop irrespective of the drop liquid properties but dependent solely on the fall time. The apparent error behind the assumption leading to the θ_{c_2} calculation may well be distributed between the equation used for internal circulation velocity, U_{ic}, calculation, i.e. Equation (14), and the assumption itself. Equation (14) is based on the Hadamard-Rybczynski (27, 64) model which is generally not applicable under actual conditions (48) and has been found to give order of magnitude deviations from data (20). Furthermore, the assumption basic to θ_{c_2} calculation is that the drops are spherical, which is not valid for the systems studied. Equation (18) was used

$$\frac{a}{b} = 1 + \frac{1.14}{9.0} E_o'' \qquad (18)$$

to calculate the degree of deformation in the drops of the systems studied. These calculations have shown that the value of a/b, for the drops in this study is in the range

$$1.2 < \frac{a}{b} < 1.7$$

showing well deformed drops. As noted in Chapter II, in deformed drops the effects of the internal circulation velocities on mass transfer are weaker than in spherical or in slightly deformed drops.

Thus, on the basis of the above discussion one is led to believe that the cup correction procedure employing Type C and Type D results, Equation (42) and the cup correction procedure employing the classical extrapolation technique both yielded unrealistic correction factors. This author, however, believes that it is hard to discard these cup

correction procedures on the basis of the relatively limited amount of data. The results shown for the six foot column height for the nC_4-nC_{10} system from the extrapolation method are supported by similar results for the four and ten foot column heights (Table X). The cause of the apparent weakness in those two procedures might be a systematic error in Type C runs. The results of the Type C runs are common to both of these correction procedures. This author believes, however, that this is very unlikely.

The general trend of the K_L values from Type A and Type B runs (concentrations corrected via Equation (39) show smaller K_L values for larger drops. A similar trend is exhibited by the predicted K_L values, i.e. $(K_L)_{c3}$, for the three systems (Table XI). This trend is contrary to the trend exhibited by the curve predicted by the assumption of only molecular diffusion. Furthermore, it is the majority belief in the related literature (20, 21, 44) that K_L should increase with drop instability which increases with drop size.

A plot of D_e/D_m versus d_e is given in Figure 19 for the corrected results obtained from Type A and Type B runs. The trends in this plot are very similar to those observed in Figures 16, 17 and 18.

Oscillation frequencies of the drops used for the systems shown in Figures 16, 17, 18 and 19 were calculated from an equation proposed by Lamb (47) and Bond and Newton (3)

$$f = \left[\frac{8\sigma}{3\pi M_d}\right]^{\frac{1}{2}} \qquad (15)$$

These frequencies are tabulated in Table XII and show higher oscillation frequencies for smaller drops. Thus, if it can be assumed that the oscillation amplitudes for different sized drops of a system

are the same, the smaller drops having higher frequencies of oscillation tend to show higher degrees of instability. It has been argued in the literature that falling drops tend to act like solid spheres soon after the start of fall (38), however some available data (17, 20) contradict this approach. The data obtained in the present study indicate drops with internal circulations and with surface oscillations of small amplitudes and varying frequencies. The low oscillation amplitudes, exhibited by most of the drops studied here, may be due to the retarding effect of surface active agents which may be present on the drop surface. The data obtained in this study are in accord with the data presented by Rabovskii and Shinyaeva (59) who also show lower mass transfer coefficients and lower D_e/D_m values for longer surface renewal times. According to their assumption, which was made in the $(K_L)_{c3}$ calculation, longer surface renewal times are analogous to larger drops.

It was noted earlier that both the K_L and D_e/D_m data showed some scatter when plotted against drop diameter. On the basis of the above discussion one can hypothesize that, if in fact some forces do exist on the drop surface which dampen the oscillation amplitudes, after a critical drop size has been reached for a given system, they are overcome by the "latent" instability of the drop.

A comparison of the K_L data versus $(K_L)_{c3}$ lines indicates to this inherent instability since n-octane drops show the highest K_L values and n-decane the lowest. The author would like to add immediately, however, that more data are necessary to establish the validity of, or to reject, the above discussion.

It is hard to decide from the results of Type A and Type B runs

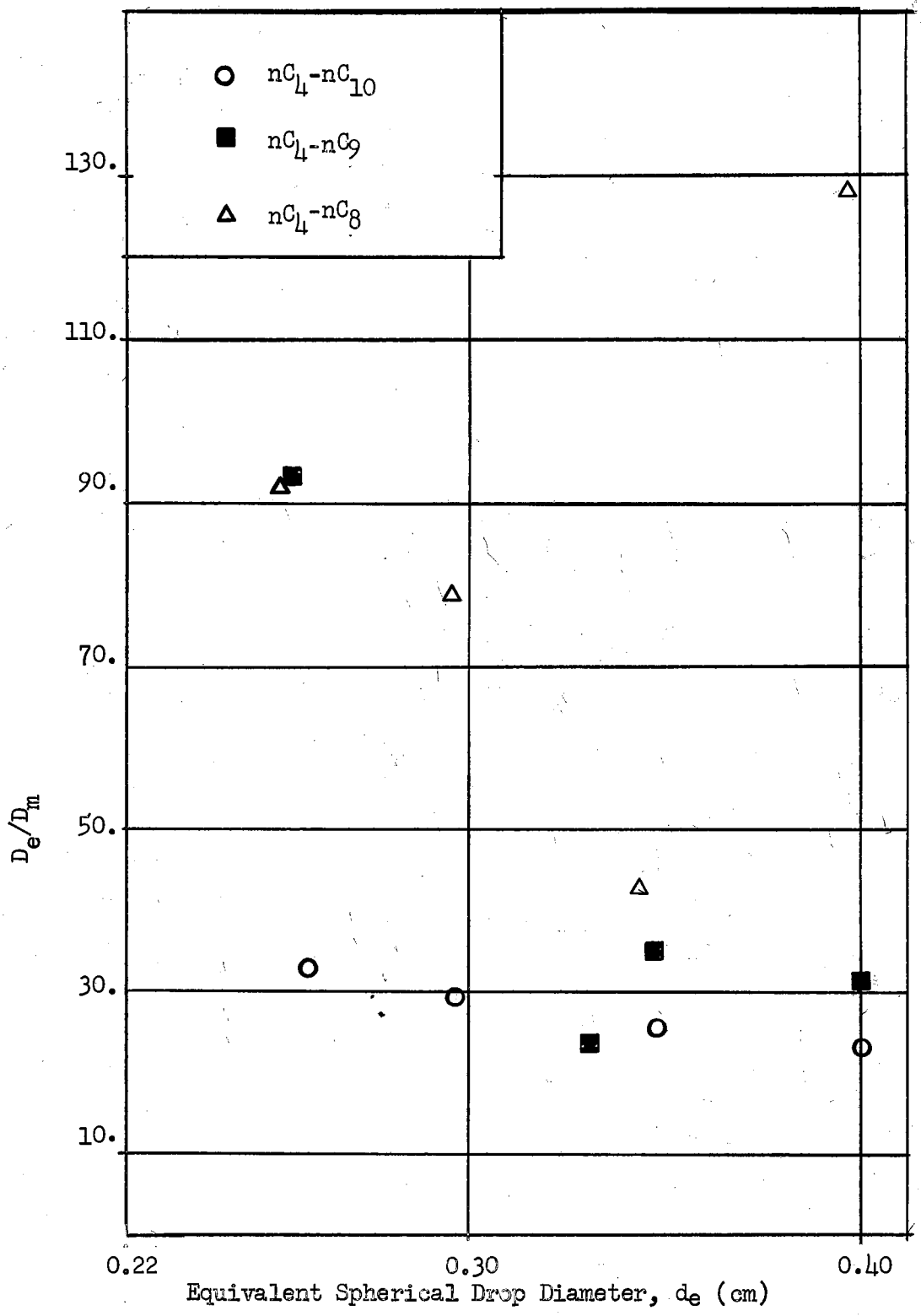

Figure 19. Effect of Drop Diameter on D_e/D_m (Results of Type A and Type B Runs in Six Foot Column)

the magnitude of the gas film resistance to mass transfer. The calculated gas and liquid resistances tabulated in Table XI all indicate that the controlling step must have been the liquid film mass transfer. Comparison of the $(K_L)_{c3}$ values with the experimentally obtained values indicate that the surface renewal mechanism chosen for the θ_{c3} calculation is near the true mechanism that existed in the drops. A shroud of inert gas probably existed around the falling liquid drops in the solute gas region of the column.

A quantitative comparison of the Type D and Type E results (Table VI) to determine the mass transfer coefficients during drop formation and during the initial fall period is not possible. Type D runs were made in a six foot long column using the nC_4-nC_9 system with drops forming in nitrogen. Type E runs were made in a four foot column fully occupied with n-butane. It was hoped that even under these conditions Type E runs will exhibit higher solute gas concentrations in the liquid sample than the Type D runs due to gas absorption during formation. The results do not confirm these expectations, except for drops formed from Tip 7.

As discussed in the first part of this thesis, drops forming in n-butane are smaller than those forming in nitrogen (from a given tip at the same drop formation time). Using n-decane rather than n-nonane should have corrected for some of this effect.

Discussion of Experimental Error

The uncertainties in the K_L values calculated from experimental data result from errors in the determination of the parameters of Equation (40)

$$K_L = \frac{d_e}{6\,\theta_a} \log_e (1 - F) \qquad (40)$$

Experimental errors observed in the liquid sample solute gas concentration are tabulated in Table VI. All Type A and Type B runs show larger errors for small drops than they do for larger drops. This trend is not followed by the results of Type C, D and E runs. The average absolute percent error for all Type A and Type B runs is 6.1% and for all runs is 4% on the solute gas concentration in the liquid sample. This error is due partially to chromatographic analysis, variations in drop formation times (2.6 - 2.8 seconds), system temperature (22.0 - 24.0°C.), column pressure and sampling time and procedure. In Appendix G data are presented showing the effect of sampling time on the solute gas concentration in the sample liquid. Based on these data, the variations in the sample solute gas concentration would be negligible even if the sampling times varied ± 5 seconds.

From Type C runs marked with (*)(Table VI) the effect of double sampling for Tip 1 drops on the observed gas concentrations is seen to be considerable. However, in general, double sampling for Tip 1 drops was necessary to obtain enough sample. Type A and Type B Tip 1 runs were treated similarly, thus they should not have been affected. This effect of double sampling would affect only the Type C runs corrected for cup effects by extrapolation. The effect of continuous sample removal from the drop catching assembly versus the sample removal technique used for most runs (90 sec. sampling time) can be seen by comparing the results of (***) marked Type C runs (Table VI) with the two previous Type C runs at identical conditions. This comparison shows that the sampling procedure does not strongly affect the results. The

reason for this is that the sample liquid, even though not in the collection cup, is still in contact with the gas in the collection chamber which has now entered the sample vial.

Variations in d_e due to possible variations in drop formation time or due to variations in drop size itself at a given drop formation time were determined to be within 1%. Variations in drop surface area due to non-sphericity from the spherical drop assumption are known to be ± 5% (17, 21).

Variations in the drop fall times and consequently the absorption periods have long been accepted to be within 2-3% (38). However, this is a biased error.

The degree of reproducibility of the experimentally determined fractional saturation values, based on the Type C run duplicates is in the range of 0.04% to 17.9%. An evident trend of decreasing percent error with increasing drop size accompany these reproducibility runs. Since the chances for a drop landing out of the drop catching unit were higher for small drops than the larger drops, the variations in sample sizes were larger for smaller drops. However, since the contact area in the drop catcher for all samples collected was about the same, the contact area to sample volume ratio in the drop catcher varied much more for smaller drops. It is believed that this fact was the major factor causing a smaller degree of reproducibility in the measured concentrations of smaller drops.

CHAPTER VI

CONCLUSIONS AND RECOMMENDATIONS

The following are concluded on the basis of the experimental data obtained and the discussion presented in this thesis:

1. The usually overlooked, or rather carelessly considered collection stage end effects in dropwise gas absorption can have a very strong effect on the mass transfer coefficients calculated for falling drops.

2. Of the three methods studied to correct for gas absorption during drop collection in an apparatus using a gas blanket at the collection point, the method employing Type A and Type B runs and Equation (26), developed in Appendix B, gave results most consistent with available theory.

3. The overall mass transfer coefficients based on the liquid side, calculated from Type A and Type B run data for falling drops of nC_8, nC_9 and nC_{10} in nC_4 were in the range 0.04 - 0.14 cm./sec. Ratios of effective to molecular diffusivities for these data were found to be in the 23 - 130 range. In general, higher mass transfer coefficients and higher ratios of effective and molecular diffusivities were observed for drops of lighter hydrocarbons, i.e. lower surface tensions. These data indicate fully circulating drops which may also have oscillations.

4. The analysis of the data shows that surface renewal times in

falling drops, for the systems studied, could be approximated by assuming one surface renewal for each diameter distance along the travel path.

5. Generally lower ratios of effective to molecular diffusivities for larger drops as indicated by the data could be the result of dampened oscillation amplitudes caused by the "hardening" of the drop surface by the probable presence of surface active agents. Thus, these larger drops being elipsoidal would benefit less from the internal circulation currents of the drop which are semi-spherical. However, the high D_e/D_m ratios obtained for the largest nC_9 and nC_8 drops indicate a possible overcoming of the surface hardening by the comparatively stronger oscillatory forces in these lower surface tension drops.

6. The analysis of the data from Type A and Type B runs show that there is evidence to the lingering of a thin layer of inert gas around a drop falling in the solute gas atmosphere, if the drop was formed in an inert gas atmosphere. This phenomenon was first hypothesized by Garner and Lane (20).

The following are recommended for future worker on this subject:

1. The effect of the collection stage could be decreased if the liquid sample is collected in a drop catching cup with a funnel like cross-section and designed to keep the exposed area of the liquid sample proportional to the sample size at all times. Furthermore, the liquid sample should be withdrawn from this receptacle continuously and as fast as possible with a large, gas tight and refrigerated syringe to decrease the amount of gas desorbed from the sample. The sample can then be pressured with an inert gas and analyzed as a liquid or it could be evaporated and analyzed as a vapor. The choice of the method of

analysis will depend on the system studied.

2. This project should be extended to use other gases and liquids as well as mixtures.

3. Research involving study of the hydrodynamic parameters pertinent to falling drops still lacks data and attention. Even though recently photoelectric cells have been used to measure drop fall times and velocities (5), the author believes that a highly accurate technique to measure drop fall times and velocities could be developed using a high speed movie camera, an accurate electronic timer and a combination of mirrors and lenses. In this technique, the mirrors and the lenses are used to make the drop image fall, at different points along the column, on a stationary point, which is constantly being photographed by the camera. Such studies, though tedious, will reveal accurate data on the drop hydrodynamics during acceleration.

BIBLIOGRAPHY

(1) Batson, J. B., M.S. Thesis, University of Tennessee (1957), as referred to in reference (54).

(2) Bayens, C. A. and Laurence, R. L., Ind. Eng. Chem. Fund. 7, 521 (1968).

(3) Bond, W. N. and Newton, D. A., Phil. Mag. 5, 794 (1958).

(4) Brock, J. R. and Bird, R. B., A.I.Ch.E., J., 1, 174 (1955).

(5) Buzzard, J. L. and Nedderman, R. M., Chem. Eng. Sci., 22, 1577 (1967).

(6) Calderbank, P. H. and Korchinski, I.J.O., Chem. Eng. Sci., 6, 65 (1956).

(7) Constan, G. L. and Calvert, S., A.I.Ch.E., J., 9, 109 (1963).

(8) Crank, J., The Mathematics of Diffusion, Oxford University Press, London (1957).

(9) Dombrowski, N. and Hooper, P. C., Chem. Abs. 57:8386g

(10) Danckwerts, P. V., Ind. Eng. Chem., 43, 1460 (1951).

(11) Davidson, J. F. and Schuler, B. O. G., Trans. Inst'n. Chem. Engr's. (London), 38, 144 (1960).

(12) Davidson, J. F. and Schuler, B. O. G., Trans. Inst'n. Chem. Engr's (London), 38, 335 (1960).

(13) Deam, J. R., Ph.D. Dissertation, Oklahoma State University, Stillwater, Oklahoma (1969).

(14) Dixon, B. E. and Russell, A. A. W., J. Soc. Chem. Ind., 69, 284 (1950).

(15) Erbar, J. H., Nonlinear Parameter Estimation Computer Program, Private Communication.

(16) Ferguson, A., Trans. Faraday Soc., 19, 407 (1923).

(17) Finlay, B. A., Ph.D. Dissertation, University of Birmingham, England (1957).

(18) Frossling, N., Gerlands Beitr. Geophys., 52, 170 (1938).

(19) Garner, F. H. and Kendrick, P., Trans. Inst'n. Chem. Engr's. (London), 37, 155 (1959)

(20) Garner, F. H. and Lane, I. J., Trans. Inst'n. Chem. Engr's. (London), 37, 162 (1959).

(21) Garner, F. H. and Lihou, D. A., Dechema Monograph, 55, 955 (1964), (English Edition, pages 155-178, published 1965).

(22) Goodridge, F. and Robb, I. D., Ind. Eng. Chem. Fund., 4, 49 (1965).

(23) Groothuis, H. and Kramers, H., Chem. Eng. Sci., 4, 17 (1955).

(24) Guyer, A., Tobler, B. and Farmer, R. H., Chem. Fabrik, Number 29/30, 265 (1934).

(25) Guyer, A., Tobler, B. and Farmer, R. H., Chem. Fabrik, Number 1/2, 5 (1936).

(26) Guyer, A. and Peterhans, E., Helv. Chim. Acta., 26, 1099 (1943).

(27) Hadamard, J., Compt. Rend. Acad. Sci. Paris, 152, 1735 (1911).

(28) Harkins, W. D. and Brown, F. E., J. Am. Chem. Soc., 41, 499 (1919).

(29) Harmathy, T. Z., A.I.Ch.E., J., 6, 281 (1960).

(30) Harper, J. F., Moore, D. W. and Pearson, J. R. A., J. Fluid Mach., 27, 361 (1967).

(31) Hatta, S. and Baba, A., J. Soc. Chem. Ind. (Japan), 37, No. 4, 162B (1934); (English Edition).

(32) Hatta, S., Veda, T. and Baba, A., J. Soc. Chem. Ind. (Japan), 37, No. 4, 164B (1934); (English Edition).

(33) Hatta, S. and Baba, A., J. Soc. Chem. Ind. (Japan), 38, No. 10, 544B (1935)(English Edition).

(34) Hatta, S. and Baba, A., J. Soc. Chem. Ind. (Japan), 38, No. 10, 546B (1935) (English Edition).

(35) Hayworth, C. B. and Treybal, E., Ind. Eng. Chem., 42, 1174 (1950).

(36) Higbie, R., Trans. Am. Inst. Chem. Eng., 31, 365 (1935).

(37) Himmelblau, E. M., Chem. Rev., 64, 527 (1964).

(38) Hughes, R. R. and Gilliland, E. R., Chem. Eng. Prog., 48, No. 10, 497 (1952).

(39) Hughes, R. R. and Gilliland, E. R., Chem. Eng. Prog. Symp. Ser., 51, (No. 16), 101 (1955).

(40) Johnstone, H. F. and Williams, G. C., Ind. Eng. Chem., 31, 993 (1939).

(41) Kenning, D. B. R., Chem. Eng. Sci., 24, 1385 (1969).

(42) Khurana, A. K. and Kumar, R., Chem. Eng. Sci., 24, 1711 (1969).

(43) King, C. J., A.I.Ch.E., J., 10, 671 (1964).

(44) Kintner, R.C. , Drop Phenomena Affecting Liquid Extraction in Advances in Chemical Engineering, Volume 4, Academic Press, New York (1965)

(45) Kronig, R. and Brink, J. C., Appl. Sci. Res., A2, 142 (1951).

(46) Kumar, R. and Kuloor, N. R., Chem. Technik, 19, 78 (1967).

(47) Lamb, H., Hydrodynamics, Sixth Edition, Dover Pub., New York (1945).

(48) Levich, V. G., Physicochemical Hydrodynamics, Prentice Hall (1962).

(49) Makino, M. and Takashima, Y., Bul. Tokyo Inst. of Techn., No. 90, 151 (1969).

(50) Marquardt, D.W., J. Soc. Ind. Appl. Math., 11, 431 (1963)

(51) Neumann, H. and Seeliger, R., Zeitschrift fur Physik, 114, 571 (1939).

(52) Null, H. R., M. S. Thesis, University of Tennessee (1951); as referred to in reference (54).

(53) Null, H. R., Ph.D. Dissertation, University of Tennessee (1955); as referred to in reference (54).

(54) Null, H. R. and Johnson, H. F., A.I.Ch.E., J., 4, 273 (1958).

(55) Plit, I. G., Zhur. Prikl. Khim. (Eng. Ed.), 38, No. 1, 135 (1965).

(56) Plit, I. G., Chem. Abs., 63:17504h.

(57) Potter, O. E., Chem. Eng. Sci., 24, 1733 (1969).

(58) Pouta̋nen, A.A. and Johnson, A.I., Can. J. Chem. Eng., 38, 93 (1960)

(59) Rabovskii, B. G. and Shinyaeva, V. S., Zhur. Prikl. Khim. (Eng. Ed.), 34, No. 2, 287 (1961).

(60) Ramakrishnan, S., Kumar, R. and Kuloor, N. R., Chem. Eng. Sci., 24, 731 (1969).

(61) Reid, R. C. and Sherwood, T. K., The Properties of Gases and Liquids, (Second Edition), McGraw Hill, New York (1966).

(62) Reinhart, A., Chem. Eng. Techn., 36, 740 (1964).

(63) Rossini, F. D., American Petroleum Institute, Project 44, Carnegie Press (1953).

(64) Rybczynski, W., Bull. Acad. Sci. Cracovie, A. 40 (1911).

(65) Satyanarayan, A., Kumar, R. and Kuloor, R., Chem. Eng. Sci., 24, 749 (1969).

(66) Shabalin, K. N., J. Appl. Chem. (U.S.S.R.), 13, 412 (1940).

(67) Vilnits, S. A. and Gelperin, N. I., Chem. Abs., 53:20941a.

(68) Vivian, J. E. and Behrman, W. C., A.I.Ch.E., J., 11, 656 (1965).

(69) Whitman, W. G., Long, L., Jr. and Wang, H. Y., Ind. Eng. Chem., 18, 363 (1926).

(70) Whitman, W. G., Chem. Met. Eng., 29, 146 (1923).

(71) Wilke, C. R. and Chang, P., A.I.Ch.E., J., 1, 264 (1955).

APPENDIX A

DERIVATION OF EQUATION (8)

A force balance on a forming liquid drop hanging vertically downward is of the form

$$F_g - F_b - F_\sigma - F_f = 0 \qquad (A\text{-}1)$$

where

F_g = gravity force = $V_d \rho_d g$

F_b = buoyant force = $V_d \rho_c g$

F_σ = surface tension force at the tip = $\pi d_2 \sigma$

F_f = force due to flow of fluid into the drop = $\dfrac{d(M_d v_n)}{d\theta}$

Harkins and Brown (28) have shown that when a liquid drop detaches from the tip not all of the hanging liquid leaves with the drop. For this purpose a correction factor, ψ, was used to account for the liquid remaining on the tip. Thus,

$$F_\sigma = \psi d_2 \pi \sigma \qquad (A\text{-}2)$$

The flow force F_f is of the form

$$F_f = \frac{d(M_d v_n)}{d\theta} = M_d \frac{d v_n}{d\theta} + v_n \frac{d M_d}{d\theta} \qquad (A\text{-}3)$$

However, since the liquid flow velocity V_f into the drop is constant, the force due to the incoming fluid which is enlarging the drop is of the form

$$F_f = v_n \frac{d M_d}{d\theta} \qquad (A\text{-}4)$$

The drop weight M is governed by the feed rate Q into the drop, thus

$$F_f = v_n \frac{d}{d\theta} \left[\rho_d \int Q \, d\theta \right] = v_n \rho_d Q \qquad \text{(A-5)}$$

Thus, Equation (A-1) can be written as

$$V_d \rho_d g - V_d \rho_c g - \psi \pi d_2 \sigma - v_n \rho_d Q = 0 \qquad \text{(A-6)}$$

However

$$V_d = M_d/\rho_d \; ; \quad Q = M_{d,final}/(\rho_d \theta_f) \text{ and } v_n = 4Q/(\pi d_1^2) \qquad \text{(A-7)}$$

Thus, Equation (A-6) becomes

$$M_d g \left(1 - (\rho_c/\rho_d) \right) = \psi \pi d_2 \sigma + (M_d/\theta_f)^2 \left(4/(\pi d_1^2 \rho_d) \right) \qquad \text{(A-8)}$$

and upon rearranging

$$M_d^2 - \left[\pi (d_1^2/4) \rho_d \theta_f^2 g \left(1 - (\rho_d/\rho_c) \right) \right] M_d + \psi d_2 \sigma d_1^2 \pi \rho_d \theta_f^2 = 0 \qquad \text{(A-9)}$$

Equation (A-9) is quadratic in M_d^2 and has two real roots. However, the value of one of these roots is very much different, i.e. orders of magnitude, from the drop weights experimentally encountered and therefore has no practical significance.

APPENDIX B

DIMENSIONAL ANALYSIS FOR EQUATION (11)

Starting with the assumption

$$\frac{(M_d)_{g,\theta_f}}{(M_d)_{air,\infty}} = \text{constant} \left(\frac{d_1}{d_2}\right)^{P_2} (\theta_f)^{P_1} (d_1)^{P_3} (\mu_d)^{P_4} (\sigma)^{P_5} (\rho_d)^{P_6} (D_m)^{P_7} \quad \text{(B-1)}$$

one proceeds to express the factors in Equation (B-1) in terms of their dimensions:

$$(-) = \text{Constant } (-)^{P_2} (\underline{\theta})^{P_1} (\underline{L})^{P_3} (\underline{M}/(\underline{L}\,\underline{\theta}))^{P_4} (\underline{M}/\underline{\theta}^2)^{P_5} (\underline{M}/\underline{L}^3)^{P_6} (\underline{L}^2/\underline{\theta})^{P_7} \quad \text{(B-2)}$$

Equating the exponents of similar dimensions on each side of Equation (B-2)

$$\underline{\theta}: \quad P_1 - P_4 - 2P_5 - P_7 = 0 \quad \text{(B-3)}$$

$$\underline{L}: \quad P_3 - P_4 - 3P_6 + 2P_7 = 0 \quad \text{(B-4)}$$

$$\underline{M}: \quad P_4 + P_5 + P_6 = 0 \quad \text{(B-5)}$$

Equations (B-3), (B-4) and (B-5) involve six unknowns. If one decides to evaluate P_4, P_5 and P_6 in terms of P_1, P_3 and P_7 one obtains

$$P_4 = -3P_1 - 2P_3 - P_7 \quad \text{(B-6)}$$

$$P_5 = 2P_1 + P_3 \quad \text{(B-7)}$$

$$P_6 = P_1 + P_3 + P_7 \quad \text{(B-8)}$$

Substituting Equations (B-6), (B-7), (B-8) into Equation (B-1) and collecting the factors with similar exponents yields

$$\frac{(M_d)_{g,\theta_f}}{(M_d)_{air,\infty}} = \text{constant} \left(\frac{d_1}{d_2}\right)^{P_2} \left(\frac{\theta_f \sigma^2 \rho_d}{\mu_d^3}\right)^{P_1} \left(\frac{d_1 \sigma \rho_d}{\mu_d^2}\right)^{P_3} \left(\frac{D_m \rho_d}{\mu_d}\right)^{P_7} \quad \text{(B-9)}$$

Equation (B-9) is in terms of dimensionless quantities. Exponents P_1, P_2, P_3 and P_7 are to be determined from the data.

Several other dimensionless equations were obtained on the basis of Equation (B-1) by choosing exponents other than the P_1, P_3 and P_7 combination. However, when fitted to the data, Equation (B-9) gave the best fit.

APPENDIX C

CONSIDERATIONS FOR THE DESIGN OF THE DROP CATCHING ASSEMBLY AND THE CHOICE OF FREON 12 AS THE BLANKET GAS

Initially a drop catching unit, very similar in design and dimensions to the one described by Garner and Kendrick (19) was constructed of glass. After a long trial and error period varying the blanket gas inlet and exit rates, the mixing of hydrocarbon gas (Type A and Type B runs) with nitrogen, which was used as the blanket gas, was eliminated in the drop catcher. However, high nitrogen flow rates had to be employed to compensate for the lower molecular weight of nitrogen than the hydrocarbon gas above it. These tests indicated that this design and method had the following drawbacks:

1. The high nitrogen flow rates that had to be employed introduced considerable amounts of nitrogen in the absorption section of the column.

2. Even though this drop catcher had been successfully tested with water drops and found to catch about 90 - 95% of the falling drops of water, it failed to catch more than 20% of the falling liquid hydrocarbon drops. Surface tensions of the hydrocarbons used are about 1/3 to 1/4 that of water. Evidently drops of low surface tension liquids tended to oscillate more than the water drops, resulting in an impact point scatter which was not handled with the 3/8 inch top opening of this drop catcher.

A new drop catching unit with a larger top opening was designed and constructed from Lucite and glass, Figure 12. Freon 12 was chosen as the blanket gas due to its high molecular weight and relatively low solubility in the hydrocarbon liquids used. Using Freon 12, a relatively low gas rate was sufficient to obtain an almost perfect gas-gas interface at the suction ring of the drop catching assembly.

APPENDIX D

GAS FLOW RATES IN THE ABSORPTION EXPERIMENTS

The gas flow rates into the absorption column, as read from rotameters R1, R2 and R3 are given below. The rotameter readings varied a maximum of ± 0.2 centimeters between runs.

The gas flow rates, in milliliters per minute, were obtained from the calibration curves supplied by the manufacturer. For Freon 12, the flow rates were calculated from the n-butane curves using the rotameter equation and assuming that the discharge coefficients were the same for both n-butane and Freon 12.

The gas rates for R4 and R5, the exit gas rotameters, are given as direct readings (centimeters), since in most cases the gases leaving the column were gas mixtures of unknown compositions. Furthermore, the exit side pressure of these rotameters were considerably lower than atmospheric due to the presence of the vacuum pump used for suction, thus eliminating the use of the curves.

Since the gas velocities in the column were low, small variations in the gas rates were not critical to the results of the experiments, i.e. interfacial gas velocity on the drop surface was unaffected. The reported readings were varied within the ± 0.2 cm. range to form and maintain sharp gas-gas interfaces.

The gas flow rates given below for each type of run are in the form: (1) Run Type; (2) Rotameter Number; (3) Rotameter Tube Number;

(4) Gas in the Rotameter; (5) Rotameter Reading (cm.); (6) Rotameter Float Giving the Reading (ss - stainless steel, py - pyrex); (7) Gas Flow Rate (milliliters per Minute).

(1)	(2)	(3)	(4)	(5)	(6)	(7)
A	R1	603	nC_4	6.0	ss	1900
A	R2	602	F12	4.0	ss	730
A	R3	603	N_2	4.0	ss	1600
A	R4	603	nC_4+F12	6.5	py	
A	R5	604	nC_4+N_2	7.5	ss	
B	R1	603	nC_4	5.9	ss	1880
B	R2	602	F12	4.0	ss	730
B	R3	603	nC_4	4.2	ss	1400
B	R4	603	nC_4+F12	6.6	py	
B	R5	604	nC_4	7.2	ss	
C	R1	603	nC_4	7.0	ss	2200
C	R3	603	N_2	3.9	ss	1600
C	R5	604	nC_4+N_2	5.9	ss	
D	R1	603	nC_4	2.0	py	400
D	R2	602	nC_4	2.6	py	500
D	R3	603	N_2	7.1	ss	2800
D	R4	603	N_2+nC_4	7.0	ss	
E	R1	603	nC_4	1.6	py	300
E	R3	602	nC_4	1.2	py	0
E	R4	603	nC_4	1.2	py	
E	R5	604	nC_4	1.2	py	

APPENDIX E

CHROMATOGRAPHIC CALIBRATIONS

The chromatographs used for the analysis of the column gas of the drop were calibrated using two different procedures. The details of these procedures and results are given below for each chromatograph.

Calibration of the Varian 1200 Chromatograph

The Varian 1200 gas chromatograph, equipped with a flame ionization detector, was used to analyze the liquid drops from both Parts I and II of this study to determine the concentration of the dissolved gas in the drop liquid sample.

The samples used to calibrate the chromatograph were of two kinds:

a. Samples of hydrocarbon liquid with dissolved hydrocarbon gas,

b. A mixture of two normal paraffinic hydrocarbon liquids.

Samples of type (a) were prepared by bubbling the hydrocarbon gas through some hydrocarbon liquid held at constant temperature in a constant temperature bath.

Samples of type (b) were prepared by adding known quantities of different hydrocarbon liquids into a sealed flask. The amount of each liquid added was determined by a Mettler balance.

Table XIII shows the calibration data. For binary liquid mixtures, the ratio of area counts of a component peak to the total peak area counts for the sample deviates about 1% from the actual composition

expressed as weight fraction. For the binary mixtures where one component was a dissolved hydrocarbon gas, i.e. n-butane, the dissolved gas fractions, as calculated from peak count ratios, deviate somewhat more from the "actual" composition than in the case of binary liquid mixtures. The "actual" compositions for the dissolved gas binaries are predictions from Raoult's law, and they are consistently higher than the compositions calculated from peak ratios. Thus, the evident discrepancy between the two compositions may well be due to Raoult's law assumption.

The data presented in Table XIII shows that the degree of reproducibility of an analysis was quite good. Based on the binary liquid mixture analyses, and also on the analyses of the n-butane - liquid hydrocarbon samples, the decision was made to use the ratio of component peak area to the total sample area as the composition of the sample, in weight fraction, for the homologous series of the paraffinic hydrocarbons used in this study.

Calibration of the FM-500 Chromatograph

The FM-500 chromatograph, equipped with a thermal conductivity detector was used to analyze the gas samples obtained from the absorption column through the gas sampling ports.

In the early stages of the experimental work it seemed almost impossible to eliminate the mixing of the blanket gases, i.e. Freon 12 and nitrogen, with the hydrocarbon gas occupying the column. Thus, it looked as if it would be necessary to accurately determine the composition profile of the column gas to be able to evaluate the mass transfer coefficients for gas absorption. This led to the calibration of the

TABLE XIII

CALIBRATION DATA FOR THE VARIAN 1200 CHROMATOGRAPH
(FLAME IONIZATION DETECTOR)

System Comp 1	System Comp 2	Counts Comp 1	Counts Comp 2	Counts Comp 1 / Counts $C_1 + C_2$	Actual Wt. Fr. Comp 1	Deviation Percent
Column: 10% SE30 on Chromasorp P (50/60 mesh)(1/8" x 10 ft.)						
Gas Rates: 40 cc/min. He, 25-27 cc/min. H_2 (at 150°C. column)						
Sample: 1 μl; Attenuation = 4						
nC_9	nC_{10}	805	1954	0.2914		
		817	1986	0.2917		
T_{sample} = 23.5°C		822	2000	0.2913		
		819	1989	0.2917		
T_{column} = 205.°C		809	1966	0.2915		
				Avg 0.2915	0.2883	1.10
nC_5	nC_{10}	478	2075	0.1872		
		460	2014	0.1860		
T_{sample} = 23.5°C		469	2048	0.1865		
		506	2129	0.1914		
T_{column} = 170.°C				Avg 0.1880	0.1910	-1.57
nC_5	nC_9	450	2479-	0.1538		
		462	2524	0.1548		
T_{column} = 150°C		458	2482	0.1546		
				Avg 0.1544	0.1520	+1.60
nC_5	nC_8	503	1797	0.2190		
		507	1852	0.2194		
T_{column} = 130°C		512	1838	0.2180		
				Avg 0.2188	0.2210	-1.00
Column: Poropak Q (100/120 mesh)(1/8" x 7')(with back flush valve)						
Gas Rate: 40 cc/min. He, 25-27 cc/min. H_2 (at 150°C. column T)						
Sample: 1 μl; Attenuation = 4						
nC_4	nC_8	4826	12121	0.284		
T_{sample} = 23.5°C		4462	11150	0.286		
				0.285	0.296*	
nC_4	nC_9	4086	11698	0.259		
		4202	12107	0.257		
T_{sample} = 23.5°C		4419	12894	0.255		
		4381	12507	0.259		
				0.258	0.276*	

TABLE XIII (Continued)

System Comp 1	System Comp 2	Counts Comp 1	Counts Comp 2	Counts Comp 1 / Counts $C_1 + C_2$	Actual Wt. Fr. Comp 1	Deviation Percent
nC_4	nC_{10}	3523	11990	0.2265		
		3528	12168	0.2248		
$T_{sample} = 23.5°C$		3760	12748	0.2272		
				0.2262	0.242(*)	

(*) Calculated from Raoult's Law using vapor pressures from Antoine equation (API Project 44(63)).

chromatograph for the gases present in the column.

The calibration procedure comprised of injecting different size samples (0.1 - 1.5 ml.) of pure gases into the chromatograph. The peak obtained for each gas varied linearly with the sample size. From these data, response factors were determined for Freon 12, n-butane, and propane relative to nitrogen.

Conditions of the calibrations for the N_2-nC_4 - Freon 12 system and the relative response factors obtained were:

Column: 50-80 mesh Poropak Q; ¼ inch x 7 feet

Column Temperature = 175°C.; Detector Block Temperature = 180°C. and Injection Port Temperature = 242°C.

Carrier Gas: Helium 45.5 ml./min.; Current: 117 mA and Attenuation = 32

Relative Response Factor (Freon 12/nitrogen) = 1.770

Relative Response Factor (n-butane/nitrogen) = 1.468

For the nitrogen-propane-Freon 12 system the conditions of calibration and the evaluated response factors were:

Column: 50-80 mesh Poropak Q; ¼ inch x 7 feet

Column Temperature = 90°C.; Detector Block Temperature = 122°C. and Injection Port Temperature = 240°C.

Carrier Gas: Helium 45.5 ml./min.; Current: 120 mA and Attenuation = 32

Relative Response Factor (Freon 12/nitrogen) = 1.927

Relative Response Factor (Propane/nitrogen) = 1.560

The relative response factors when used to predict the composition of a gas mixture of "known" composition, gave acceptable predictions. However, in general the Freon 12 values checked the best (within 1%).

The predicted nitrogen concentrations were in general lower (7%) than the actual and the predicted n-butane concentrations were in general higher than the actual (5%). For the nitrogen-propane-Freon 12 system the predicted and actual compositions compared much more favorably (0.5%).

The gas mixtures of known compositions were prepared in the laboratory by introducing different amounts (partial pressure) of nitrogen, Freon 12 and propane or n-butane into an initially evacuated flask. The relative response factors were applied to the peak ratios to predict the composition of the mixture in mole fractions.

However, it was later possible to virtually eliminate the mixing of the blanket gases into the hydrocarbon gas in the column during a run. Thus, the calibrations on the FM-500 chromatograph were not used. Any gas mixing noticed during absorption runs were not more than two-three counts per thousand counts. In most of the runs the chromatographic analysis showed no gas mixing at all.

APPENDIX F

CORRECTIONS FOR MASS TRANSFER DURING SAMPLE COLLECTION

(DERIVATIONS)

The mechanism governing the liquid and the surrounding gas atmosphere in the drop collection chamber of the absorption column is described by the mass balance

$$\frac{d(Q\theta C)}{d\theta} = k_1 A \Delta C + Q C_d \qquad (F\text{-}1)$$

Equation (F-1) approximates the periodic addition of the drops to the sample liquid in the drop collection cup with a constant liquid feed rate Q. The liquid feed rate, Q is defined as

$$Q = \frac{1}{\theta_s} \sum_{1}^{N} (V_d)_i \qquad (F\text{-}2)$$

Furthermore, Equation (F-1) also assumes that the collected sample is perfectly mixed at all times during sampling.

Derivation of the Cup Correction Factor from the Results of Type A and Type B Runs

For the liquid sample collected in the drop catcher during Type A and Type B runs Equation (F-1) takes the form

$$\frac{d(Q\theta C)}{d\theta} = -k_1 A (C - C_g) + Q C_d \qquad (F\text{-}3)$$

The minus sign preceding the first term on the right hand side signifies desorption. Rearranging Equation (F-3) one obtains

$$C + \theta \frac{dC}{d\theta} = -\left(\frac{k_1 A}{Q}\right) C + \left(\frac{k_1 A}{Q}\right) C_g + C_d \qquad (F\text{-}4)$$

Letting M1 = $k_1 A/Q$ and rearranging to integrate

$$\int_{C_d}^{C_s} \frac{dC}{(M1\, C_g + C_d) - (1+M1)C} = \int_{1}^{\theta_s} \frac{d\theta}{\theta} \qquad (F\text{-}5)$$

where C_s is obtained from the chromatographic analysis of the liquid sample. The lower limit of the right hand side integral in Equation (F-5) has to be greater than zero, since at zero time there is no liquid in the collection cup. If time units are chosen small, e.g. milliseconds, a limit of 1 could be used without introducing an appreciable error to the calculations.

Integrating Equation (F-5) one obtains

$$\frac{1}{1+M1} \ln \left[\frac{M1\, C_g + C_d - (1+M1)\, C_d}{M1\, C_g + C_d - (1+M1)\, C_d}\right] = \ln \theta_s \qquad (F\text{-}6)$$

Rearranging and taking the exponential

$$\frac{M1\, C_g + C_d - (1+M1)\, C_s}{M1\, C_g + C_d - (1+M1)\, C_d} = \theta_s^{-(1+M1)} = \theta_s^{-(1+\frac{k_1 A}{Q})} \qquad (F\text{-}6)$$

In Type A runs, C_d is unknown, C_g will be replaced by C_g^A to identify the type of run and C_s will be replaced by C_s^A to designate the origin of the analyzed liquid sample. Thus, for Type A runs, Equation (F-6) becomes

$$\frac{M1\, C_g^A + C_d - (1+M1)\, C_s^A}{M1\, C_g^A + C_d - (1+M1)\, C_d} = \theta_s^{-(1+M1)} = \theta_s^{-(1+\frac{k_1 A}{Q})} \qquad (F\text{-}7)$$

In Type B runs, C_d is equal to C*, the equilibrium concentration

of the hydrocarbon gas in the drop liquid at run temperature and pressure. Furthermore, in Equation (F-7) C_g is replaced by C_g^B and C_s by C_s^B to obtain

$$\frac{M1\,C_g^B + C^* - (1+M1)\,C_s^B}{M1\,C_g^B + C^* - (1+M1)\,C^*} = \theta_s^{-(1+M1)} = \theta_s^{-(1+\frac{k_1 A}{Q})} \qquad (F\text{-}8)$$

Drop formation rates and sampling times are held the same for both type A and type B runs, thus Q has the same value in Equation (F-7) and in Equation (F-8). The transfer area A is constant since the samples are collected in the tube above valve V20.

Assuming that the transfer coefficient k_1 is constant for both runs, i.e. k_1 is independent of concentration, the right hand sides of Equations (F-7) and (F-8) become identical in value. Thus, equating the left hand side terms of Equations (F-7) and (F-8) one obtains,

$$\frac{M1\,C_g^A + C_d - (1+M1)\,C_s^A}{M1\,C_g^A + C_d - (1+M1)\,C_d} = \frac{M1\,C_g^B + C^* - (1+M1)\,C_s^B}{M1\,C_g^B + C^* - (1+M1)\,C^*} \qquad (F\text{-}9)$$

Rearranging Equation (F-9) and solving for C_d, the unknown, one obtains

$$C_d = \{C_g^B[M1(M1+1)C_s^A] + C_g^A[M1(M1+1)C^* - M1(M1+1)C_s^B] - M1(M1+1)\,C^*C_s^A\} \Big/ \{M1(M1+1)C_g^B - M1(M1+1)C_s^B\} \qquad (F\text{-}10)$$

dividing by M1(M1+1)

$$C_d = \left[C_g^B + C_g^A(C^* - C_s^B) - C^*C_s^A\right] \Big/ \left[C_g^B - C_s^B\right] \qquad (F\text{-}11)$$

Thus, knowing C_s^A, C_s^B, C^*, C_g^A and C_g^B experimentally one can determine C_d. However, assuming that the concentration of the hydrocarbon gas in the Freon 12 atmosphere is negligible, i.e. $C_g^A \approx 0.0$, Equation (F-11) becomes

$$C_d = \left(\frac{C_s^A}{C_s^B}\right) C^* \qquad (F\text{-}12)$$

Derivation of the Cup Correction Factor from the Results of Type C and Type D Runs

For the liquid sample collected in the drop catcher during type C and type D runs, Equation (F-3) takes the form

$$\frac{d(Q\theta C)}{d\theta} = k_2 A (C^* - C) + Q C_d \qquad (F\text{-}13)$$

where, C^* is the equilibrium concentration of the hydrocarbon gas in the film of the collected sample in contact with the hydrocarbon gas in the drop catcher. The plus sign preceding the first term on the right hand side of Equation (F-13) can be brought to the integrable form, with

$M2 = k_2 A / Q$

$$\int_{C_d}^{C_s} \frac{dC}{(M2\,C^* + C_d) - (1+M2)C} = \int_1^{\theta_s} \frac{d\theta}{\theta} \qquad (F\text{-}14)$$

Upon integrating Equation (F-14) and taking the exponential of both sides, one obtains

$$\frac{M2\,C^* + C_d - (M2+1)\,C_s^C}{M2\,C^* + C_d - (M2+1)\,C_d} = \theta_s^{-(1+M2)} \qquad (F\text{-}15)$$

In type D runs $C_d = 0.0$, since the drops fall in nitrogen until they splash in the hydrocarbon gas atmosphere of the drop catcher. Setting $C_d = 0.0$ and replacing C_s by C_s^D in Equation (F-16) one obtains

$$\frac{M2\,C^* - (M2+1)\,C_s^D}{M2\,C^*} = \theta_s^{-(1+M2)} \qquad (F\text{-}17)$$

Following the same arguments previously stated,

$$\frac{M2\,C^* + C_d - (M2+1)\,C_s^C}{M2\,C^* + C_d - (M2+1)\,C_d} = \frac{M2\,C^* - (M2+1)C_s^D}{M2\,C^*} \qquad (F\text{-}18)$$

Upon simplification of Equation (F-18) one solves for C_d to obtain

$$C_d = \frac{C_s^C - C_s^D}{1 - (C_s^D/C^*)} \qquad (F\text{-}19)$$

Closing Remarks

Equations (F-12) and (F-19) derived from Equation (F-3) and Equation (F-13),respectively, can also be obtained from Equations (F-20) and (F-21) respectively, assuming C_g=0.0 in Equation (F-20). However, Equations (F-20) and (F-21) do not give a true picture of the mass transfer mechanism during drop collection. They assume that all through the sampling period, including time zero, a liquid sample of volume equal to to the final liquid sample volume V_s of concentration C_d is present in the drop catcher. Equations (F-20) and (F-21) are integrated with the assumption that during the sampling period the sample gas concentrations change from the initial concentration C_d to the final concentration (observed) C_s. Furthermore, solution of Equation (F-20) can not be used to take into account the hydrocarbon gas concentration in the Freon 12 atmosphere, if such a measurement is made and found significant. This type of problem could easily be solved using Equation (F-12) which is the result of the general approach.

For the special case dictated by the assumptions used, both mechanisms, i.e. simple and general, give identical cup corretion factors. However, the difference between the two approaches becomes evident when one compares Equations (F-12) and (F-19) and the solution of Equations (F-20) and (f-21), which is of the form

$$V_s \frac{dC}{d\theta} = -kA(C - C_g) \qquad (F\text{-}20)$$

$$V_s \frac{dC}{d\theta} = k'A(C^* - C) \qquad (F\text{-}21)$$

$$\log_e [(\Delta C)_1/(\Delta C)_2] = \left(\frac{kA}{V_s}\right)\theta_s \qquad (F\text{-}22)$$

APPENDIX G

EFFECT OF DROP LIQUID SAMPLING TIME

ON OBSERVED LIQUID COMPOSITION

Observed solute gas concentrations in the liquid sample are plotted in Figure 20 as a function of the sampling time. These runs with a four foot long column at the Type E run conditions for the nC_4-nC_{10} system using Tip 3. The results show that a small variation in the sampling time (like ± 5 seconds) would have almost neglibible effect (± 0.001 weight fraction nC_4 in nC_{10}) on the sample composition.

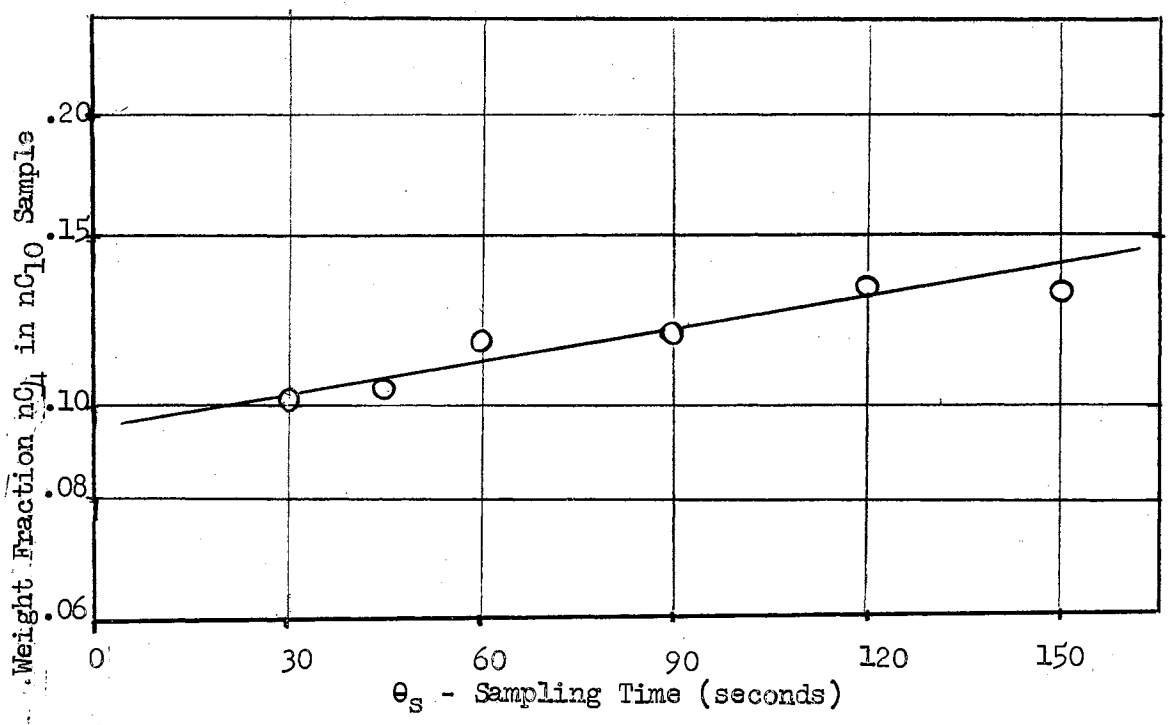

Figure 20. Effect of Sampling Time on Sample Solute Gas Concentration

APPENDIX H

NOMENCLATURE

A - Drop surface area ($\underline{L}^2$)

a - Major axis of ellipsoidal drop ($\underline{L}$)

B - Drop oscillation amplitude ($\underline{L}$)

B_o - Initial Drop Oscillation Amplitude ($\underline{L}$)

b - Minor axis of ellipsoidal drop ($\underline{L}$)

C - Solute gas concentration in liquid at any time θ ($\underline{M}/\underline{M}$)

C^* - Saturation solute gas concentration in drop ($\underline{M}/\underline{M}$)

C_o - Initial solute gas concentration in drop ($\underline{M}/\underline{M}$)

C_D - Drag coefficient for falling drops (-)

C_d - Drop solute gas concentration at the end of drop fall period ($\underline{M}/\underline{M}$)

C_g - Gas phase solute gas concentration ($\underline{M}/\underline{M}$)

C_s^A - Liquid sample solute gas concentration: Type A runs ($\underline{M}/\underline{M}$)

C_s^B - Liquid sample solute gas concentration: Type B runs ($\underline{M}/\underline{M}$)

C_s^C - Liquid sample solute gas concentration: Type C runs ($\underline{M}/\underline{M}$)

C_s^D - Liquid sample solute gas concentration: Type D runs ($\underline{M}/\underline{M}$)

C_g^A - Solute gas concentration in Collection Chamber gas (Type A runs)($\underline{M}/\underline{M}$)

D_c - Eddy diffusivity ($\underline{L}^2/\underline{\theta}$)

D_e - Effective diffusivity ($\underline{L}^2/\underline{\theta}$)

D_m - Molecular diffusivity (Liquid Phase)($\underline{L}^2/\underline{\theta}$)

D_v - Molecular diffusivity (Vapor Phase)($\underline{L}^2/\underline{\theta}$)

d_1 - Internal tip diameter ($\underline{L}$)

d_2 - External tip diameter ($\underline{L}$)

d_e - Diameter of equivalent spherical drop ($\underline{L}$)

E_o - Eötvos Number, $(\rho_d - \rho_c)d_e^2 g/\sigma$

F - Fractional saturation (-)

F_b - Buoyant force ($\underline{M}\underline{L}/\underline{\theta}^2$)

F_f - Force due to flow ($\underline{M}\,\underline{L}/\underline{\theta}^2$)

F_k - Kinetic Force

F_σ - Surface tension force ($\underline{M}\,\underline{L}/\underline{\theta}^2$)

f - Drop oscillation frequency ($1/\underline{\theta}$)

G - Amount of absorbed gas ($\underline{M}$)

g - Gravitational acceleration ($\underline{L}/\underline{\theta}^2$)

g_c - Conversion constant (Force-Mass)

K_e - Vapor-Liquid equilibrium constant

K_g - Overall mass transfer coefficient based on the gas side ($\underline{M}/\underline{L}^2\underline{\theta}$)

K_L - Overall mass transfer coefficient based on the liquid side ($\underline{M}/(\underline{L}^2\underline{\theta})$)

k_c - Gas film mass transfer coefficient ($\underline{M}/\underline{L}^2\underline{\theta}$)

k_g - $\frac{k_c}{RT}$ gas film mass transfer coefficient

k_L - Liquid film mass transfer coefficient ($\underline{M}/\underline{L}^2\underline{\theta}$)

k - Mass transfer coefficient ($\underline{M}/\underline{L}^2\underline{\theta}$)

k', k_1, k'', k_2 - Mass transfer coefficients in drop catcher ($\underline{M}/\underline{L}^2\underline{\theta}$)

L - Drop fall distance ($\underline{L}$)

M_d - Drop mass ($\underline{M}$)

MW_d - Molecular weight of discontinuous phase

N_μ - Nusselt number $\frac{k\,d_e}{D_m}$

P_r - Prandtl number ($\mu_d / \rho_d D_m$)

Q - Liquid feed rate (L^3/θ)

R - Gas constant

R_e - Reynolds number ($d_e U \rho_c / \mu_c$)

$(R_e)_i$ - Internal Reynolds number ($d_e U_{ic} \rho_d / \mu_d$)

S_c - Schmidt number = Prandtl number

S_h - Sherwood number = Nusselt number

T - Temperature

T_i - $\mu_d \theta / (\rho_d d_e^2)$

U - Drop velocity (L/θ)

U_g - Gas velocity (L/θ)

U_{ic} - Drop internal circulation velocity

V_d - Drop volume (L^3)

V_k - Drop volume equivalent to kinetic force (L^3)

V_s - Sample volume from drop catcher (L^3)

V_σ - Drop volume equivalent to surface tension force (L^3)

V_g - Drop volume equivalent to buoyant force (L^3)

v_n - Nozzle (tip) fluid flow rate (L/θ)

vm_c - Continuous (solute) phase molal volume (L^3/M)

x_e - Saturation solute concentration in liquid

y_e - Saturation solute concentration in vapor

Greek Letters

α - Association parameter

σ - Surface tension

μ - Viscosity

ρ - Density (M/L^3)

θ - Time ($\underline{\theta}$)

θ_a - Absorption time ($\underline{\theta}$)

θ_c - Surface renewal time ($\underline{\theta}$)

θ_f - Drop formation time ($\underline{\theta}$)

θ_{fl} - Drop fall time ($\underline{\theta}$)

θ_s - Sampling time ($\underline{\theta}$)

ψ - Constant in Equation (9)

ϕ - Constant in Equation (9)

Dimension

$\underline{M}$ - Mass

$\underline{L}$ - Distance

$\underline{\theta}$ - Time

Subscripts

c - Continuous phase (gas)

d - Discontinuous phase (liquid)

g - Gas phase

m - Saturated gas - liquid mixture

θ - Time

∞ - Long time ($\theta \to \infty$)

VITA

Öner Hortaçsu

Candidate for the Degree of

Doctor of Philosophy

Thesis: PART I - EFFECT OF THE SURROUNDING GAS ATMOSPHERE ON THE LIQUID CONTENT OF FORMING HYDROCARBON DROPS

PART II - GAS ABSORPTION BY FALLING LIQUID DROPS: HYDROCARBON SYSTEMS

Major Field: Chemical Engineering

Biographical:

Personal Data: Born in İzmir, Turkey, February 26, 1940, the son of Ali and Müşerref Hortaçsu; married to Amable G. Dorotan on June 7, 1968 in Stillwater, Oklahoma.

Education: Attended primary school in İstanbul, Turkey; graduated from Robert Academy, İstanbul, in 1956, and from Robert College in June, 1963; received the Master of Science degree from Oklahoma State University in August, 1965; completed the requirements for the degree of Doctor of Philosophy in July, 1970.

Professional Experience: Employed by Mensucat Santral T.A.Ş. in İstanbul in the summer of 1961 and also by Mobil Oil Austria A.G., in Vienna, Austria in the summer of 1962 as Summer Engineering Trainee. Employed by Atlantic-Richfield Company, Harvey (Illinois) Technical Center as a Chemical Engineer since April, 1969.

Membership in Organizations: Member of American Institute of Chemical Engineers, American Chemical Society, Society of Sigma Xi, Catalysis Club of Chicago and Omega Chi Epsilon.